U–Pb zircon geochronology of Proterozoic and Paleozoic rocks, North Islesboro, coastal Maine (USA): links to West Africa and Penobscottian orogenesis in southeastern Ganderia?

Douglas N. Reusch[1], Christopher S. Holm-Denoma[2], and John F. Slack[3,†]

1. Department of Geology, University of Maine, Farmington, Maine 04938, USA
2. U.S. Geological Survey, MS 973, Denver, Colorado 80225, USA
3. U.S. Geological Survey, MS 954, Reston, Virginia 20192, USA
†. Present address: U.S. Geological Survey (Emeritus), Farmington, Maine 04938, USA

*Corresponding author <reusch@maine.edu>

Date received: 29 July 2017 ¶ Date accepted: 30 March 2018

ABSTRACT

Within the Ganderian inlier of Penobscot Bay, coastal Maine, the Islesboro fault block occupies a central position between the St. Croix terrane of continental affinity and, to the east, the Ellsworth terrane of oceanic affinity. New field, petrographic, geochemical, and U–Pb LA-ICP-MS geochronological data on detrital and magmatic zircon grains constrain the provenance and transfer history of these terranes from Gondwana to the Appalachian margin of Laurentia. On North Islesboro, the Coombs Limestone and Hutchins Island Quartzite (new name), intruded by E-MORB amphibolite, constitute a newly recognized local inlier of Proterozoic basement. Together with the nearby Seven Hundred Acre Island Formation, these mature, carbonate-rich strata record deposition on a low-latitude passive margin. Abundant detrital zircon grains in the Hutchins Island Quartzite, all older than ca. 1.8 Ga, have a predominant population at ca. 2.0 Ga and a small peak between ca. 2.8 Ga and 2.4 Ga, an age spectrum strikingly similar to those of both the Paleoproterozoic Taghdout Quartzite in Morocco, on the West African craton, and basement rocks from Georges Bank, offshore Massachusetts.

The overlying Neoproterozoic–Cambrian Islesboro Formation records a second period of extension (interstratified E-MORB greenstone) synchronous with accumulation of interbedded siliciclastic and carbonate sediment, prior to recumbent folding. At the base of the moderately deformed Turtle Head Cove (new name) cover sequence, immature greywacke has a youngest zircon population of ca. 515 Ma, large late Neoproterozoic populations (ca. 624 Ma and 678 Ma), a small peak at 1.2 Ga, a moderate number of ca. 1.5 Ga to 2.0 Ga grains, and a few Late Archean grains. Compared with many similar Ganderian age spectra reported from Vermont to New Brunswick, which are all consistent with a source in either the Amazonian or West African cratons, this new age spectrum most closely resembles those from quartzites in the Grand Manaan and Brookville terranes of coastal New Brunswick. Significantly, exotic blocks lithologically indistinguishable from Proterozoic strata on Islesboro occur in the St. Croix terrane within a Lower Ordovician black shale mélange at the base of the Penobscot Formation, suggesting that the St. Croix terrane, Islesboro block, and Ellsworth terrane were initially juxtaposed by Penobscottian thrusting prior to the Middle Ordovician. Subsequently, the Islesboro block was isolated between the bounding post-Silurian, pre-Late Devonian Turtle Head and Penobscot Bay dextral strike-slip faults. Along the North Islesboro fault, a fault-bounded lens of foliated pyritic felsic volcanic and volcaniclastic rock, dated at ca. 372 Ma and containing Devonian to Archean detrital zircons, records late Paleozoic deformation recognized previously in coastal New Brunswick but not in Penobscot Bay.

RÉSUMÉ

Dans la baie Penobscot, sur la côte du Maine, le bloc de failles d'Islesboro occupe une position centrale entre le terrane d'affinité continentale de St. Croix et, à l'est, le terrane d'affinité océanique d'Ellsworth. De nouvelles données géochronologiques de terrain, pétrographiques, géochimiques et U-Pb LA-ICP-MS sur les grains de zircon détritique et magmatique limitent la provenance et l'historique de transfert de ces terranes du Gondwana à la marge appalachienne de la Laurentie. À Islesboro

0843-5561|18|000189-221 $5.95|0

Nord, le calcaire de Coombs et le quartzite de Hutchins Island (nouveau nom), intrusés par l'amphibolite de la basalte de dorsale médio-océanique, constituent une nouvelle entaille locale du socle protérozoïque. Conjointement avec la formation de Seven Hundred Acre Island située à proximité, ces strates matures et riches en carbonates témoignent d'un dépôt sur une marge passive de faible latitude. Les grains de zircon détritiques abondants dans le quartzite de Hutchins Island, tous âgés de plus de 1,8 Ga, ont une population prédominante aux environs de 2,0 Ga et un petit pic entre la période de 2,8 Ga et 2,4 Ga, un spectre d'âge étonnamment similaire à ceux du quartzite palzoprotérozoïque Taghdout au Maroc, sur le craton ouest-africain, et des roches du socle de Georges Bank, au large du Massachusetts.

La formation d'Islesboro datant du Néoprotérozoïque-Cambrien sus-jacent enregistre une seconde période d'extension (interstratification de roches vertes de la basalte de dorsale médio-océanique) synchrone avec l'accumulation de sédiments siliciclastiques et carbonatés interstratifiés, avant le plissement du gisement. À la base de la séquence de couverture de Turtle Head Cove (nouveau nom) modérément déformée, le greywacke immature a une plus jeune population de zircon d'environ 515 Ma, de grandes populations néoprotérozoïques tardives (624 Ma, 678 Ma), un petit pic à 1,2 Ga, un nombre modéré de grains de 1,5 Ga à 2,0 Ga, et quelques grains de l'Archéen tardif. Comparé à de nombreux spectres d'âge ganderiens similaires du Vermont au Nouveau-Brunswick, qui correspondent tous à une source dans les cratons amazoniens ou ouest-africains, ce nouveau spectre d'âge ressemble le plus à ceux des quartzites des terres côtières de Grand Manan et de Brookville au Nouveau- Brunswick. De manière significative, des blocs exotiques lithologiquement indiscernables des strates protérozoïques d'Islesboro se trouvent dans le terrane de St. Croix à l'intérieur de la formation de Penobscot, ce qui suggère que le terrane de St. Croix, le bloc d'Islesboro et le terrane d'Ellsworth étaient initialement juxtaposés. par une poussée de l'arc penobscottien avant l'Ordovicien moyen. Par la suite, le bloc d'Islesboro a été isolé entre les failles limites post-siluriennes de Turtle Head datant du pré-Dévonien tardif et les failles de décrochement dextres de la baie Penobscot. Le long de la faille d'Islesboro Nord, une lentille fendue de roches volcaniques pyriteuses felsiques et volcanoclastiques, datée d'environ 372 Ma et contenant des zircons détritiques du Dévonien à l'Archéen, enregistre la déformation tardive du Paléozoïque reconnue précédemment sur les côtes du Nouveau-Brunswick, mais pas dans la baie Penobscot.

[Traduit par la redaction]

INTRODUCTION

The Appalachian–Caledonide orogen (Hibbard *et al.* 2006; Fig. 1) has yielded fundamental insights into Earth history, paleogeography, and processes (e.g., Wilson 1966), yet continues to present significant questions. In contrast to the western peri-Laurentian flank of the orogen, which is relatively well understood in terms of Ordovician continent-arc collision (e.g., Karabinos *et al.* 2017), the eastern peri-Gondwanan realm comprises a complex mosaic of pre-Silurian terranes with a much more contentious tectonic evolution (Murphy *et al.* 2004; Fyffe *et al.* 2011; Pollock *et al.* 2012). Ganderia, the most outboard of several peripheral Gondwanan domains, was first to accrete to Laurentia and has proved especially challenging to interpret owing to a protracted history of deformation and magmatism (e.g., Hibbard *et al.* 2007).

In Penobscot Bay, Maine, a Ganderian inlier of Ordovician and older rocks exposes the St. Croix terrane of continental affinity and, to the east, the Ellsworth terrane of sharply contrasting oceanic affinity (e.g., ε_{Nd} [500 Ma] +5.6 to +8.6; Schulz *et al.* 2008) that contains abundant marine volcanic rock and rare upper-mantle peridotite (Fig. 2). The inlier is juxtaposed via the Sennebec Pond Fault against strata of the Fredericton Trough on the northwest; it underlies by angular unconformity Silurian strata of the Coastal Volcanic Belt on the southeast. The narrow Islesboro block (Stewart *et al.* 1995; Stewart 1998), bounded by the Turtle Head and Penobscot Bay faults, occupies a central position within the inlier (Fig. 2). This block hosts the oldest known Precambrian basement in Maine plus distinctive carbonate units, and as well shares several lithologic and structural features with both the St. Croix and Ellsworth terranes (Berry and Osberg 1989; Stewart 1998).

Previous work

Williams (1978) originally included the St. Croix terrane within the Avalon zone based on correlation with strata in the Saint John area of coastal New Brunswick. Subsequently, informed by a field trip in the Penobscot Bay region led by D.B. Stewart in 1999, van Staal *et al.* (2004) assigned the St. Croix terrane to Ganderia (Fig. 1). In particular, the Megunticook Formation was found to closely resemble the Crocker Hill Formation of the Lower Cookson Group in southwestern New Brunswick. This re-interpretation allows for the existence of an Avalon Seaway that accounts for the distribution of arc rocks, high-pressure metamorphism, and seismic reflections related to the latest Silurian–Middle Devonian Acadian collision between Avalonia and Ganderia (van Staal *et al.* 2009). Additionally, van Staal *et al.* (1998, 2012) presented extensive arguments for Ganderia having originated near the Columbian margin of South America and for a Middle to Late Cambrian depar-

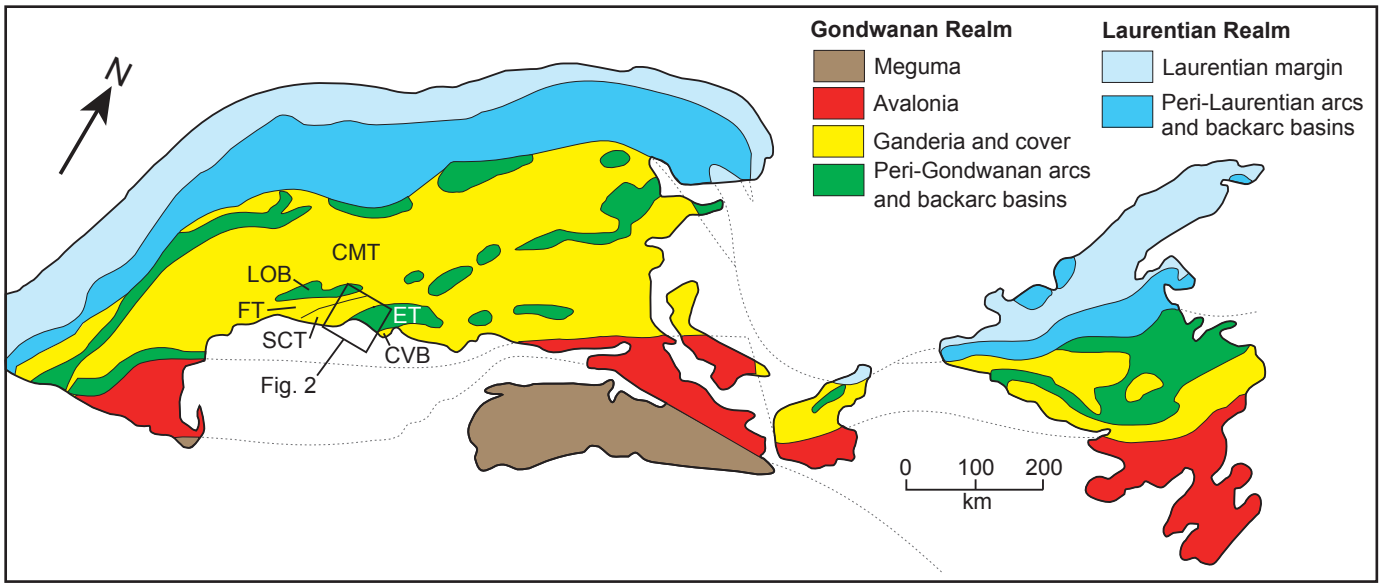

Figure 1. Lithotectonic divisions of the northeastern Appalachian orogen (after Hibbard *et al.* 2006). Abbreviations: CMT = Central Maine Trough; CVB = Coastal Volcanic Belt; ET = Ellsworth Terrane; FT = Fredericton Trough; LOB = Liberty-Orrington Belt; SCT = St. Croix Terrane.

ture from Gondwana. Johnson *et al.* (2012) documented pre-Middle Ordovician (Penobscottian) deformation in the Annidale terrane of New Brunswick; Reusch and van Staal (2012) speculated that a quartz-pebble conglomerate in southwestern Penobscot Bay might record a nearby pre-Middle Ordovician Penobscottian event.

Smith *et al.* (1907) defined the Islesboro Formation (Fig. 2) including carbonate members and the uppermost Coombs Limestone member, and correlated overlying rocks with the Battie Quartzite of the St. Croix terrane. Stewart and Lux (1988) reported Neoproterozoic ages for the amphibolite-facies Seven Hundred Acre Island Formation, exposed beneath the Islesboro Formation along an antiform. Berry and Osberg (1989) described a third sequence, which we refer to here informally as the Turtle Head Cove unit, interpreted to overlie both the Islesboro and Seven Hundred Acre Island formations with profound unconformity; of note, Stewart (1998) did not separate this third sequence from the Islesboro Formation.

Purpose and scope

In general, the identities of peri-Gondwanan elements (e.g., Landing 1996; Fyffe *et al.* 2011; Pothier *et al.* 2015), their provenance (e.g., Nance *et al.* 2008; Barr *et al.* 2012, 2014), and mechanisms of transfer to the Appalachian margin of Laurentia (e.g., Neuman and Max 1989; van Staal *et al.* 2012; Waldron *et al.* 2014b) remain matters of ongoing debate. Fundamental problems of both local and broader significance include (1) provenance of the Islesboro basement; (2) relationship to the rifting of Ganderia from Gondwana and subsequent opening of the Rheic Ocean (Schulz *et al.* 2008; Nance *et al.* 2012; van Staal *et al.* 2012); (3) mechanism of juxtaposition of the St. Croix-Ellsworth terranes; (4) timing of the juxtaposition; and (5) whether, during closure of the Iapetus Ocean (between Ganderia and Laurentia), subduction was initiated internally (van Staal *et al.* 2012) or not (Waldron *et al.* 2014).

The purpose of our reconnaissance investigation of Islesboro is to expand the geochronological database by U–Pb dating of detrital and igneous zircon in samples of metasedimentary and volcaniclastic rock from this critical area. We collected samples from a quartzite that Stewart (1998) showed at the top of the Islesboro Formation (Fig. 3); greywacke from the base of the Turtle Head Cove unit (Fig. 4); and a volcaniclastic rock from the Kedears Hill sulphide prospect (Fig. 4). The geochronological results require a re-evaluation of both local field relationships and, in light of recent detrital zircon studies in West Africa (Abati *et al.* 2010; Bradley *et al.* 2015) and offshore Massachusetts (Kuiper *et al.* 2017), global paleogeography.

GEOLOGIC SETTING

St. Croix terrane

West of the Turtle Head Fault (Fig. 2), the St. Croix terrane (Tucker *et al.* 2001) comprises, in ascending stratigraphic order, the Rockport, Cookson, and Benner Hill groups. The Proterozoic Rockport Group (Berry in press) is capped by the Coombs Limestone and Rockport Quartzite, which are in turn unconformably overlain by conglomerate and sandstone of the Simonton Corners Formation. The latter basal unit of the Cookson Group is correlated across the West Rockport Fault with the Megunticook Formation

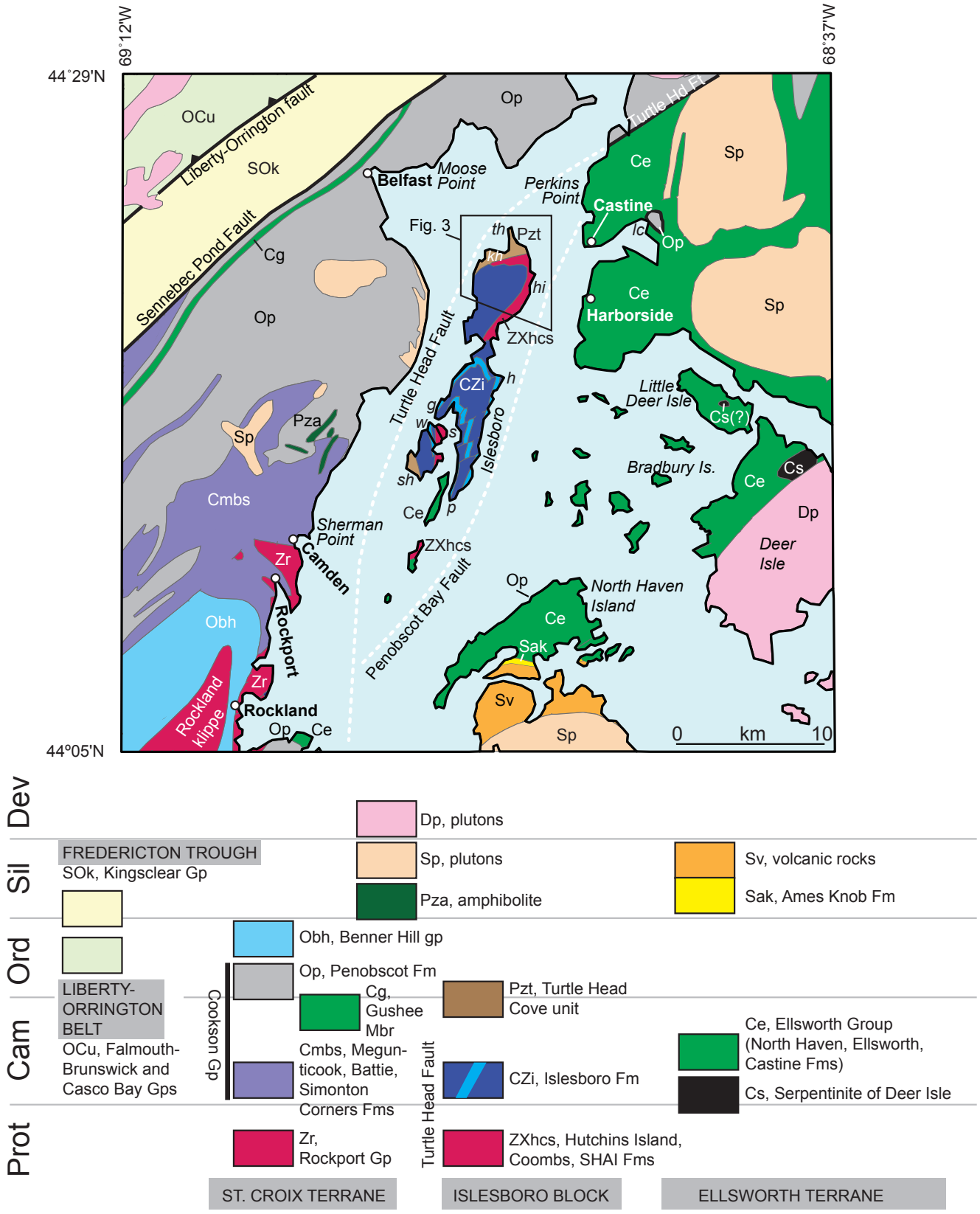

Figure 2. Regional geologic map showing location of Islesboro in Penobscot Bay, Maine, USA (modified from Osberg *et al.* 1985). In the Islesboro Formation (CZi), light blue indicates the distinctive carbonate member(s). Abbreviations: g = Grindel Point; h = Hewes Point; hi = Hutchins Island; kh = Kedears Hill; lc = Lord's Cove; p = Pendleton Point; s = Spruce Island; sh = Seven Hundred Acre Island; th = Turtle Head; w = Warren Island.

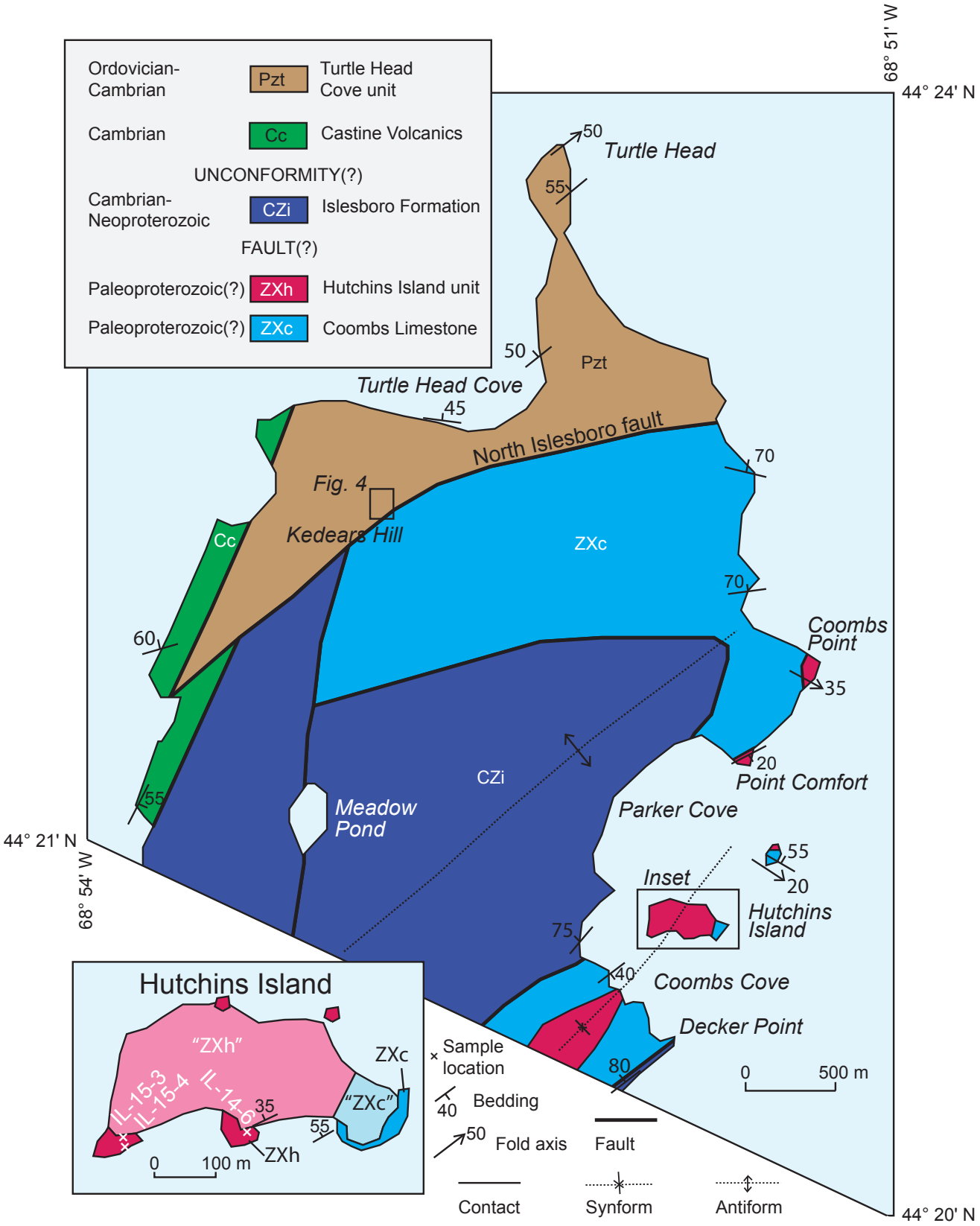

Figure 3. Simplified geologic map of North Islesboro (modified from Stewart 1998). Map unit symbols same as in Figure 2, plus ZXc = Coombs Limestone; ZXh = Hutchins Island Quartzite. On the inset, "ZXc" and "ZXh" are covered areas. Kedears Hill tuff is too thin to be shown on Figure 3 but is shown on Figure 4.

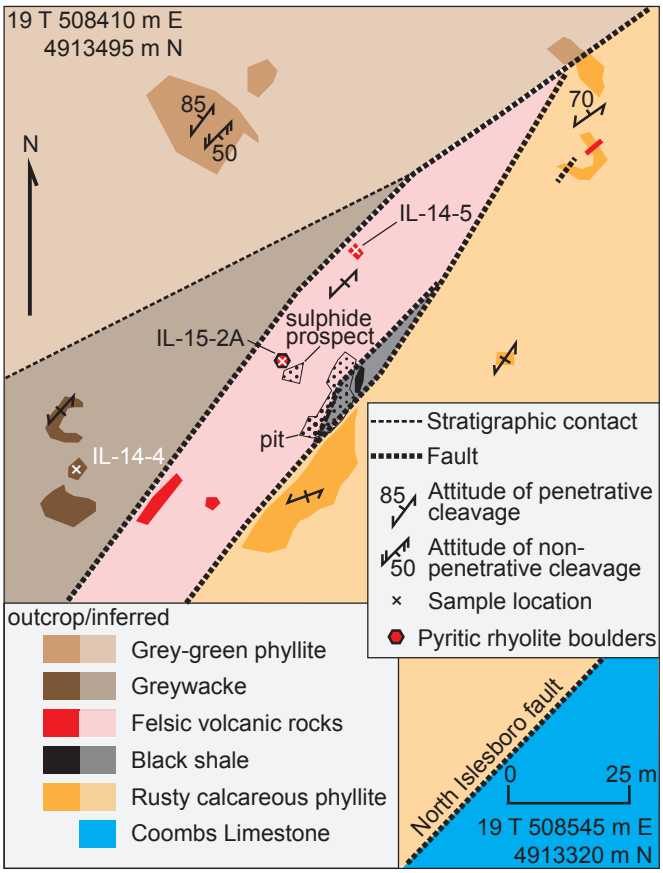

Figure 4. Detailed geologic map of Kedears Hill area showing North Islesboro fault (location after Stewart 1998) and splays. Location of corners is indicated by UTM coordinates.

that is locally underlain conformably by the Battie Quartzite. The Megunticook Formation comprises a sequence of quartzite and quartz-mica schist (Bickel 1971; Berry and Osberg 2000). The structurally overlying Penobscot Formation, also part of the Cookson Group, consists of rusty black schist with rare quartzose sandstone (Bickel 1971). The Penobscot Formation is correlated with the Calais Formation, which near the Maine-New Brunswick border contains Tremadocian graptolites (Fyffe *et al.* 2011). The latest Cambrian Gushee Member of the Penobscot displays a clear island-arc geochemical signature (Burke *et al.* 2016). Highest in the sequence, the Benner Hill Group is notable for containing the only pre-Silurian fossils in the region, which are highly stretched brachiopods of Caradocian (~Sandbian) age (Berry *et al.* 2000).

Ellsworth terrane

The Ellsworth terrane comprises a structurally complex assemblage of low-grade, but highly deformed, chlorite-quartz-feldspar schist, Middle Cambrian marine bimodal volcanic rock (e.g., North Haven Greenstone, Castine Volcanics), rare pelagic sedimentary rock, and rare serpentinized peridotite (Fig. 2). The thickness of this terrane, based on seismic studies, is on the order of several kilometers (Stewart 1998). The presumed steeply dipping Turtle Head Fault juxtaposes the Ellsworth and St. Croix terranes both to the northeast and southwest of Islesboro. However, in several locations (Fig. 2), Ellsworth rocks directly overlie black shale of the Penobscot Formation in an inferred thrust fault relationship. East of Castine, the Penobscot Formation is exposed in the Lord's Cove window (Osberg *et al.* 1985; Reusch 2002a, 2002b). On the northwest shore of North Haven Island, Penobscot Formation black shale is injected into overlying fractured North Haven Greenstone (Reusch *et al.* 2003); east of Rockland, pillow lavas of the North Haven Greenstone are thrust over Penobscot Formation (Osberg *et al.* 1985). The maximum age of this thrusting event is Early Ordovician. The Turtle Head and related steep faults, according to Stewart *et al.* (2001), show dextral offsets of Late Silurian isograds that pre-date Late Devonian plutons. On North Islesboro, Stewart (1998) showed a narrow belt of Middle Cambrian Castine Volcanics, one of the marine volcanic units of the Ellsworth terrane, bounded by splays of the Turtle Head Fault (Fig. 2).

Islesboro block

Strata within the Islesboro fault block (Stewart 1998) include, in ascending order, the amphibolite-facies Seven Hundred Acre Island Formation of Proterozoic age (Stewart *et al.* 2001), the greenschist-facies Islesboro Formation of undefined age (Smith *et al.* 1907), and the third sequence of Berry and Osberg (1989) here referred to as the Turtle Head Cove unit.

The Seven Hundred Acre Island Formation (Brookins 1976; Stewart 1998) comprises a platform sequence of marble (Fig. 5E), quartzite, quartz-rich schist, and sparse amphibolite. It was metamorphosed to amphibolite facies during the Neoproterozoic based on $^{40}Ar/^{39}Ar$ ages of ca. 670 to 650 Ma for hornblende from amphibolite, and on a U–Pb age of 646.7 ± 2.7 Ma for zircon from a cross-cutting granitic pegmatite (Stewart *et al.* 2001).

The Islesboro Formation, which surrounds fault-bounded inliers of the Seven Hundred Acre Island Formation (Stewart 1998), consists of heterogeneous siliciclastic rock (Fig. 5D) and lesser carbonate rock. Distinctive brown-weathering carbonate members (Figs. 2 and 5A), shown separately on previous maps, constrain the internal structure of this unit.

The Turtle Head Cove unit consists of low-grade sedimentary rock present on the west side of Seven Hundred Acre Island and northwest side of North Islesboro. On Seven Hundred Acre Island, a basal conglomerate and sandstone grade upward into predominant phyllite and lesser sandstone (Fig. 5B and 5C). This unit was interpreted by Berry and Osberg to overlie the Islesboro and Seven Hundred Acre Island formations with angular unconformity.

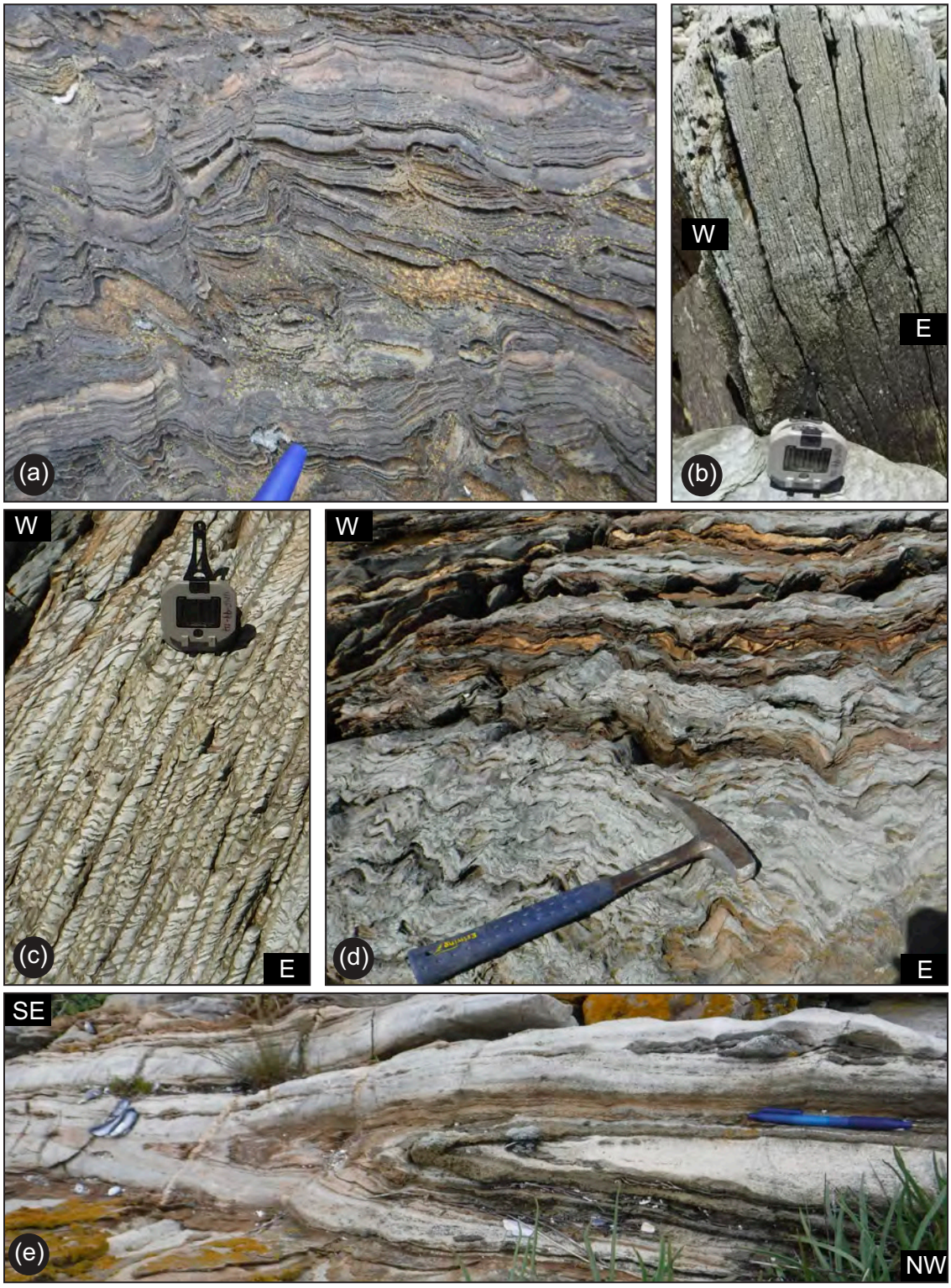

Figure 5. Outcrop photographs showing wide range of structural features in Islesboro Formation of Stewart (1998). (a) = thinly laminated, brown-weathering limestone member of Islesboro Formation, headland 1.6 km south of Hewes Point. (b) = steeply west-dipping, upright sandstone bed and steeply east-dipping cleavage, south point of Seven Hundred Acre Island. (c) = phyllite showing two cleavages, early one dips moderately northeast, second cleavage dips steeply west, location several hundred meters west of B. (d) = crenulated, interbedded siliciclastic and tan-weathering carbonate strata, Grindel Point. (e) = isoclinally folded marble on ledge ca. 500 m northeast of Hutchins Island. In (b) and (c), Brunton compass points north, pen for scale in (a) and (e). Abbreviations: E = east; NW = northwest; SE = southeast; W = west.

FIELD RELATIONSHIPS AND PETROGRAPHY

On North Islesboro (Fig. 3), the first published geologic map (Smith *et al.* 1907) shows two gently plunging synclines cored by Battie Quartzite, one in the west extending north towards Kedears Hill and the other located in the Parker Cove-Hutchins Island-Coombs Cove area. The map by Osberg *et al.* (1985) delineates the intervening, northeast-plunging anticline. In addition, Osberg *et al.* (1985) added a thrust fault that places the Islesboro Formation over presumably younger rocks to the north on Turtle Head. Stewart *et al.* (2001) retained the central anticline and eastern syncline, returned the rocks on Turtle Head to the Islesboro Formation, retained a fault, here named the North Islesboro Fault, in the same location as the thrust of Osberg *et al.* (1985), and added several other faults. Figure 3 attempts to reconcile our reconnaissance field observations with the geology shown on these previously published maps.

Proterozoic basement

In the eastern part of North Islesboro (Fig. 3), the Coombs Limestone (ZXc) and overlying Hutchins Island Quartzite (ZXh) constitute a newly recognized area of high-grade Proterozoic basement. Our field observations generally support the quartzite-cored syncline shown on previous geologic maps (Smith *et al.* 1907; Osberg *et al.* 1985; Stewart 1998) that extends southward from east of Coombs Point through Hutchins Island to the central small headland on the south shore of Coombs Cove. Specifically, the quartzite unit overlies the carbonate unit at Point Comfort, in Coombs Cove on the western limb of the syncline close to its axial trace, at the eastern headland of Hutchins Island on the eastern limb, and at the north end of the small ledge to the northeast (Fig. 3). Not shown on previous maps are small lenses of amphibolite present in the southwestern part of Hutchins Island (sample locations IL-15-3 and -4).

The type locality of the Coombs Limestone (Smith *et al.* 1907) is Coombs Point. This carbonate unit crops out between Coombs Point and Point Comfort, along the southern shore of Coombs Cove, the eastern headland of Hutchins Island, and on a small ledge to the northeast. It consists of thin- to thick-bedded, grey calcitic and buff to brown-weathering dolomitic marble (Fig. 5E), minor quartzite, both white and pink, and sparse calc-silicate rock.

The Hutchins Island Quartzite crops out at Coombs Point, Point Comfort, Hutchins Island, and on the hill south of Coombs Cove. An occurrence of cross beds at Point Comfort (H.N. Berry IV, written communication, 1999) suggests that the quartzite conformably overlies the Coombs Limestone. On the south shore of Hutchins Island, thick-bedded white quartzite was sampled for detrital zircon (Fig. 3; Sample IL-14-6; 44°21.042'N, 68°52.244'W). Thin sections of the quartzite reveal locally abundant chlorite and feldspar, and a strong penetrative fabric (Fig. 6A). Nearby outcrops and those in the southwest part of the island are quartzo-feldspathic gneiss and schist, and rare, discontinuous, thin (<1 m) lenses of amphibolite. The amphibolite is medium grained, contains abundant chloritized hornblende and sericitized plagioclase, and displays a strong fabric (Fig. 6D).

At least two generations of folds are present. A presumably older generation consists of open to isoclinal, variably northwest- to southeast-plunging folds with a steeply dipping axial-planar foliation. These folds are nearly perpendicular to the contacts with adjacent Islesboro Formation, suggesting a structural discordance. Other observed structures include common boudinaged beds of quartzite and dolomitic marble, southwest-plunging folds, and late faults.

Several observations suggest that the contact relationship of the Proterozoic basement with the adjacent Islesboro Formation (CZi) may be a fault. On the western shore of Coombs Cove, in rocks mapped as Islesboro Formation, graded beds indicate tops to the northwest, opposite the inferred east-younging direction of the western limb of the syncline. On the east shore of Decker Point, rocks mapped as Islesboro Formation (Stewart 1998) are lithologically distinct compared to those on the western shore of Coombs Cove. Finally, the presence of amphibolite on Hutchins Island indicates a metamorphic discordance across the contact, in addition to the structural discordance described above. We are unable to determine whether the Precambrian basement inliers are horsts or klippes.

Based on lithologies and field relationships, the Proterozoic basement of Coombs Limestone and Hutchins Island Quartzite on North Islesboro correlates with the Seven Hundred Acre Island Formation of Stewart (1998) exposed in nearby inliers. In addition, these rocks may also be equivalent to the upper part of the Rockport Group of Osberg *et al.* (1985) exposed on the western shore of Penobscot Bay.

Islesboro Formation

Smith *et al.* (1907) did not designate a specific type locality for the Islesboro Formation. However, the shoreline outcrops of interbedded siliciclastic and minor carbonate rock at Grindel Point (Figs. 2 and 5D) have been taken as representative (e.g., Berry 2007). The presence there of interstratified and discordant greenstone distinguishes the Islesboro Formation from the amphibolite-bearing Seven Hundred Acre Island Formation, and also from the weakly metamorphosed and less-deformed (Fig. 5B) Turtle Head Cove unit in which greenstone is evidently absent. At Grindel Point, thin-bedded siliciclastic strata and distinctive orange-weathering carbonate are interbedded (Fig. 5D). Rare sandstone lenses several millimeters thick and several centimeters long, oriented obliquely to bedding, are possible worm burrows (e.g., Berry 2007, photo 10, near center). Beds dip generally north, display very tight horizontal folds (Berry 2007), and are strongly

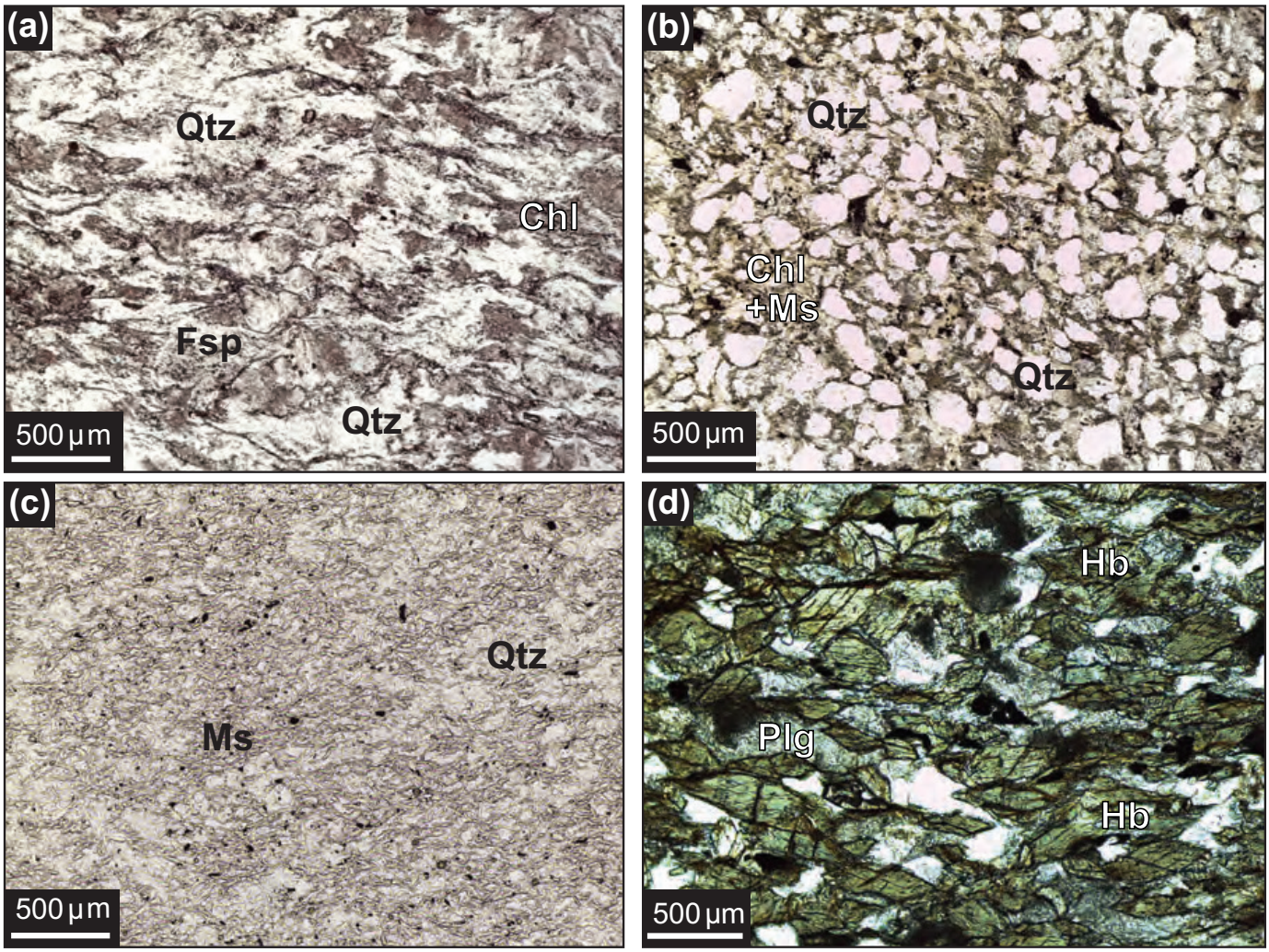

Figure 6. Photomicrographs in plane-polarized transmitted light. (a) = chlorite-rich portion of quartzite, to show strong fabric, from Hutchins Island, sample IL-14-6. (b) = greywacke from near Kedears Hill, sample IL-14-4. (c) = felsic volcaniclastic tuff from near Kedears Hill, sample IL-14-5. (d) = amphibolite from Hutchins Island, sample IL-15-4. List of mineral abbreviations: Chl = chlorite; Fsp = feldspar; Hb = hornblende; Ms = muscovite; Plg = plagioclase; Qtz = quartz.

crenulated on moderately north-plunging folds. Conformable greenstone beds, likely mafic tuff, occur in places. Discordant greenstone dykes up to 5 m thick cut the foliation. The thinly bedded, crenulated aspect of these outcrops and presence of abundant greenstone are features of the Ellsworth Schist (Reusch 2003), a potential correlative.

The Islesboro Formation is lithologically heterogeneous. On the western shore of Coombs Cove, to the southwest of Hutchins Island, distinctively thin-bedded, fine-grained siliciclastic strata display graded beds; similar distinctively thin-bedded strata, including packages of "ribbon" carbonate, are present on the west shore of Pendleton Point (Fig. 2). To the east of Coombs Cove, in cliffs along the eastern shore of Decker Point (Fig. 3), steeply dipping, massive, light-weathering strata (feldspathic slate of Stewart 1998) strike south-southeast; similar massive, light-weathering rocks at Hewes Point (Fig. 2), a few kilometers to the southeast, display two cleavages but extremely sparse bedding. Decker Point itself is held up by a resistant siliceous rock of uncertain protolith and relationship to adjacent units.

Castine Volcanics

A narrow belt of Castine Volcanics crops out along the western shore of North Islesboro (Stewart 1998). At the headland west of Meadow Pond (Fig. 3), this unit, although shown as quartzite and conglomerate by Stewart *et al.* (2001), consists of thick-bedded tuffaceous sedimentary rock, tuff, and lithic tuff. The outcrops are rusty due to minor disseminated pyrite. These strata display only a weak penetrative deformation. Possible correlatives include the felsic volcanic and volcaniclastic rocks at the Kedears Hill sulphide prospect (in which case this unit was incorrectly correlated with the Castine Volcanics), and also the undated volcaniclastic rocks at Perkins Point (Fig. 2) north of Castine (Smith *et al.* 1907).

Rocks northwest of the North Islesboro fault

Rocks northwest of the North Islesboro fault (Fig. 3) display a low grade of metamorphism relative to those southeast of the fault. Whereas locally two cleavages are present in these northwestern strata (e.g., Gregg 1979; Fig. 5C), in general the structure is characterized by a relatively open fold style and steeply dipping slaty cleavage of presumed pressure-solution origin (Gregg 1986).

The Kedears Hill area contains important outcrops used for geochronology in this study. Our mapping (Fig. 4) suggests that several unrelated units are juxtaposed along splays of the North Islesboro fault. In the excavated area on the northeast side of Kedears Hill, the four units we recognize are therefore described in geographic order.

The first unit, occurring in the most southeastern exposures, is orange-weathering calcareous phyllite that carries a well-developed, steeply dipping foliation and in places is highly sheared and cut by irregular quartz ± carbonate veins. A recent excavation exposes a thin tuff bed and southeast-dipping fault surface (Fig. 4).

Northwest of the calcareous phyllite and a thin strip of pyritic black shale is the second unit that comprises poorly exposed felsic volcanic rocks within the excavated area, including a previously undescribed sulphide prospect (Fig. 4). Massive white albite-rich rhyolite occurs along a ridge located approximately 40 m to the southwest of the prospect, in nearby sub-crop, and as several 2- to 3-m, iron-stained boulders that contain abundant, 1–3 cm clots of coarse pyrite. A small roadbed 25 m to the north of the excavated area exposes a rusty weathering, strongly foliated felsic rock that was sampled for zircon (IL-14-5; 44°22.454'N, 68°53.613'W). The wide range of ages obtained for this rock (see below) supports an origin as a volcaniclastic sediment, referred to here for simplicity as a tuff. Thin section study shows predominant quartz with lesser muscovite (Fig. 6C); textures, including the presence of doubly terminated euhedral zircon grains without evidence of sedimentary abrasion, suggest a significant ash component.

Approximately 40 to 50 m to the southwest of the prospect is the third unit in the excavated area, consisting of several outcrops of massive, quartz-rich greywacke (sample IL-14-4; 44°22.429'N, 68°53.652'W). We consider these strata to be the basal part of the Turtle Head Cove unit based on more complete exposures of a nearly identical sequence on the southwestern shore of Seven Hundred Acre Island. Minor pyrite occurs in disseminations and locally in thin (1–3 mm) laminae. In thin section (Fig. 6B), the sand grains are angular and poorly size-sorted, surrounded by a volumetrically minor matrix of chlorite and muscovite.

The fourth unit, considered to conformably overlie the greywacke, is extensively exposed in the larger, non-metallic quarry to the northwest (Fig. 4) and on both shores of Turtle Head Cove ca. 1 km to the northeast (Fig. 3; Gregg 1979). This unit consists of pervasively Mn-stained, grey-green mudstone and shale locally containing sparse, white, centimeter-sized possible lapilli and elongate, small (1–2 cm) lenses of quartz ± carbonate. Interbedded greywacke is volumetrically minor. These rocks are at most weakly metamorphosed and display a prominent, steeply dipping, northeast-striking cleavage; a second cleavage is much less prominent, more widely spaced, and dips moderately southeast.

The east shore of Turtle Head contains nearly continuous outcrops of moderately northwest-dipping, interbedded sandstone and grey to black shale. Many of these outcrops have a white-weathering rind, thus suggesting a tuffaceous component. Carbonate-rich sandstone is locally present, including several beds that contain angular clasts of pyrite up to ~1 cm in diameter. The northernmost headland—Turtle Head—displays open folds that plunge gently northeast around a near-vertical cleavage (Fig. 3).

ANALYTICAL METHODS

Samples for whole-rock geochemistry were pulverized in an alumina-ceramic mortar and analyzed at Activation Laboratories Ltd.in Ancaster, Ontario. Analyses were made on duplicate samples and on 8 to 12 standards. Precision and accuracy for concentrations ≥100 × the minimum detection limit (MDL) generally were better than ±5% relative, and in many cases, such as for major elements, were better than ±1% relative. For concentrations approximately 10× the MDL, precision and accuracy were about ±10 to 20% relative, depending on the method used. Major, most trace, and all rare earth elements (REE) were determined by inductively coupled plasma-mass spectrometry (ICP-MS) on rock powders fused with lithium metaborate/tetraborate in order to insure complete acid dissolution of resistate minerals prior to analysis. Instrumental neutron activation analysis (INAA) was used for Au, As, Sb, Se, Sc, Cr, Br, and Ir because of lower detection limits. Total carbon and sulphur were determined by a LECO infrared analyzer, and CO_2 by coulometry after digestion with 2N perchloric acid. Details of the various analytical methods are available online at www.actlabs.com.

Analyses of zircon grains were conducted using a Nu Instruments AttoM ES™ high-resolution, sector-field, ICP-MS coupled to a Photon Machines Excite™ 193 nm ArF excimer laser (LA-ICP-MS) at the USGS Southwest Isotope Research Laboratory in Denver, Colorado. Zircon was ablated using a ~25 um spot size, 150 total bursts per analysis with a repetition rate of 5 Hz, laser energy of ~3 mJ, and energy density of 4.11 J/cm^2. Pit depths are typically ~20 μm or less. The rate of He carrier gas flow from the HelEx cell of the laser was ~0.6 L/min. Make-up Ar gas (~0.2 L/min) was added to the sample stream prior to its introduction into the plasma. Nitrogen with a flow rate of 5.5 mL/min was added to the sample stream to allow for significant reduction in ThO+/Th+ (<0.5%) and improved the ionization of refractory Th (Hu *et al.* 2008). With the magnet set at a constant mass, the flat tops of the isotope peaks of ^{202}Hg,

^{204}(Hg + Pb), ^{206}Pb, ^{207}Pb, ^{208}Pb, ^{232}Th, ^{235}U, and ^{238}U were measured by rapidly deflecting the ion beam with a 30 s on-peak background measured prior to each 30-s analysis. Raw data were reduced off-line using Iolite™ 2.5 (Paton *et al.* 2011) to subtract on-peak background signals, correct for U–Pb downhole fractionation, and normalize the instrumental mass bias using external mineral reference materials, the ages of which were determined previously by ID-TIMS. Ages were corrected by standard sample bracketing with the primary zircon reference material Temora2 (ca. 417 Ma; Black *et al.* 2004) and secondary reference material Plešovice (ca. 337 Ma; Sláma *et al.* 2008), and an in-house standard WRP-63-08 (ca. 1707 Ma; W. Premo, personal communication, 2016). For igneous zircon, rims and cores were analyzed if revealed in SEM-CL and large enough for analysis. Reduced data were compiled using Isoplot 4.15 (Ludwig 2012). ^{206}Pb/^{238}U ages are reported for igneous zircon samples less than ~1300 Ma, whereas ^{207}Pb/^{206}Pb ages are used for older ages (Appendix A) following the recommendations of Gehrels (2011). Analyses that are more than 15% discordant (^{206}Pb/^{238}U age relative to ^{207}Pb/^{206}Pb age), or more negative than -10% discordant, are excluded from the probability density plots.

RESULTS

Whole-rock geochemistry

Whole-rock analyses of metasedimentary and meta-igneous rocks are presented in Table 1. On the south side of Hutchins Island, quartzite sample IL-14-6 is distinguished by high SiO_2 (80.92 wt %). Nearby amphibolite samples IL-15-3 and IL-15-4, within the same sequence, contain relatively high $Fe_2O_3^T$ (13.90 and 13.78 wt %, respectively) and TiO_2 (2.05 and 1.78 wt %, respectively). Plagioclase-chlorite schist sample IL-15-5 from Grindel Point is broadly similar to the amphibolite samples in terms of major-element contents, but differs in some trace elements such as having much higher Cr (463 ppm vs ≤93 ppm) and Ni (130 ppm vs ≤30 ppm). Greywacke sample IL-14-4, from the north side of Kedears Hill, has relatively high contents of Al_2O_3 (11.38 wt %) and TiO_2 (1.07 wt %). Nearby sample IL-14-5 of felsic tuff contains appreciable K_2O (3.57 wt %) but sparse Na_2O (0.15 wt %), whereas pyritic rhyolite IL-15-2A, from the same area, has low K_2O (0.05 wt %) but high Na_2O (10.06 wt %).

Figure 7 shows geochemical plots for the mafic meta-igneous rocks based on whole-rock compositions. Data for the amphibolite samples from Hutchins Island and Seven Hundred Acre Island, and the plagioclase-chlorite schist from Grindel Point, all plot within the basalt field (Fig. 7A) and the field for Enriched-Mid-Ocean Ridge Basalt (E-MORB) (Fig. 7B). REE data show abundances of ~10× to ~100× chondrite and slightly elevated light rare earth elements (LREE), with amphibolite sample IL-15-4 from Hutchins Island having a positive Eu anomaly (Eu/Eu* = 1.52; Table 1); one amphibolite from Seven Hundred Acre Island is distinct in displaying a higher abundance of LREE and a higher La/Yb ratio (Fig. 7C). Excluding scatter shown by mobile elements (e.g., U, K, and Sr), most samples of the mafic meta-igneous rocks display broadly similar patterns based on Primitive Mantle normalization, including a lack of negative Ta anomalies and large positive Pb anomalies (Fig. 7D).

Detrital zircon geochronology

Sample IL-14-6 of quartzite, collected from the south shore of Hutchins Island, yielded 120 concordant U–Pb zircon ages (Fig. 8). Most are centered on ca. 2008 Ma, with minor peaks at ca. 2070, 1965, and 1895 Ma. No ages are younger than ca. 1800 Ma; five fall in the range of ca. 2300 to 2100 Ma. A gap is present between ca. 2400 and 2300 Ma. Nineteen ages are fairly evenly distributed between ca. 2750 and 2400 Ma.

Sample IL-14-4, a greywacke collected from near Kedears Hill, yielded 109 concordant U–Pb zircon ages (Fig. 8). A strong late Neoproterozoic maximum at ca. 624 Ma is flanked by lesser peaks at ca. 678, 577, and 515 Ma. The weighted average age of the three youngest grains is 515 ± 5 Ma and defines the maximum depositional age. Over half of the ages are Mesoproterozoic and Paleoproterozoic (ca. 2000–1000 Ma), with a peak at ca. 1204 Ma and 26 ages between ca. 2100 Ma and 1800 Ma. A gap is present between ca. 2550 Ma and 2100 Ma. The seven oldest ages, all Archean, are in the range of ca. 2750 Ma to 2550 Ma.

Sample IL-14-5 was collected from a felsic volcaniclastic rock. The sample had a relatively low yield of zircon (45 grains). Cathodoluminescence imaging of the zircon grains revealed several core-rim relationships as well as various morphologies including euhedral to anhedral; several of the zircon grains are fragments (Fig. 9). Because of the complex internal textural relationships, several grains were analyzed multiple times to try to date both cores and rims. Inherited cores (and several grains without core-rim relationships) are older than rims. The youngest coherent six grains analyzed define a proposed igneous age of 371.8 ± 5.7 Ma (Fig. 9B). In addition to these youngest Late Devonian ages, described below, the sample includes grains as old as Archean (Fig. 8). Within this older set of ages, all but six are late Paleoproterozoic to early Neoproterozoic (ca. 1900–800 Ma); two are latest Neoproterozoic. The oldest ages include one at ca. 2100 Ma (Paleoproterozoic), one at ca. 2600 Ma (Neoarchean), and two at ca. 3000 Ma (Mesoarchean).

DISCUSSION

Our data provide important new constraints on several fundamental problems of local as well as broader significance and establish a framework for future investigations in the region. Below, we discuss field, petrographic, geochemical, and geochronological data in the context of new stratigraphy.

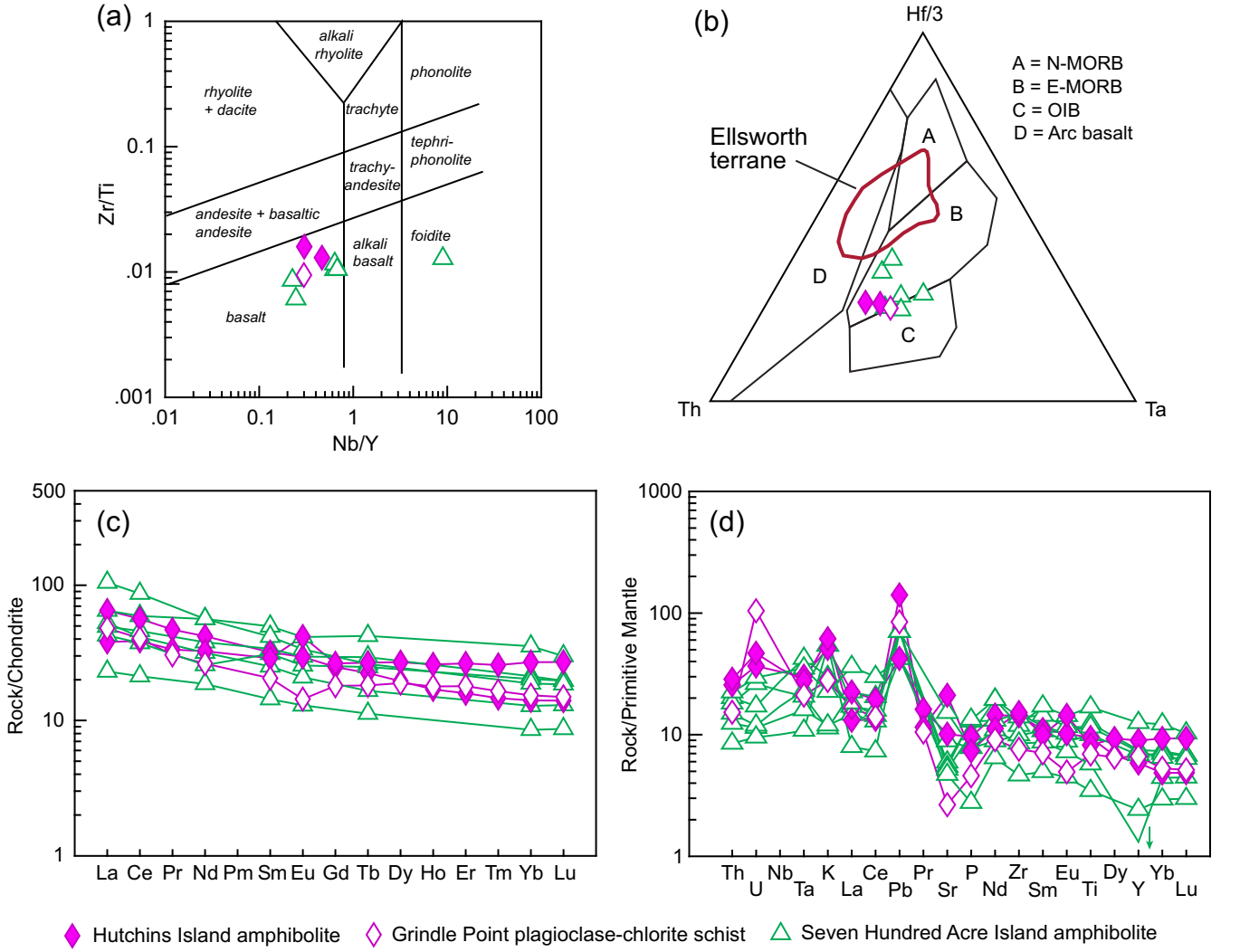

Figure 7. Plots of whole-rock geochemical data for amphibolite and mafic schist. (a) = Zr/Ti vs Nb/Y plot (Pearce 1996). (b) = Th-Hf/3-Ta plot (Wood 1980). (c) = Chondrite-normalized REE plot; (d) = Primitive Mantle-normalized spider plot; note that one amphibolite from Seven Hundred Acre Island (arrow) has a normalized Y value of 0.5 (below plot); Nb data are not shown due to analytical problems. Data for Seven Hundred Acre Island samples are from Stewart *et al.* (2001). Chondrite and primitive mantle values are from Sun and McDonough (1989). Red line in (b) encloses Ellsworth data from Schulz *et al.* (2008). N-MORB = normal mid-ocean ridge basalt, E-MORB = enriched mid-ocean ridge basalt, OIB = ocean island basalt.

Proterozoic basement

Geochemical constraints

Stewart *et al.* (2001) proposed a platform setting for the Seven Hundred Acre Island Formation, and our geochemical data are consistent with a low-latitude, passive-margin setting for the Coombs Limestone and Hutchins Island Quartzite (cf. McLennan *et al.* 1993). The quartzite has a relatively high Th/Sc ratio of 0.78, which records a predominantly felsic source. A high Zr/Sc ratio of 37.5 for the quartzite implies abundant zircon and/or significant zircon recycling.

Depositional age and provenance

The distinctive age spectrum of detrital zircon in the quartzite sample (IL-14-6) is unique in the Appalachian orogen, including Gondwanan and peri-Gondwanan terranes, in lacking grains younger than ca. 1800 Ma, its maximum depositional age. The minimum depositional age, based on correlation with the Seven Hundred Acre Island Formation and the age of metamorphism therein, is ca. 670 Ma (Stewart *et al.* 2001). Of note, the IL-14-6 age spectrum bears a close resemblance to those from strata in Mauritania (West African craton) dated at ca. 1107 Ma but with no zircon younger than ca. 1.8 Ga (Char barcode of Bradley *et al.* 2015). However, we consider a Paleoproterozoic depositional age for our sample more likely, given (1) a low-

Table 1. Whole-rock geochemistry of metasedimentary and metaigneous rocks.

Sample	IL-14-4	IL-14-5	IL-14-6	IL-15-2A	IL-15-3	IL-15-4	IL-15-5
SiO_2 (wt %)	72.41	79.82	80.92	68.02	48.31	46.69	49.11
TiO_2	1.073	0.458	0.350	0.186	2.054	1.783	1.501
Al_2O_3	11.38	10.68	8.12	17.49	15.37	15.64	16.87
$Fe_2O_3^T$	6.66	1.23	2.76	2.91	13.9	13.78	14.81
MnO	< 0.001	0.009	< 0.001	0.004	0.196	0.185	0.083
MgO	1.24	0.70	1.49	0.01	7.06	7.29	8.97
CaO	0.49	0.06	0.65	0.08	6.19	7.59	0.30
Na_2O	0.08	0.15	2.03	10.06	2.55	1.02	2.01
K_2O	2.97	3.57	1.58	0.05	1.54	1.85	0.84
P_2O_5	0.38	< 0.01	0.14	< 0.01	0.21	0.16	0.10
LOI	2.46	2.07	1.49	2.12	2.71	3.45	5.95
Total	99.14	98.75	99.51	100.9	100.1	99.44	100.6
Total C	0.02	0.01	0.03	< 0.01	0.02	0.01	0.04
CO_2	0.05	0.02	0.08	0.03	0.03	0.05	0.10
Total S	< 0.01	< 0.01	0.01	2.09	0.17	0.11	0.08
Sc (ppm)	16.0	9.5	5.8	0.7	27.8	31.3	33.8
Be	3	2	1	< 1	2	3	2
V	114	68	39	7	283	284	238
Cr	93	69	42	< 5	33	62	463
Hf	4.9	1.6	4.7	1.8	3.6	3.9	2.1
Ta	0.80	0.60	0.45	0.58	1.23	1.13	0.86
Th	8.92	3.99	4.68	2.07	2.18	2.43	1.30
U	2.16	0.87	1.01	0.75	0.77	0.98	2.19
Co	9	1	4	31	35	29	43
Ni	< 20	< 20	< 20	30	< 20	< 20	130
Cu	< 10	< 10	< 10	20	< 10	20	< 10
Zn	40	< 30	40	< 30	110	110	160
Ga	18	15	9	17	17	22	20
Ge	1.8	1.6	< 0.5	1.4	1.6	2.7	1.7
Y	68.5	5.9	14.2	4.5	26.6	40.8	30.1
Zr	219	65	225	75	160	170	85
Nb	7.3	4.6	3.9	4.1	12.4	12.3	9.0
Mo	< 2	< 2	< 2	2	< 2	< 2	< 2
Ag	0.6	< 0.5	0.6	0.5	< 0.5	< 0.5	< 0.5
Tl	0.52	0.65	0.31	< 0.05	0.14	0.25	< 0.05
Pb	6	< 5	< 5	7	< 5	10	6
Bi	0.2	< 0.1	< 0.1	0.2	< 0.1	0.2	< 0.1
In	0.1	< 0.1	< 0.1	< 0.1	< 0.1	< 0.1	< 0.1
W	1.7	7.1	1	1.9	< 0.5	< 0.5	< 0.5
Sn	2	1	< 1	< 1	< 1	2	1
Sb	0.7	1.1	0.3	1.1	1.5	2.7	1.1
As	15.0	8.2	3.4	9.5	10.3	11.2	2.9
Rb	111	118	58	< 1	50	61	29
Sr	36	7	129	38	213	445	56
Cs	4.8	2.8	0.9	0.1	0.9	1.1	0.6
Ba	379	208	372	16	338	393	225
La	58.90	6.03	21.80	4.60	15.40	9.02	11.40
Ce	163	11.5	43.3	10.2	34.6	23.7	24.8
Pr	16.40	1.30	5.25	1.13	4.46	3.18	2.90
Nd	66.70	4.39	19.20	4.65	19.60	15.20	12.30

Table 1. Continued.

Sample	IL-14-4	IL-14-5	IL-14-6	IL-15-2A	IL-15-3	IL-15-4	IL-15-5
Sm	15.50	0.92	3.57	0.84	4.89	4.42	3.14
Eu	3.670	0.144	0.941	0.168	1.710	2.420	0.834
Gd	15.30	0.71	2.89	0.69	5.10	5.43	3.71
Tb	2.43	0.15	0.41	0.12	0.84	1.00	0.68
Dy	14.20	0.91	2.42	0.70	4.96	6.85	4.80
Ho	2.51	0.20	0.47	0.15	0.96	1.47	1.01
Er	6.81	0.66	1.42	0.48	2.63	4.37	2.97
Tm	0.889	0.115	0.221	0.083	0.373	0.655	0.420
Yb	5.05	0.91	1.40	0.70	2.39	4.59	2.61
Lu	0.680	0.132	0.231	0.115	0.356	0.687	0.379
Ce/Ce*	1.256	1.003	0.980	1.045	0.981	1.045	1.004
Eu/Eu*	0.733	0.548	0.901	0.678	1.053	1.519	0.751

Sample lithologies and locations:

IL-14-4, greywacke, northwest side of Kedears Hill (44°22.429'N, 68°53.652'W)

IL-14-5, felsic tuff, north side of Kedears Hill (44°22.454'N, 68°53.613'W)

IL-14-6, quartzite, south side of Hutchins Island (44°21.045'N, 68°52.227'W)

IL-15-2A, pyritic rhyolite, north side of Kedears Hill (44°22.442'N, 68°53.624'W)

IL-15-3, amphibolite, south side of Hutchins Island (44°21.036'N, 68°52.370'W)

IL-15-4, amphibolite, south side of Hutchins Island (44°21.028'N, 68°52.367'W)

IL-15-5, chlorite-plagioclase schist, Grindle Point (~44°16.935'N, ~68°56.588'W)

Elements not detected and their lower limits of determination (ppm; in parentheses): Au (<2); Se (<3); Br (<0.5); Ir (<5)

$Fe_2O_3^T$, total iron as Fe_2O_3; LOI, Loss on Ignition

Ce and Eu anomalies (Ce/Ce* and Eu/Eu*) are calculated by chondrite normalization using data of Sun and McDonough (1989); Ce/Ce* = 2Ce/(La+Pr); Eu/Eu* = 2Eu/(Sm+Gd).

latitude, passive-margin setting, and (2) a striking resemblance of the barcode to the detrital zircon age spectrum of a lithologically similar, dated Paleoproterozoic sequence in Morocco.

First, Neoproterozoic and Paleoproterozoic passive margins are common but Mesoproterozoic passive margins are not (Bradley 2008). During the Neoproterozoic, Gondwana was located at high paleolatitude (Fyffe *et al.* 2011; van Staal and Barr 2012). A caveat, however, is that Barr *et al.* (2014) considered the Neoproterozoic carbonate-rich Ashburn Formation of the Green Head Group in the Brookville terrane, southern New Brunswick, to have been deposited at mid-latitude on the passive Amazonian margin of the Puncoviscana Ocean.

Second, both the lithologic assemblage and zircon age spectrum of sample IL-14-6 bear a striking resemblance to those of the Paleoproterozoic Taghdout Group (Fig. 10), located in the Anti-Atlas region of Morocco and considered the passive margin to the Archean-Paleoproterozoic West African craton (Abati *et al.* 2010; Ikenne *et al.* 2017). Recently studied metasedimentary rocks from a deep test well on Georges Bank, offshore Massachusetts, USA (Kuiper *et al.* 2017), which also display a strikingly similar age spectrum to IL-14-6 (Fig. 10), are best explained as a fragment of African crust stranded on the North American plate during the break-up of Pangea. Unlike other terranes of the West African craton known in the Appalachians (i.e., Meguma and Suwannee; see Kuiper *et al.* 2017), the Taghdout Group, Georges Bank, and Hutchins Island Quartzite lack detrital zircon younger than ca. 1800 Ma, and hence are likely vestiges of the Paleoproterozoic passive margin of the northern West African craton. If this interpretation is correct, a ca. 1800 Ma depositional age implies that the Hutchins Island Quartzite is the oldest known rock unit in the Appalachians.

We interpret the zircon grains that constitute the dominant ca. 2 Ga population to be sourced from the Eburnian (ca. 2.1–2.0 Ga) and/or Birimian (ca. 2.2–2.1 Ga) orogens located in the West African craton. An alternative source, near the West African craton, is the Hoggar terrane in southern and western Algeria that contains several quartzite ± marble sequences of ca. 2 Ga age (Caby 2003; Bechiri-Benmerzoug *et al.* 2017). The relatively small number of ca. 2750–2450 Ma zircon grains may be from the Liberian orogen (ca. 2.9–2.7 Ma). The lack of zircon grains in the range of ca. 2.4 Ma to 2.3 Ma is also consistent with the absence of rocks of this age in the West African craton (Abati *et al.* 2010). However, the Amazonian craton contains a spectrum of ages that is also broadly similar (Tassinari and Macambira 1999; Abati *et al.* 2010). For example, the ca. 2750 Ma

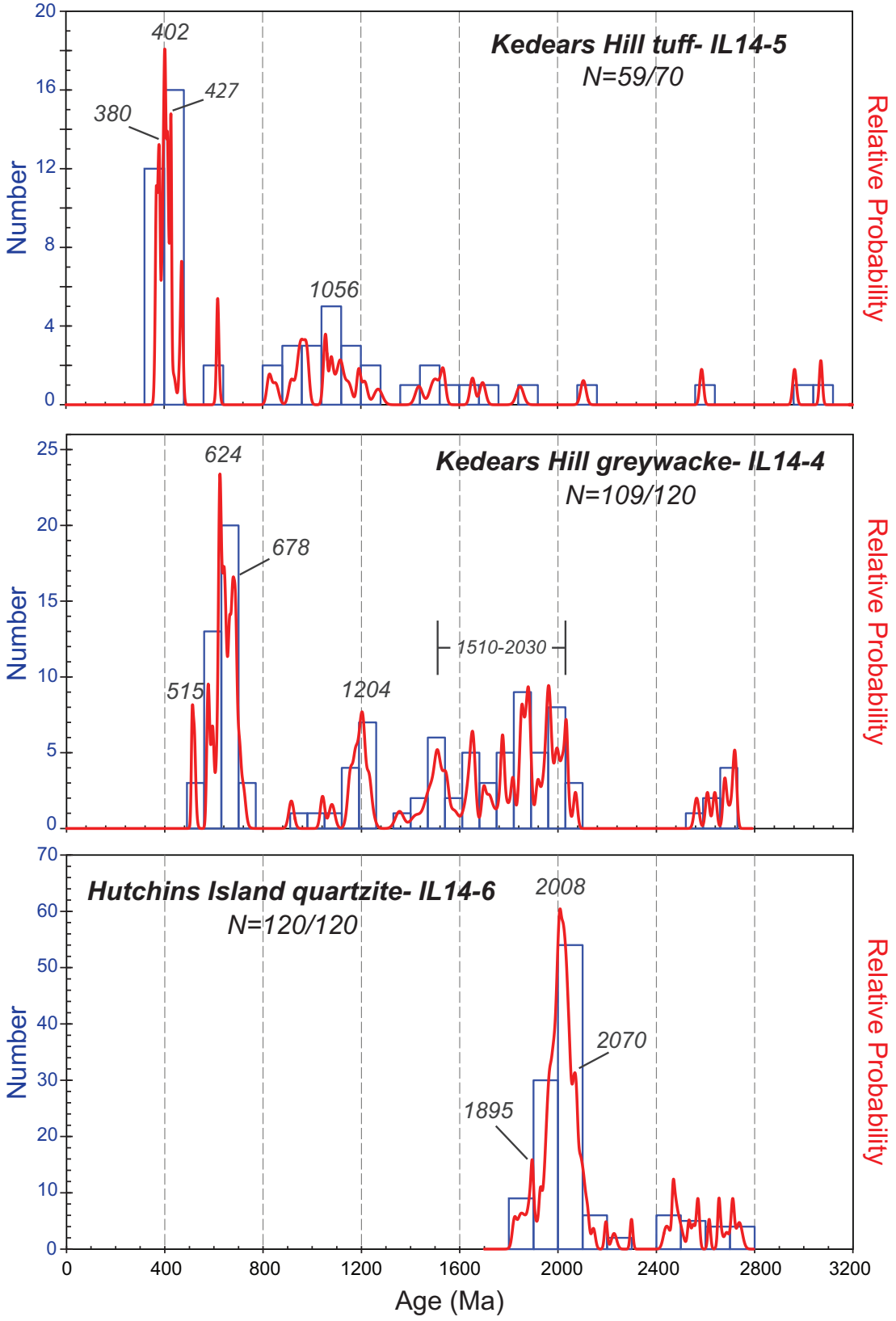

Figure 8. Probability density plots of U–Pb ages of zircons listed in Appendix A. Samples IL4-14 and IL4-16 are wholly detrital zircons. Sample IL14-5 is a tuffaceous volcaniclastic rock; forty-five grains were analyzed, some with multiple spots where rim-core relationships were determined by cathodoluminescence imaging (Fig. 9). N = number of concordant analyses/number of total analyses. Data are from Appendix A.

to 2450 Ma zircons grains in the Hutchins Island Quartzite could be from similar-aged rock in central Amazonia (Restrepo-Pace and Cediel 2010). Detrital zircon data for IL-14-6 alone, therefore, may be insufficient to distinguish between a West African and Amazonian provenance.

Correlation

Prior to this study, the Ashburn Formation of the Green Head Group in the Brookville terrane of southern New Brunswick, based on an abundance of marble, was considered potentially correlative with the Coombs Limestone (Berry and Osberg 1989). However, the Ashburn Formation contains abundant Neoproterozoic zircon in sharp contrast to the absence of zircon younger than ca. 1.8 Ga in sample IL-14-6. Nonetheless, the lithologic resemblance between the Maine and New Brunswick marbles is provocative, and data presented below suggest a close tie between Islesboro and the Grand Manaan and/or Brookville terranes. Within the Grand Manaan terrane, the pre-Ediacaran basement, as on North Islesboro, consists of a carbonate unit (Kent Island Formation) overlain by a quartzite (Thoroughfare Formation) (Fyffe *et al.* 2009).

Whereas geochronological data for the Seven Hundred Acre Island Formation and Rockport Group do not exist, we see no reason not to correlate the Coombs Limestone and Hutchins Island Quartzite with the Seven Hundred Acre Island Formation exposed nearby along strike. Moreover, we agree with Osberg *et al.* (1985) in their correlation of Proterozoic rocks of Islesboro and the Rockport area. In addition, John Waldron has suggested (oral communication, 2015) that exotic marble in a mélange at the base of the Penobscot Formation at Sherman Point (Fig. 2) might be Proterozoic. Subsequent field observations strongly suggest that these exotic blocks of marble, massive orthoquartzite, and a distinctively bedded quartzite are sourced from the Proterozoic sequence that occurs on Islesboro. Below, we discuss the significance of these blocks in relation to Ordovician tectonism.

Amphibolite

Whole-rock geochemical data for relatively immobile trace elements indicate that protoliths of the mafic meta-igneous rocks (amphibolites) from Hutchins Island are basalt (Fig. 7A) having an E-MORB signature (Fig. 7B). Slightly elevated LREE/HREE ratios (Fig. 7C) are consistent with this classification. Importantly, the primitive mantle-normalized plot (Fig. 7D) lacks negative Ta anomalies, which would be evidence of an arc or subduction-related source for the parent basalts (e.g., Pearce *et al.* 2005). Very similar data reported by Stewart *et al.* (2001) for amphibolite from the Seven Hundred Acre Island Formation—including large positive Pb anomalies—suggest a common petrogenetic setting. One sample from Stewart *et al.* (2001) has a high Nb/Y ratio (Fig. 7A), which may be due to analytical error.

Islesboro Formation

Interstratified siliciclastic and carbonate strata and greenstone in the Islesboro Formation are suggestive of a rift setting. Specifically, sample IL-15-5 is a metabasalt with an E-MORB (non-arc) affinity (Figs. 7B and 7D). A mechanism to explain the interstratified siliciclastic and carbonate metasedimentary rocks is by the erosion of horsts of Proterozoic basement composed of mixed siliciclastic and carbonate strata.

The age of the Islesboro Formation is bracketed only between ca. 647 Ma and 420 Ma. However, the present study adds two new constraints. This formation apparently underlies the ca. 515 Ma to 420 Ma Turtle Head Cove unit (Berry and Osberg 1989), discussed below. Newly recognized burrow-like structures, if indeed of this origin, may imply a post-Neoproterozoic age (e.g., Bromley 1996). Although Smith *et al.* (1907) considered the Islesboro Formation to unconformably overlie the Ellsworth Schist of Middle Cambrian age (Schulz *et al.* 2008), the two formations share several features, notably the presence of abundant greenstone and a similar deformational style, thus it is possible they are equivalent or nearly so. The Ellsworth terrane, which includes substantial bimodal tuff, has been argued to record Middle Cambrian separation of Ganderia from Gondwana as the Rheic Ocean began to open (Schulz *et al.* 2008). In this rifting context, inliers of Proterozoic basement and the Deer Isle serpentinite (Fig. 2), viewed as hyperextended basement by Reusch and Rust (2001), may be compared to Grenvillian inliers in the western Appalachians that originated as horsts later decapitated by thrust faults (Karabinos *et al.* 2017). Hence, the Islesboro Formation may record deposition within adjacent grabens, and the Rockland klippe (Fig. 2) of Proterozoic hanging wall on Ordovician (~Sandbian) footwall may represent an example of a thrust fault-decapitated horst.

Van Staal *et al.* (2012) incorporated the Middle Cambrian rift interpretation of the Ellsworth into a larger framework in which Ganderia departed Gondwana from a location on the Amazonian margin near present-day Columbia. These workers provided extensive arguments for an Amazonian provenance, but a cornerstone of the interpretation is the absence of a Mesoproterozoic sediment source in West Africa. The recent discovery of Mesoproterozoic detrital zircon ages in the foreland of the Mauritanide orogen (Bradley *et al.* 2015) permits a West African provenance for Ganderia as well. While it is appropriate here to resurrect West Africa as the potential birthplace of Ganderia and to suggest that a West African provenance might imply a simpler tectonic evolution, it is beyond the scope of this paper to fully evaluate all of the arguments for an Amazonian provenance of Ganderia.

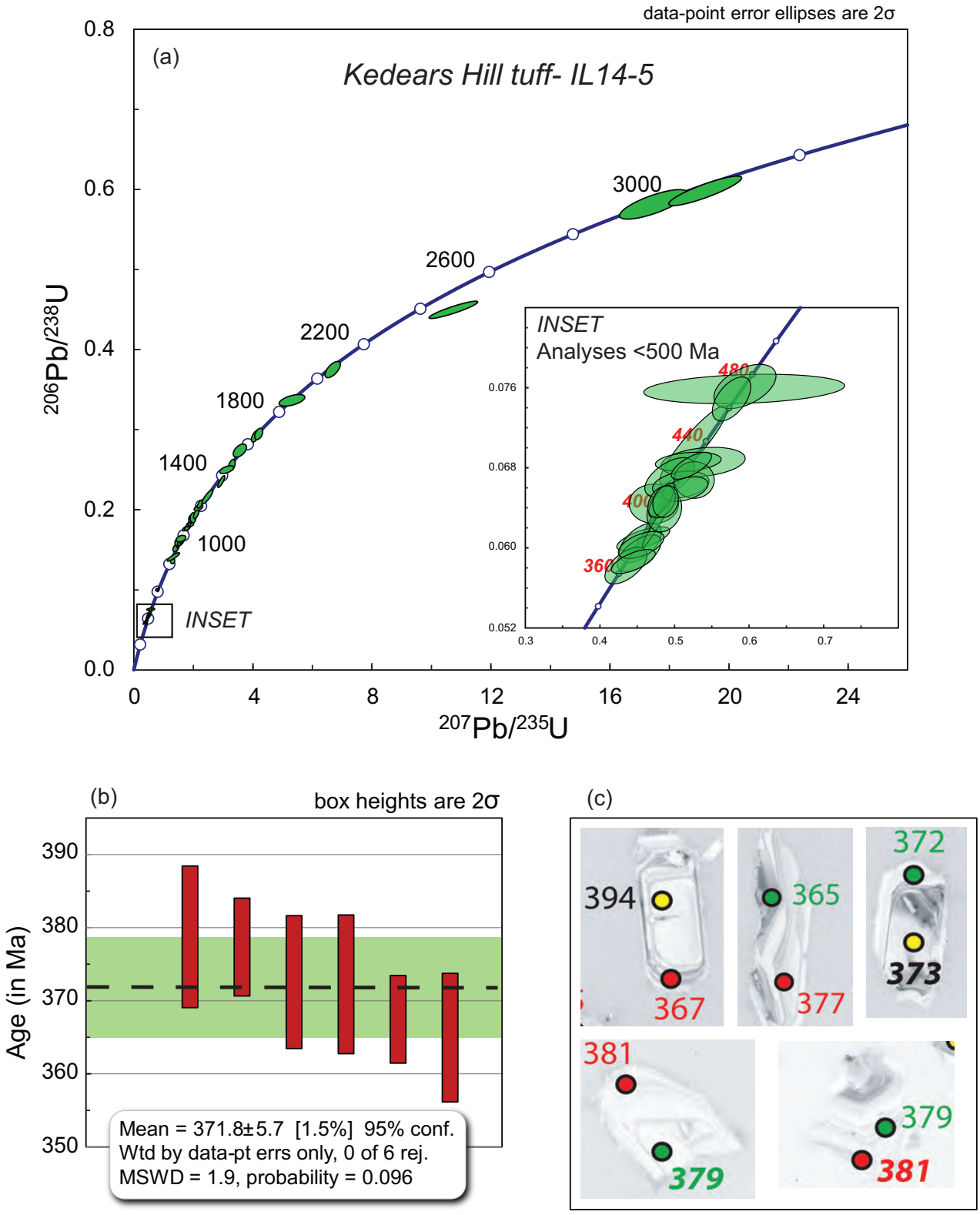

Figure 9. Zircon U–Pb geochronology for Kedears Hill tuff (sample IL14-5). (a) = conventional concordia plot of relatively concordant (<15% discordant) analyses of zircon. Inset shows analyses at less than ca. 500 Ma in detail. (b) = weighted average/mean age of six youngest coherent analyses. (c) = cathodoluminescence images of youngest zircons and locations of analyzed spots and matching ages. Colors of spots/text are associated with different analytical sessions: Red-analytical session dated zircon rims, Yellow/Black-analytical session dated zircon cores, Green-analytical session collected additional age data. Bold italic font indicates ages with greater than 15% discordance. U–Pb data listed in Appendix A.

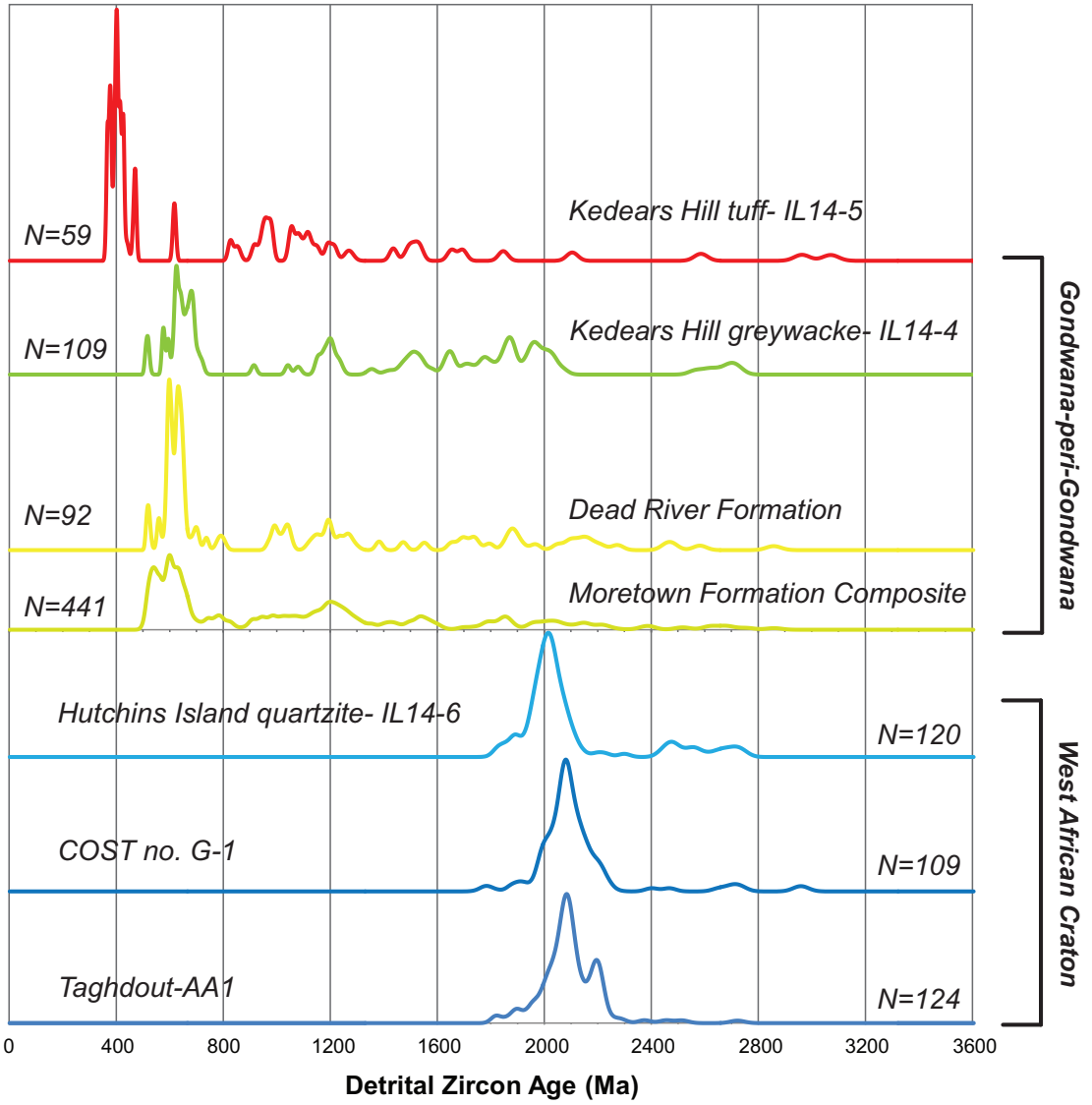

Figure 10. Normalized probability density plots of samples from this study and reference samples. N = number of analyses included in sample plots. Taghdout-AA1 (Abati *et al.* 2010; data filtered using the same discordance cutoff as for IL-14-6); COST no. G-1 (Kuiper *et al.* 2017); Hutchins Island Quartzite-IL14-6 (this study); Moretown Formation composite (Macdonald *et al.* 2014; Karabinos *et al.* 2017); Dead River Formation (C. Gerbi, written communication 2017); Kedears Hill greywacke- IL14-4 (this study); Kedears Hill tuff-IL14-5 (this study).

Turtle Head Cove unit

Greywacke at the base of the Turtle Head Cove unit in the Kedears Hill area displays an immature texture and composition. This rock (Sample IL-14-4) has an intermediate Th/Sc ratio of 0.52, implying a mix of mafic and felsic detritus, and Zr/Sc ratio of 12.9, both of which are lower than in the mature Hutchins Island Quartzite (respectively 0.78 and 37.5). Together, these features argue against a passive-margin setting for the greywacke, the only setting in which maximum depositional age and depositional age are known to differ significantly; we therefore suggest that the sediment age may be close to the maximum depositional age.

Depositional age

The depositional age of the greywacke is constrained by the maximum depositional age of 515 ± 5 Ma (Middle Cambrian) defined by detrital zircon geochronology and the minimum depositional age of Late Silurian based on cross-cutting plutons (Tucker *et al.* 2001). Regional stratigraphic relationships yield a minimum depositional age of late Llandovery, the age of the oldest fossils in the Ames Knob Formation (Brookins *et al.* 1973) that unconform-

ably overlies both the Ellsworth and St. Croix terranes (Gates 1989). Hence, although a Middle–Late Cambrian age seems most plausible for the greywacke (cf. Nelson 2001), we also consider below the intriguing possibility of an Ordovician depositional age.

The detrital zircon signature for this sample, which includes peaks at ca. 624 Ma, 678 Ma, and 577 Ma, is broadly similar to those of other Ganderian metasedimentary units in New England, New Brunswick, and Newfoundland. It is also nearly identical to the Oujeft detrital-zircon barcode, which includes peaks at ca. 624 Ma and 579 Ma, from the younger (late Neoproterozoic) Pan-African foreland basin in Mauritania (Bradley *et al.* 2015). Sample IL-14-4 has the same maximum depositional age as the Moretown Formation of western New England, the westernmost fragment of Ganderia (Fig. 10; Macdonald *et al.* 2014; Karabinos *et al.* 2017). All of the age spectra from these units display large Neoproterozoic–Cambrian peaks between ca. 700 and 500 Ma. In detail, however, the age of the main population(s) across data sets is different. Perhaps the closest match of detrital zircon age population signatures is with that for the Flagg Cove Formation (611 ± 7 Ma with secondary peak at 574 ± 4 Ma) in the Grand Manaan terrane, and for the Martinon Formation (635 ± 4 Ma with secondary peak at 674 ± 8 Ma) in the Brookville terrane (Fyffe *et al.* 2009).

The greywacke displays the well-established detrital zircon signature of Gondwanan provenance—a prominent late Neoproterozoic–Early Cambrian age population (e.g., Barr *et al.* 2003) in combination with the near-absence of ca. 1 Ga ages. The youngest age populations in the greywacke and in the Ellsworth Schist (Fyffe *et al.* 2009) overlap, suggesting a common source in the Middle Cambrian. In contrast to the Ellsworth age spectrum, the greywacke lacks a large age population at ca. 545 Ma. The ca. 624 Ma peak matches the age of rocks in the older arc assemblage in the Brookville terrane (Barr *et al.* 2014). The distribution of Mesoproterozoic ages is consistent with an Amazonian provenance, but also with recently dated rocks of Mesoproterozoic age in West Africa (Bradley *et al.* 2015). Hence, the small number of ages at ca. 1200 Ma might be linked to sources in either Amazonia or West Africa.

A Penobscottian cover sequence?

In New Brunswick, pre-Middle Ordovician deformation is documented in the Annidale terrane (Johnson *et al.* 2012). New River basement was thrust northwest over equivalents of the Gushee Volcanics Member of the Penobscot Formation prior to intrusion of the ca. 474 Ma Stewarton Gabbro. In Penobscot Bay, the Ellsworth terrane is in similar thrust relationship with black shale of the Penobscot Formation (Reusch 2002b), but neither stitching plutons nor an overlap sequence has been recognized. An Ordovician age for the Turtle Head Cove unit would strongly suggest that it represents Penobscottian cover. A point in favor of this interpretation is the abundance of Mn-coated pelite in strata of the Turtle Head Cove unit, which is a characteristic of the Davidsville Group that constitutes Penobscottian cover in Newfoundland (Waldron *et al.* 2014a).

A compelling argument for pre-Middle Ordovician (Penobscottian) deformation locally is based on recognition during this study of exotic blocks in mélange at the base of the Early Ordovician Penobscot Formation (Sherman Point, Fig. 2) that are lithologically indistinguishable from Proterozoic strata on Islesboro. In particular, marble, orthoquartzite, and distinctively bedded quartzite occur both as exotic blocks in the mélange and as coherent strata of the Coombs Limestone and Hutchins Island Quartzite on North Islesboro. Regardless of whether the mélange is an olistostrome or tectonic in origin, Proterozoic basement must have been exhumed by the Early Ordovician. We consider this strong evidence for primary juxtaposition of the St. Croix terrane, Islesboro block, and Ellsworth terrane at this time as along the Cold Spring Melange in a similar tectonic setting in Newfoundland (Williams and Piasecki 1990). Previous hyperextension during Middle Cambrian rifting is a likely mechanism to have exhumed the basement.

It remains unclear whether the Turtle Head Cove unit constitutes a typical "older Gander margin" quartzose apron or a post-Early Ordovician "younger Gander margin" on the Penobscottian orogen. This unresolved issue has great significance for a first-order problem in Appalachian tectonics, as to whether closure of the Iapetus Ocean occurred (1) by subduction initiated internally (van Staal *et al.* 2012), or (2) by subduction having entered Iapetus from outside (subduction infection of Waldron *et al.* 2014b). More recently, Waldron *et al.* (2015) have argued that if the timing of strong northwest-vergent deformation of the Ellsworth terrane was pre-Middle Ordovician, then subduction can be explained more easily by a Caribbean-style subduction infection scenario (Waldron *et al.* 2014b) than by an internal, orogen-parallel initiation of subduction (van Staal *et al.* 2012).

Ganderia not Avalonia

Ganderia and Avalonia are less easily distinguished in Maine and New Brunswick than in the type area of Newfoundland (Fig. 1). Landing (1996) recognized lower Paleozoic formations characteristic of Avalonia in the New River terrane (Ellsworth correlative) of coastal New Brunswick. However, other workers (e.g., van Staal *et al.* 2004; van Staal and Barr 2012) have emphasized contrasts, and include both the New River and Brookville terranes within Ganderia. As an example of one contrast, Ganderia is characterized by basement that is more isotopically evolved than that in Avalonia (van Staal *et al.* 2009). The presence

of Proterozoic continental basement on Islesboro as well as detrital zircon ages in the range ca. 1.2 Ga to 2 Ga in quartzite sample IL-14-4, therefore, support a Ganderian affinity (cf. Stewart and Lux 1988).

Kedears Hill tuff

Depositional age

The youngest zircon age population (based on the youngest three grains) in the volcaniclastic tuff is 371.8 ± 5.7 Ma. These Famennian zircon grains are euhedral (Fig. 9C), which strongly suggests an igneous source and minimal sedimentary transport. An alternative interpretation for this young population involving contamination of a Cambrian–Ordovician rock by glacial detritus cannot be ruled out, but is considered unlikely because of the very small fraction of material with such a possible origin, relative to that of the rock, and because of the absence of abundant Cambrian and Neoproterozoic grains that characterize the nearby greywacke (Fig. 10).

Correlation

The Famennian age proposed here for the felsic tuffaceous rock, while common for some local plutons, is young in the context of other sedimentary and volcanic strata of Maine. A possible correlative is rhyolitic tuff of the Carrow Formation (Piskahegan Group) in southern New Brunswick, sourced from the Mount Pleasant caldera (McCutcheon *et al.* 1997), which has a TIMS U–Pb age of 363.8 ± 2.2 Ma (Tucker *et al.* 1998). Felsic igneous rocks of similar age also occur in the Magdalen basin of eastern Canada (Dunning *et al.* 2002) and the Narragansett basin of southeastern New England (Thompson and Hermes 2003). However, the euhedral crystals that make up the youngest age population in the Kedears Hill tuff argue for minimal if any long-distance fluvial transport, thus favoring a model involving the deposition of this population from a widely dispersed, caldera-sourced pyroclastic sheet.

Significantly, the pyrite prospect in this same area—within nearby albitized rhyolite—is the only post-Acadian, submarine volcanogenic sulphide occurrence in the Appalachians (e.g., Gair and Slack 1980; Sangster 1980). The original sulphide mineralization is interpreted to have formed on or near the seafloor, based on the presence of stratiform thin layers of pyrite in black shale at the prospect, and detrital grains of coarse pyrite within calcareous sandstone in shoreline outcrops on the east side of Turtle Head near the neck.

Provenance

The tuff includes a detrital zircon signature traditionally interpreted as Grenvillian, specifically a broad peak at ca. 1 Ga (Fig. 8). The age spectrum also includes (1) minor contributions from a Neoproterozoic source, presumably peri-Gondwanan rocks that by the Late Devonian were accreted to Laurentia; (2) Mesoproterozoic ages as occur in the greywacke; and (3) oldest grains of ca. 3 Ga having possible sources either in the Leonean belt of the West African craton or the Nain craton of Laurentia.

Tectonic significance

Post-Late Devonian deformation, documented southwest of Saint John, New Brunswick, by the presence of several klippen of Proterozoic rocks on Carboniferous strata (Barr *et al.* 2014), has not been recognized previously in Penobscot Bay. Hence, the discovery of Late Devonian volcaniclastic rock with a penetrative fabric may represent the first local example of Neoacadian or Alleghanian deformation.

CONCLUSIONS

U–Pb zircon geochronology of metasedimentary and metavolcaniclastic rocks from North Islesboro, Penobscot Bay, Maine, confirms a Ganderian identity for the Islesboro block located between the St. Croix and Ellsworth terranes. In the context of recently dated detrital zircon from foreland basin strata in Mauritania (Bradley *et al.* 2015), these data permit a West African craton provenance for Ganderia. A mélange at the base of the nearby Lower Ordovician Penobscot Formation contains exotic blocks lithologically indistinguishable from Proterozoic strata on Islesboro, relationships consistent with previously suggested lithospheric extension (Reusch and Rust 2001) during the Middle Cambrian departure of Ganderia from Gondwana (Schulz *et al.* 2008; van Staal *et al.* 2012) and subsequent Penobscottian collision during the initial stage of closure of the Iapetus Ocean (Johnson *et al.* 2012; Waldron *et al.* 2015). Quartzite on Hutchins Island is potentially the oldest rock known in the Appalachian orogen; the foliated Late Devonian volcaniclastic rock in the Kedears Hill area represents the first documentation of late Paleozoic deformation in Penobscot Bay.

ACKNOWLEDGMENTS

We are grateful to Renee Pillers of the USGS (Denver) for preparing zircon separations and mounts. Thanks to Henry Berry (Maine Geological Survey) and Dwight Bradley (USGS Emeritus) for helpful discussions, and to John Waldron (University of Alberta) and Justin Strauss (Dartmouth College) for discussions in the field. Carter Hearn (USGS Emeritus) provided copies of unpublished 1968 field notes and maps of Islesboro prepared by Dave Stewart and colleagues. We also thank Byron Crosby and Sandy Sabaka (Maine Bureau of Parks and Lands) for boat transport. Field work on Islesboro by Reusch was supported in part by the Maine Geological Survey. Klaus

Schulz (USGC), Dwight Bradley, Yvette Kuiper (Colorado School of Mines), and an anonymous referee provided very thorough and helpful reviews of the manuscript.

REFERENCES

Abati, J., Aghzer, A.M., Gerdes, A., and Ennih, N. 2010. Detrital zircon ages of Neoproterozoic sequences of the Moroccan Anti-Atlas belt. Precambrian Research, 181, pp. 115–128. https://doi.org/10.1016/j.precamres.2010.05.018

Barr, S.M., Davis, D.W., Kamo, S., and White, C.E. 2003. Significance of U–Pb detrital zircon ages in quartzite from peri-Gondwanan terranes, New Brunswick and Nova Scotia, Canada. Precambrian Research, 126, pp. 123–145. https://doi.org/10.1016/S0301-9268(03)00192-X

Barr, S.M., Hamilton, M.A., Samson, S.D., Satkoski, A.M., and White, C.E. 2012. Provenance variations in northern Appalachian Avalonia based on detrital zircon age patterns in Ediacaran and Cambrian sedimentary rocks, New Brunswick and Nova Scotia, Canada. Canadian Journal of Earth Sciences, 49, pp. 533–546.https://doi.org/10.1139/e11-070

Barr, S.M., White, C.E., Davis, D.W., McClelland, W.C., and van Staal, C.R. 2014. Infrastructure and provenance of Ganderia: evidence from detrital zircon ages in the Brookville terrane, southern New Brunswick, Canada. Precambrian Research, 246, pp. 358–370. https://doi.org/10.1016/j.precamres.2014.03.022

Bechiri-Benmerzoug, F, Bonin, B., Bechiri, H., Khéloui, R., Talmat-Bouzeguela, S., and Bouzid, K. 2017. Hoggar geochronology: a historical review of published isotopic data. Arabian Journal of Geosciences, 10:351, 32 p. https://doi.org/10.1007/s12517-017-3134-6

Berry, H.N., IV 2007, Grindle Point, Islesboro, Maine. Maine Geological Survey, Augusta, Maine, Maine geologic facts and localities, 12 p. URL <http://digitalmaine.com/cgi/viewcontent.cgi?article=1418&context=mgs_publications>, 20 July, 2017.

Berry, H.N, IV. *(Compiler)*. in press. Bedrock geology of the Augusta 1:100 000 quadrangle, Maine. Maine Geological Survey, Augusta, Maine, USA, scale 1:100 000.

Berry, H.N., IV and Osberg, P.H. 1989. A stratigraphic synthesis of eastern Maine and western New Brunswick. *In* Structure and stratigraphy. *Edited by* R.D. Tucker and R.G. Marvinney. Maine Geological Survey, Augusta, Maine, Studies in Maine Geology, 2, pp. 1–32.

Berry, H.N., IV and Osberg, P.H. 2000. The Megunticook Formation. *In* Guidebook for field trips in coastal and east-central Maine. *Edited by* M.G. Yates, D.R. Lux, and J.T. Kelley. New England Intercollegiate Geological Conference, 92nd Annual Meeting, October 6–8, 2000, Orono, Maine, pp. 54–70.

Berry, H.N., IV, Schoonmaker, A., and Guidotti, C.V. 2000. The Benner Hill sequence. *In* Guidebook for field trips in coastal and east-central Maine. *Edited by* M.G. Yates, D.R. Lux, and J.T. Kelley. New England Intercollegiate Geological Conference, 92nd Annual Meeting, October 6–8, 2000, Orono, Maine, pp. 187–207.

Bickel, C.E. 1971. Bedrock geology of the Belfast quadrangle, Maine. Unpublished Ph.D. thesis, Harvard University, Cambridge, Massachusetts, 342 p.

Black, L.P., Kamo, S.L., Allen, C.M., Davis, D.W., Aleinikoff, J.N., Valley, J.W., Mudil, R., Campbell, I.H., Korsch, R.J., Williams, I.S., and Foudoulis, C. 2004. Improved $^{206}Pb/^{238}U$ microprobe geochronology by the monitoring of a trace-element-related matrix effect; SHRIMP, ID-TIMS, ELA-ICPMS and oxygen isotope documentation for a series of zircon standards. Chemical Geology, 205, pp. 115–140. https://doi.org/10.1016/j.chemgeo.2004.01.003

Bradley, D.C. 2008. Passive margins through Earth history. Earth-Science Reviews, 91, pp. 1–26. https://doi.org/10.1016/j.earscirev.2008.08.001

Bradley, D.C., O'Sullivan, P., Cosca, M.A., Motts, H.A., Horton, J.D., Taylor, C.D., Beaudoin, G., Lee, G.K., Ramezani, J., Bradley, D.B., Jones, J.V., and Bowring, S. 2015. Synthesis of geological, structural, and geochronologic data (phase V, deliverable 53). *In* Second projet de renforcement institutionnel du secteur minier de la République Islamique de Mauritanie (PRISM-II). *Edited by* C.D. Taylor. U.S. Geological Survey Open-File Report 2013–1280-A, 328 p. [In English and French.] URL <https://doi.org/10.3133/ofr20131280A>, 20 July, 2017.

Bromley, R.G. 1996. Trace fossils: biology, taphonomy and applications (2nd edition). Chapman and Hall, London, 361 p. https://doi.org/10.1007/978-1-4899-2875-7

Brookins, D.G. 1976. Geochronologic contributions to stratigraphic interpretation and correlation in the Penobscot Bay area, eastern Maine. *In* Contributions to the stratigraphy of New England. *Edited by* L.R. Page. Geological Society of America Memoir, 148, pp. 129–145. https://doi.org/10.1130/MEM148-p129

Brookins, D.G., Berdan, J.M., and Stewart, D.B. 1973. Isotopic and paleontologic evidence for correlating three volcanic sequences in the Maine coastal volcanic belt. Geological Society of America Bulletin, 84, pp. 1619–1628. https://doi.org/10.1130/0016-7606(1973)84<1619:IAPEFC>2.0.CO;2

Burke, W., West, D.P., Jr., and Coish, R. 2016. Petrology and geochemistry of metamorphosed Cambrian–Ordovician volcanic rocks of the St. Croix belt, western Penobscot Bay, Maine. Geological Society of America Abstracts with Programs, 48(2), unpaginated.

Caby, R. 2003. Terrane assembly and geodynamic evolution of central-western Hoggar: a synthesis. Journal of African Earth Sciences, 37, pp. 133–159. https://doi.org/10.1016/j.jafrearsci.2003.05.003

Dunning, G.R., Barr, S.M., Giles, P.S., McGregor, D.C., Pe-Piper, G., and Piper, D.J.W. 2002. Chronology of Devonian to early Carboniferous rifting and igneous activity in southern Magdalen basin based on U–Pb (zircon) dating. Canadian Journal of Earth Sciences, 39, pp. 1219–1237. https://doi.org/10.1139/e02-037

Fyffe, L.R., Barr, S.M., Johnson, S.C., McLeod, M.J., McNicoll, V.J., Valverde-Vaquero, P., van Staal, C.R., and White, C.E. 2009. Detrital zircon ages from Neoproterozoic and early Paleozoic conglomerate and sandstone units of New Brunswick and coastal Maine: implications for the tectonic evolution of Ganderia. Atlantic Geology, 45, pp. 110–144. https://doi.org/10.4138/atlgeol.2009.006

Fyffe, L.R., Johnson, S.C., and van Staal, C.R. 2011. A review of Proterozoic to early Paleozoic lithotectonic terranes in the northeastern Appalachian orogen of New Brunswick, Canada, and their tectonic evolution during Penobscot, Taconic, Salinic, and Acadian orogenesis. Atlantic Geology, 47, pp. 211–248. https://doi.org/10.4138/atlgeol.2011.010

Gair, J.E. and Slack, J.F. 1980. Stratabound massive sulfide deposits of the U.S. Appalachians. *In* Review of Caledonian-Appalachian stratabound sulphides. *Edited by* F.M. Vokes and E. Zachrisson. Geological Survey of Ireland Special Paper, 5, pp. 67–81.

Gates, O. 1989. Silurian roundstone conglomerates of coastal Maine and adjacent New Brunswick. *In* Studies in Maine geology. *Edited by* R.D. Tucker and R.G. Marvinney. Maine Geological Survey, Augusta, Maine, pp. 127–144.

Gehrels, G. 2011. Detrital zircon U–Pb geochronology: current methods and new opportunities. *In* Tectonics of sedimentary basins: recent advances. *Edited by* C. Busby and A. Azor. John Wiley and Sons, Ltd., Chichester, U.K., pp. 47–62. https://doi.org/10.1002/9781444347166.ch2

Gregg, W.J. 1979. The development of foliations in low, medium, and high grade metamorphic tectonites. Unpublished Ph.D. thesis, State University of New York at Albany, Albany, New York, 230 p.

Gregg, W.J. 1986. Deformation of chlorite-mica aggregates in cleaved psammitic and pelitic rocks from Islesboro, Maine, U.S.A. Journal of Structural Geology, 8, pp. 59–68. https://doi.org/10.1016/0191-8141(86)90017-9

Hibbard, J.P., van Staal, C.R., Rankin, D.W., and Williams, H. 2006. Lithotectonic map of the Appalachian orogen (North), Canada–United States of America. Geological Survey of Canada, Map 02042A, scale 1:1 500 000.

Hibbard, J.P., van Staal, C.R., and Rankin, D.W. 2007. A comparative analysis of pre-Silurian crustal building blocks of the northern and the southern Appalachian orogen. American Journal of Science, 307, pp. 23–45. https://doi.org/10.2475/01.2007.02

Hu, Z., Gao, S., Liu, Y., Hu, S., Chen, H. and Yuan, H. 2008. Signal enhancement in laser ablation ICP-MS by addition of nitrogen in the central channel gas. Journal of Analytical Atomic Spectrometry, 23, pp. 1093–1101. https://doi.org/10.1039/b804760j

Ikenne, M., Söderlund, U., Ernst, R.E., Pin, C., Youbi, N., El Aouli, E.H., and Hafid, A. 2017. A c. 1710 Ma mafic sill emplaced into a quartzite and calcareous series from Ighrem, Anti-Atlas—Morocco: evidence that the Taghdout passive margin sedimentary group is nearly 1 Ga older than previously thought. Journal of African Earth Sciences, 127, pp. 62–76. https://doi.org/10.1016/j.jafrearsci.2016.08.020

Johnson, S.C., Fyffe, L.R., McLeod, M.J., and Dunning, G.R. 2012. U–Pb ages, geochemistry, and tectonomagmatic history of the Cambro–Ordovician Annidale Group: a remnant of the Penobscot arc system in southern New Brunswick? Canadian Journal of Earth Sciences, 49, pp. 166–188. https://doi.org/10.1139/e11-031

Karabinos, P., MacDonald, F.A., and Crowley, J.L. 2017. Bridging the gap between the foreland and hinterland I: geochronology and plate tectonic geometry of Ordovician magmatism and terrane accretion on the Laurentian margin of New England. American Journal of Science, 317, pp. 515–554. https://doi.org/10.2475/05.2017.01

Kuiper, Y.D., Thompson, M.D., Barr, S.M., White, C.E., Hepburn, J.C., and Crowley, J.L. 2017. Detrital zircon evidence for Paleoproterozoic West African crust along the eastern North American continental margin, Georges Bank, offshore Massachusetts, USA. Geology, 45, pp. 811–814. https://doi.org/10.1130/G39203.1

Landing, E. 1996. Avalon: insular continent by the latest Precambrian. *In* Avalonian and related peri-Gondwanan terranes of the Circum-North Atlantic. *Edited by* R.D. Nance and M.D. Thompson. Geological Society of America Special Paper, 304, pp. 29–63. https://doi.org/10.1130/0-8137-2304-3.29

Ludwig, K.R. 2012. User's Manual for Isoplot/Ex, Version 3.75. A geochronological toolkit for Microsoft Excel: Berkeley Geochronology Center, Berkeley, California, Special Publication, 5, revised January 2012, 75 p.

Macdonald, F.A., Ryan-Davis, J., Coish, R.A., Crowley, J.L., and Karabinos, P. 2014. A newly identified Gondwanan terrane in the northern Appalachian Mountains: implications for the Taconic orogeny and closure of the Iapetus Ocean. Geology, 42, pp. 539–542. https://doi.org/10.1130/G35659.1

McCutcheon, S.R., Anderson, H.E., and Robinson, P.T. 1997. Stratigraphy and eruptive history of the Late Devonian Mount Pleasant caldera complex, Canadian Appalachians. Geological Magazine, 134, pp. 17–36. https://doi.org/10.1017/S0016756897006213

McLennan, S.M., Hemming, S., McDaniel, D.K., and Hanson, G.N. 1993. Geochemical approaches to sedimentation, provenance, and tectonics. *In* Processes controlling the composition of clastic sediments. *Edited by* M.J. Johnsson and A. Basu. Geological Society of America Special Paper, 284, pp. 21–40. https://doi.org/10.1130/SPE284-p21

Murphy, J.B., Pisarevsky, S.A., Nance, R.D., and Keppie, J.D. 2004. Neoproterozoic-early Paleozoic evolution of peri-Gondwanan terranes: implications for Laurentia-Gondwana connections. International Journal of Earth Sciences, 93, pp. 659–682. https://doi.org/10.1007/s00531-004-0412-9

Nance, R.D., Murphy, J.B., Strachan, R.A., Keppie, J.D., Gutiérrez-Alonzo, G., Fernández-Suárez, J., Quesada, C., Linnemann, U., D'Lemos, R., and Pisarevsky, S.A. 2008. Neoproterozoic-early Palaeozoic tectonostratigraphy and palaeogeography of the peri-Gondwanan terranes: Amazonian v. West African connections. *In* The boundaries of the West African craton. *Edited by* N. Ennih and J.-P. Liégeois. Geological Society of London Special Publication, 297, pp. 345–383. https://doi.org/10.1144/SP297.17

Nance, R.D., Gutiérrez-Alonso, G., Keppie, J.D., Linnemann, U., Murphy, J.B., Quesada, C., Strachan, R.A., and Woodcock, N.H. 2012. A brief history of the Rheic Ocean. Geoscience Frontiers, 3, pp. 125–135. https://doi.org/10.1016/j.gsf.2011.11.008

Nelson, D.R. 2001. An assessment of the determination of depositional ages for Precambrian clastic sedimentary rocks by U–Pb dating of detrital zircons. Sedimentary Geology, 141–142, pp. 37–60. https://doi.org/10.1016/S0037-0738(01)00067-7

Neuman, R.B. and Max, M.D. 1989. Penobscottian-Grampian-Finnmarkian orogenies as indicators of terrane linkages. *In* Terranes in the circum-Atlantic Paleozoic orogens. *Edited by* R.D. Dallmeyer. Geological Society of America Special Paper, 230, pp. 31–45. https://doi.org/10.1130/SPE230-p31

Osberg, P.H., Hussey, A.M., II, and Boone, G.M. *(Editors)*. 1985. Bedrock geologic map of Maine. Maine Geological Survey, Augusta, Maine, scale 1:500 000.

Paton, C., Hellstrom, J., Paul, B., Woodhead, J., and Hergt, J. 2011. Iolite: freeware for the visualization and processing of mass spectrometric data. Journal of Analytical Atomic Spectrometry, 26, pp. 2508–2518. https://doi.org/10.1039/c1ja10172b

Pearce, J.A. 1996. A user's guide to basalt discriminant diagrams. *In* Trace element geochemistry of volcanic rocks: applications for massive sulphide exploration. *Edited by* A.H. Bailes et al. Geological Association of Canada Short Course Notes, 12, pp. 79–113.

Pearce, J.A., Stern, R.J., Bloomer, S.H., and Fryer, P. 2005. Geochemical mapping of the Mariana arc-basin system: implications for the nature and distribution of subduction components: Geochemistry, Geophysics, Geosystems, 6, 27 p.

Pollock, J.C., Hibbard, J.P., and van Staal, C.R. 2012. A paleogeographical review of the peri-Gondwanan realm of the Appalachian orogen. Canadian Journal of Earth Sciences, 49, pp. 259–288. https://doi.org/10.1139/e11-049

Pothier, H.D., Waldron, J.W.F., Schofield, D.I., and DuFrane, S.A. 2015. Peri-Gondwanan terrane interactions recorded in the Cambrian–Ordovician detrital zircon geochronology of north Wales. Gondwana Research, 28, pp. 987–1001. https://doi.org/10.1016/j.gr.2014.08.009

Restrepo-Pace, P.A., and Cediel, F. 2010. Northern South America basement tectonics and implications for paleocontinental reconstructions of the Americas. Journal of South American Earth Sciences, 29, pp. 764–771. https://doi.org/10.1016/j.jsames.2010.06.002

Reusch, D.N. 2002a. The Ellsworth Schist, Maine: Acadian-telescoped rift sequence or Penobscottian accretionary complex? Geological Society of America Abstracts with Programs, 34(1), p. 76.

Reusch, D.N. 2002b. Tectonic evolution of the Ellsworth terrane. Unpublished field guide for Geological Society of Maine Summer Field Trip, August 2-4, 2002, 13 figures, 16 p.

Reusch, D.N. 2003. Bedrock geology of the mainland portion of the Newbury Neck and Salsbury Cove 7.5-minute quadrangles. Maine Geological Survey, Open-File No. 03–92, 14 p.

Reusch, D.N. and Rust, K.L. 2001. Post-rifting fate of the peri-Gondwanan Ellsworth Schist, Newbury Neck, Maine. Geological Society of America Abstracts with Programs, 33(1), p. A-79.

Reusch, D.N. and van Staal, C.R. 2012. The Dog Bay–Liberty line and its significance for Silurian tectonics of the northern Appalachian orogen. Canadian Journal of Earth Sciences, 49, pp. 239–258. https://doi.org/10.1139/e11-024

Reusch, D.N., van Staal, C., Barr, S.M., and Yates, M. 2003. Ultramafic and sedimentary dikes, Penobscot Bay: Cambrian extension and Ordovician accretion along southeastern Ganderia. Geological Society of America Abstracts with Programs, 35(3), pp.78–79.

Sangster, D.F. 1980. A review of Appalachian stratabound sulphide deposits in Canada. *In* Review of Caledonian-Appalachian stratabound sulphides. *Edited by* F.M. Vokes and E. Zachrisson. Geological Survey of Ireland Special Paper, 5, pp. 7–18.

Schulz, K.J., Stewart, D.B., Tucker, R.D., Pollock, J.C., and Ayuso, R.A. 2008. The Ellsworth terrane, coastal Maine: geochronology, geochemistry, and Nd-Pb isotopic composition—implications for the rifting of Ganderia. Geological Society of America Bulletin, 120, pp. 1134–1158. https://doi.org/10.1130/B26336.1

Sláma, J., Kosler, J., Condon, D.J., Crowley, J.L., Gerdes, A., Hanchar, J.M., Horstwood, M.S.A., Morris, G.A., Nasdala, L., Norberg, N., Schaltegger, U., Schoene, B., Tubrett, M.N., and Whitehouse, M.J. 2008. Plešovice zircon—a new natural reference material for U–Pb and Hf isotopic microanalysis. Chemical Geology, 249, pp. 1–35. https://doi.org/10.1016/j.chemgeo.2007.11.005

Smith, G.O., Basin, E.S., and Brown, C.W. 1907. Description of the Penobscot Bay quadrangle, Maine. U.S. Geological Survey Geologic Atlas, Folio 149, 14 p., scale 1:125 000.

Stewart, D.B. 1998. Geology of northern Penobscot Bay, Maine. U.S. Geological Survey Miscellaneous Investigations Series Map I-2551, 2 sheets, scale 1:62 500.

Stewart, D.B. and Lux, D.R. 1988. Lithologies and metamorphic age of the Precambrian rocks of Seven Hundred Acre Island and vicinity, Islesboro, Penobscot Bay, Maine. Geological Society of America Abstracts with Programs, 20(3), p. 73

Stewart, D.B., Unger, J.D., and Hutchinson, D.R. 1995. Silurian tectonic history of Penobscot Bay region, Maine. Atlantic Geology, 31, pp. 67–79. https://doi.org/10.4138/2098

Stewart, D.B., Tucker, R.D., Ayuso, R.A., and Lux, D.R. 2001. Minimum age of the Neoproterozoic Seven Hundred Acre Island Formation and the tectonic setting of the Islesboro Formation, Islesboro block, Maine. Atlantic Geology, 37, pp. 41–59. https://doi.org/10.4138/1971

Sun, S.-s. and McDonough, W.F. 1989. Chemical and isotopic systematics of oceanic basalts: implications for mantle composition and processes. *In* Magmatism in the ocean basins. *Edited by* A.D. Saunders and M.J. Norry. Geological Society Special Publication, 42, pp. 313–345. https://doi.org/10.1144/GSL.SP.1989.042.01.19

Tassinari, C.C.G. and Macambira, M.J.B. 1999. Geochronological provinces of the Amazonian craton. Episodes, 22, pp. 174–182.

Thompson, M.D. and Hermes, O.D. 2003. Early rifting in the Narragansett basin, Massachusetts-Rhode Island: evidence from Late Devonian bimodal volcanic rocks. The Journal of Geology, 111, pp. 597–604. https://doi.org/10.1086/376768

Tucker, R.D., Bradley, D.C., Ver Straeten, C.A., Harris, A.G., Ebert, J.R., and McCutcheon, S.R. 1998. New U–Pb zircon ages and the duration and division of Devonian time. Earth and Planetary Science Letters, 158, pp. 175–186. https://doi.org/10.1016/S0012-821X(98)00050-8

Tucker, R.D., Osberg, P.H., and Berry, H.N., IV. 2001. The geology of a part of Acadia and the nature of the Acadian orogeny across central and eastern Maine. American Journal of Science, 301, pp. 205–260. https://doi.org/10.2475/ajs.301.3.205

Van Staal, C.R. and Barr, S.M. 2012. Lithospheric architecture and tectonic evolution of the Canadian Appalachians and associated Atlantic margin. *In* Tectonic styles in Canada: the Lithoprobe perspective. *Edited by* J.A. Percival, F.A. Cook, and R.M. Clowes. Geological Association of Canada Special Paper, 49, pp. 41–95.

Van Staal, C.R., Dewey, J.F., MacNiocaill, C., and McKerrow, W.S. 1998. The Cambrian-Silurian tectonic evolution of the northern Appalachians and British Caledonides: history of a complex, west and southwest Pacific-type segment of Iapetus. *In* Lyell: the past is the key to the present. *Edited by* D.J. Blundell and A.C. Scott. Geological Society of London Special Publication, 143, pp. 199–242. https://doi.org/10.1144/GSL.SP.1998.143.01.17

Van Staal, C.R., McNicoll, V., Valverde-Vaquero, P., Barr, S.M., Fyffe, L.R., and Reusch, D.N. 2004. Ganderia, Avalonia, and the Salinic and Acadian orogenies. Geological Society of America Abstracts with Programs, 36(2), p. 128.

Van Staal, C.R., Whalen, J.B., Valverde-Vaquero, P., Zagorevski, A., and Rogers, N. 2009. Pre- Carboniferous, episodic accretion-related, orogenesis along the Laurentian margin of the northern Appalachians. *In* Ancient orogens and modern analogues. *Edited by* J.B. Murphy, J.D. Keppie, and A.J. Hynes. Geological Society of London Special Publication, 327, pp. 271–316. https://doi.org/10.1144/SP327.13

Van Staal, C.R., Barr, S.M., and Murphy, J.B. 2012. Provenance and tectonic evolution of Ganderia: constraints on the evolution of the Iapetus and Rheic oceans. Geology, 40, pp. 987–990. https://doi.org/10.1130/G33302.1

Waldron, J.W.F., Schofield, D.I., DuFrane, S.A., Floyd, J.D., Crowley, Q.G., Simonetti, A., Dokken, R.J., and Pothier, H.D. 2014a. Ganderia-Laurentia collision in the Caledonides of Great Britain and Ireland. Journal of the Geological Society, 171, pp. 555–569. https://doi.org/10.1144/jgs2013-131

Waldron, J.W.F., Schofield, D.I., Murphy, J.B., and Thomas, C.W. 2014b. How was the Iapetus Ocean infected with subduction? Geology, 42, pp. 1095–1098. https://doi.org/10.1130/G36194.1

Waldron, J.W.F., Schofield, D.I., and Reusch, D.N. 2015. Arc-microcontinent interaction in the early history of the Iapetus Ocean. Geological Society of America Abstracts with Programs, 47(7), p. 861.

Williams, H. 1978. Tectonic-lithofacies map of the Appalachian orogen. Memorial University of Newfoundland, St. John's, Newfoundland, Map no. 1, scale 1:2 000 000.

Williams, H. and Piasecki, M.A.J. 1990. The Cold Spring Melange and a possible model for Dunnage–Gander zone interaction in central Newfoundland. Canadian Journal of Earth Sciences, 27, pp. 1126–1134. https://doi.org/10.1139/e90-117

Wilson, J.T. 1966. Did the Atlantic close and then re-open? Nature, 211, pp. 676–681. https://doi.org/10.1038/211676a0

Wood, D.A. 1980. The application of a Th-Hf-Ta diagram to problems of tectonomagmatic classification and establishing the nature of crustal contamination of basaltic lavas of the British Tertiary volcanic province. Earth and Planetary Science Letters, 50, pp. 11–30. https://doi.org/10.1016/0012-821X(80)90116-8

Editorial responsibility: Sandra M. Barr

Appendix A. LA–ICP-MS U–Pb isotopic analyses of zircon grains.

					Isotopic ratios										Final isopotic ages								
Sample number and analysis[1]	Source file[2]	Date[3]	Time	(s)[4]	$^{207}Pb/^{235}U$	2σ	$^{206}Pb/^{238}U$	2σ	ρ	$^{238}U/^{206}Pb$	2σ	$^{207}Pb/^{206}Pb$	2σ	EC[5]	$^{207}Pb/^{235}U$	2σ	$^{206}Pb/^{238}U$	2σ	$^{207}Pb/^{206}Pb$	2σ	% D[6]	PA[7]	2σ
(IL14-5)-core-19	6551	20/11 (6)	13:51.0	24	0.459	0.016	0.0594	0.0016	0.41431	16.83502	0.4534685	0.056	0.002	0.368	383.2	11	372.2	9.5	445	62	16.4	372.2	9.5
(IL14-5)-core-8	6551	20/11 (6)	49:49.0	25	0.476	0.016	0.0625	0.002	0.96881	16.00000	0.512	0.05499	0.0015	0.31223	394.9	11	391	12	410	36	4.6	391.0	12.0
(IL14-5)-core-15	6551	20/11 (6)	03:24.0	25	0.469	0.018	0.0626	0.0024	0.98703	15.97444	0.6124386	0.05476	0.0014	0.58452	390.0	12	392	15	401	26	2.2	392.0	15.0
(IL14-5)-core-16	6551	20/11 (6)	10:43.0	24	0.462	0.018	0.0635	0.0014	0.13827	15.73812	0.3467637	0.053	0.0021	0.25391	385.4	12	397.1	8.5	339	68	-17.1	397.1	8.5
(IL14-5)-core-17	6551	20/11 (6)	11:45.0	24	0.486	0.019	0.0637	0.0017	0.19836	15.69859	0.4189576	0.0558	0.0023	0.3583	404	14	398.2	10	433	78	8.0	398.2	10.0
(IL14-5)-core-22	6551	20/11 (6)	23:14.0	25	0.4823	0.015	0.0646	0.0013	0.33391	15.47748	0.3114181	0.054	0.0016	0.32108	399.5	10	403.6	7.7	387	37	-4.3	403.6	7.7
(IL14-5)-core-23	6551	20/11 (6)	24:17.0	25	0.4877	0.014	0.0647	0.0013	0.17375	15.4679	0.3110329	0.0547	0.0017	0.42028	403.3	9.6	403.9	8.1	396	46	-2.0	403.9	8.1
(IL14-5)-core-9	6551	20/11 (6)	50:52.0	25	0.4824	0.014	0.0648	0.0014	0.74141	15.43448	0.3335125	0.05416	0.0014	0.12947	399.7	9.6	404.7	8.6	376	28	-7.6	404.7	8.6
(IL14-5)-core-20	6551	20/11 (6)	14:53.0	24	0.526	0.022	0.0668	0.0015	0.001	14.97006	0.336154	0.0574	0.0027	0.43373	429	15	416.8	9	493	91	15.5	416.8	9.0
(IL14-5)-core-11	6551	20/11 (6)	59:14.0	24	0.523	0.021	0.0716	0.0014	0.14535	13.97038	0.2732402	0.0536	0.0022	0.23208	427	14	445.7	8.3	365	84	-22.1	445.7	8.3
(IL14-5)-core-21	6551	20/11 (6)	22:12.0	24	0.576	0.021	0.0749	0.0018	0.54667	13.35113	0.320855	0.0564	0.002	0.07477	465	15	465.5	11	462	59	-0.8	465.5	11.0
(IL14-5)-core-5	6551	20/11 (6)	40:26.0	24	0.853	0.027	0.1008	0.0022	0.61433	9.920635	0.2165218	0.06186	0.0017	0.19273	626.1	15	618.8	13	668	32	7.4	618.8	13.0
(IL14-5)-core-12	6551	20/11 (6)	00:17.0	23	1.326	0.06	0.1369	0.0033	0.001	7.304602	0.1760788	0.0704	0.0037	0.61832	856	26	827	19	923	98	10.4	827.0	19.0
(IL14-5)-core-10	6551	20/11 (6)	51:55.0	24	1.533	0.064	0.1578	0.004	0.54088	6.337136	0.1606372	0.0706	0.0027	0.19941	942	26	944	22	953	66	0.9	944.0	22.0
(IL14-5)-core-25	6551	20/11 (6)	26:23.0	23	1.608	0.05	0.1633	0.0039	0.26941	6.123699	0.1462488	0.0719	0.0022	0.4829	973	20	975	22	979	42	0.4	975.0	22.0
(IL14-5)-core-13	6551	20/11 (6)	01:19.0	24	1.914	0.057	0.1846	0.0046	0.75094	5.417118	0.1349878	0.07421	0.0019	0.27087	1086	20	1092	25	1046	26	-4.4	1092.0	25.0
(IL14-5)-core-18	6551	20/11 (6)	12:48.0	24	1.964	0.075	0.1888	0.0041	0.13963	5.29661	0.1150217	0.075	0.0029	0.40859	1102	26	1115	22	1074	66	-3.8	1115.0	22.0
(IL14-5)-core-14	6551	20/11 (6)	02:22.0	24	2.017	0.077	0.1904	0.0051	0.07241	5.252101	0.1406813	0.0771	0.0032	0.44167	1120	26	1123	28	1115	69	-0.7	1123.0	28.0
(IL14-5)-core-3	6551	20/11 (6)	38:21.0	23	2.127	0.075	0.1954	0.005	0.64041	5.117707	0.1309546	0.0794	0.0022	0.21798	1157	25	1151	27	1181	34	2.5	1151.0	27.0
(IL14-5)-core-6	6551	20/11 (6)	47:44.0	24	2.252	0.076	0.2074	0.0043	0.66411	4.821601	0.0999657	0.0798	0.0023	-0.0651	1197	24	1215	23	1191	36	-2.0	1215.0	23.0
(IL14-5)-core-1	6551	20/11 (6)	36:15.0	24	2.962	0.098	0.2355	0.006	0.83573	4.246285	0.1081856	0.0905	0.0024	-0.2876	1397	25	1363	31	1436	29	5.1	1436.0	29.0
(IL14-5)-core-4	6551	20/11 (6)	39:23.0	24	3.324	0.092	0.2563	0.0057	0.40242	3.901678	0.0867716	0.0934	0.0026	0.52203	1486	22	1471	29	1493	32	1.5	1493.0	32.0
(IL14-5)-core-24	6551	20/11 (6)	25:20.0	24	4.109	0.11	0.2923	0.006	0.5794	3.421143	0.0702253	0.1017	0.0025	0.31895	1655.8	21	1653	30	1654	20	0.1	1654.0	20.0
(IL14-5)-core-7	6551	20/11 (6)	48:47.0	24	4.223	0.11	0.2951	0.0058	0.41461	3.388682	0.0666024	0.1037	0.0026	0.45139	1678	22	1667	29	1695	24	1.7	1695.0	24.0
(IL14-5)-core-2	6551	20/11 (6)	37:18.0	24	6.71	0.21	0.3756	0.0083	0.63403	2.662407	0.0588338	0.13	0.0035	0.0827	2078	26	2055	39	2105	22	2.4	2105.0	22.0
(IL14-5)-rim-19	6550	19/11 (5)	48:54.0	28	0.4445	0.024	0.0587	0.001	0.6589	17.0503	0.2848984	0.05527	0.0007	0.46453	373.3	10	367.4	6	421	29	12.7	367.4	6.0
(IL14-5)-rim-20	6550	19/11 (5)	49:57.0	25	0.455	0.025	0.0603	0.0011	0.54188	16.58375	0.3025228	0.0545	0.001	0.29282	380.7	10	377.3	6.7	387	41	2.5	377.3	6.7
(IL14-5)-rim-4	6550	19/11 (5)	14:24.0	25	0.4479	0.023	0.0608	0.001	0.62058	16.44737	0.2596953	0.05307	0.0008	0.19657	375.8	9.7	380.5	5.8	330	32	-15.3	380.5	5.8
(IL14-5)-rim-25	6550	19/11 (5)	01:26.0	26	0.4578	0.029	0.0609	0.001	0.66856	16.41228	0.2639756	0.05489	0.0009	0.28248	382.6	12	381.3	5.9	405	36	5.9	381.3	5.9
(IL14-5)-rim-1	6550	19/11 (5)	11:16.0	26	0.479	0.11	0.0635	0.0052	0.99543	15.74803	1.289603	0.05414	0.0008	0.43984	396	38	396	31	375	33	-5.6	396.0	31.0
(IL14-5)-rim-10	6550	19/11 (5)	26:58.0	26	0.484	0.11	0.0647	0.0052	0.99548	15.45595	1.242209	0.0557	0.0007	0.24322	399	40	404	31	446	28	9.4	404.0	31.0
(IL14-5)-rim-24	6550	19/11 (5)	00:23.0	26	0.514	0.025	0.0659	0.001	0.41873	15.17681	0.2303356	0.0566	0.001	0.21466	421.1	9.9	411.3	6.2	482	45	14.7	411.3	6.2
(IL14-5)-rim-23	6550	19/11 (5)	59:21.0	25	0.508	0.031	0.0663	0.0011	0.26966	15.07841	0.2500942	0.0559	0.0012	0.42923	417	12	413.9	6.5	444	47	6.8	413.9	6.5
(IL14-5)-rim-18	6550	19/11 (5)	47:52.0	26	0.5223	0.022	0.0682	0.0011	0.69364	14.65631	0.2362882	0.05628	0.0005	0.36015	426.6	8.6	425.5	6.6	463	20	8.1	425.5	6.6
(IL14-5)-rim-21	6550	19/11 (5)	57:16.0	24	0.538	0.046	0.0686	0.0012	0.25284	14.57726	0.2549958	0.0561	0.0015	0.35956	436.7	17	427.5	7.3	449	60	4.8	427.5	7.3

Appendix A. Continued.

					Isotopic ratios										Final isopotic ages								
Sample number and analysis[1]	Source file[2]	Date[3]	Time	(s)[4]	$^{207}Pb/^{235}U$	2σ	$^{206}Pb/^{238}U$	2σ	ρ	$^{238}U/^{206}Pb$	2σ	$^{207}Pb/^{206}Pb$	2σ	EC[5]	$^{207}Pb/^{235}U$	2σ	$^{206}Pb/^{238}U$	2σ	$^{207}Pb/^{206}Pb$	2σ	% D[6]	PA[7]	2σ
(IL14-5)-rim-16	6550	19/11 (5)	45:46.0	25	0.518	0.036	0.0686	0.0008	0.26055	14.57301	0.1656507	0.0561	0.0012	0.25634	425.2	15	427.8	4.7	453	48	5.6	427.8	4.7
(IL14-5)-rim-13	6550	19/11 (5)	36:21.0	24	0.605	0.096	0.0715	0.0021	0.49905	13.98601	0.410778	0.0599	0.0025	-0.0132	479	33	445	13	587	90	24.2	445.0	13.0
(IL14-5)-rim-22	6550	19/11 (5)	58:18.0	24	0.593	0.11	0.0759	0.0012	0.22239	13.17523	0.208304	0.0567	0.0034	0.14637	471	37	471.5	7.5	450	130	-4.8	471.5	7.5
(IL14-5)-rim-7	6550	19/11 (5)	23:50.0	24	0.603	0.053	0.0764	0.0009	0.001	13.09415	0.1560256	0.0595	0.0017	0.50563	479	18	474.4	5.4	590	69	19.6	474.4	5.4
(IL14-5)-rim-5	6550	19/11 (5)	15:27.0	24	0.814	0.043	0.1005	0.0014	0.34171	9.950249	0.1386104	0.05887	0.001	0.33386	604.7	12	617.1	8	560	37	-10.2	617.1	8.0
(IL14-5)-rim-14	6550	19/11 (5)	37:24.0	25	1.354	0.17	0.1415	0.0044	0.88175	7.067138	0.2197555	0.0679	0.0011	-0.28	868	32	853	25	863	34	1.2	853.0	25.0
(IL14-5)-rim-8	6550	19/11 (5)	24:53.0	23	1.612	0.13	0.1644	0.0032	0.35381	6.082725	0.1183985	0.0743	0.0019	0.4192	974	21	981	18	1045	54	6.1	981.0	18.0
(IL14-5)-rim-3	6550	19/11 (5)	13:22.0	24	1.786	0.1	0.1773	0.0027	0.65474	5.640158	0.0858907	0.0734	0.0009	0.22885	1040	15	1052	15	1024	25	-2.7	1052.0	15.0
(IL14-5)-rim-17	6550	19/11 (5)	46:49.0	24	1.829	0.084	0.1778	0.0025	0.60015	5.624297	0.0790818	0.0754	0.001	0.24012	1055.5	13	1058	13	1078	27	1.9	1058.0	13.0
(IL14-5)-rim-12	6550	19/11 (5)	35:19.0	24	1.917	0.098	0.1821	0.0027	0.35031	5.491488	0.0814224	0.0738	0.0011	0.37488	1087	14	1078	15	1035	30	-4.2	1078.0	15.0
(IL14-5)-rim-9	6550	19/11 (5)	25:55.0	24	2.2	0.12	0.2029	0.003	0.51563	4.928536	0.0728714	0.0818	0.0012	0.27427	1181	15	1191	16	1238	30	3.8	1191.0	16.0
(IL14-5)-rim-6	6550	19/11 (5)	22:47.0	24	3.145	0.19	0.2505	0.0039	0.54365	3.992016	0.0621512	0.0944	0.0017	0.22115	1450	15	1441	20	1515	35	4.9	1515.0	35.0
(IL14-5)-rim-11	6550	19/11 (5)	34:16.0	24	4.272	0.29	0.3087	0.0079	0.88518	3.239391	0.0828999	0.09676	0.0009	0.34093	1687	20	1734	39	1562	17	-11.0	1562.0	17.0
(IL14-5)-rim-15	6550	19/11 (5)	38:27.0	24	5.34	0.35	0.3372	0.0059	0.53599	2.965599	0.0518892	0.113	0.0019	0.23063	1875	20	1873	28	1847	29	-1.4	1847.0	29.0
(IL14-5)-rim-2	6550	19/11 (5)	12:19.0	24	10.76	0.67	0.4502	0.0089	0.90976	2.221235	0.0439116	0.173	0.0016	0.15511	2505	18	2396	39	2586	15	7.3	2586.0	15.0
(IL14-5)-add-12	6552	20/11 (6)	52:17.0	25	0.4345	0.023	0.0582	0.0015	0.5793	17.17033	0.4422303	0.05337	0.0026	0.04417	366.3	18	364.9	8.8	351	37	-4.0	364.9	8.8
(IL14-5)-add-13	6552	20/11 (6)	53:20.0	25	0.4522	0.024	0.0595	0.0015	0.59521	16.81237	0.4239839	0.05496	0.0027	0.34651	378.7	17	372.5	9.1	408	38	8.7	372.5	9.1
(IL14-5)-add-1	6552	20/11 (6)	28:15.0	25	0.4538	0.023	0.0605	0.0016	0.52858	16.52619	0.4369841	0.05395	0.0026	0.4723	379.9	16	378.7	9.7	367	31	-3.2	378.7	9.7
(IL14-5)-add-18	6552	20/11 (6)	04:50.0	24	0.4279	0.023	0.0606	0.0014	0.57913	16.49621	0.3809747	0.0528	0.0027	0.17342	361.6	17	379.4	8.6	329	41	-15.3	379.4	8.6
(IL14-5)-add-11	6552	20/11 (6)	51:15.0	24	0.4979	0.025	0.0629	0.0016	0.25061	15.90331	0.4046643	0.05657	0.0027	0.62413	410.2	17	393.1	9.5	472	38	16.7	393.1	9.5
(IL14-5)-add-9	6552	20/11 (6)	42:53.0	25	0.493	0.027	0.0632	0.0019	0.90707	15.82278	0.475685	0.05743	0.0027	0.22394	406.4	19	395.3	12	507	22	22.0	395.3	12.0
(IL14-5)-add-17	6552	20/11 (6)	03:48.0	24	0.472	0.027	0.0644	0.0016	0.001	15.52313	0.3855481	0.0544	0.0029	0.50332	392.6	18	402.4	9.6	381	59	-5.6	402.4	9.6
(IL14-5)-add-8	6552	20/11 (6)	41:51.0	24	0.493	0.027	0.0671	0.0016	0.56305	14.9098	0.3556832	0.0546	0.0027	0.05586	406.8	19	418.5	9.9	392	44	-6.8	418.5	9.9
(IL14-5)-add-15	6552	20/11 (6)	55:26.0	24	0.501	0.027	0.0675	0.0018	0.63936	14.81481	0.3950617	0.05378	0.0026	0.12301	412.3	18	421.3	11	360	33	-17.0	421.3	11.0
(IL14-5)-add-10	6552	20/11 (6)	43:56.0	24	0.582	0.031	0.0692	0.0018	0.30707	14.45087	0.3758896	0.0604	0.0032	0.13257	465.9	20	431.4	11	627	56	31.2	431.4	11.0
(IL14-5)-add-19	6552	20/11 (6)	05:53.0	24	0.525	0.037	0.0703	0.0032	0.91004	14.22475	0.6474993	0.0552	0.0028	-0.0844	428	25	438	19	418	42	-4.8	438.0	19.0
(IL14-5)-add-14	6552	20/11 (6)	54:23.0	24	0.628	0.036	0.0723	0.0021	0.001	13.83126	0.4017378	0.0628	0.0036	0.54513	495	22	449.7	13	691	72	34.9	449.7	13.0
(IL14-5)-add-3	6552	20/11 (6)	30:21.0	25	0.594	0.034	0.0762	0.0018	0.4771	13.13198	0.3104078	0.0565	0.0029	-0.1035	475.1	20	473.1	11	470	48	-0.7	473.1	11.0
(IL14-5)-add-20	6552	20/11 (6)	06:55.0	24	1.443	0.083	0.1529	0.0039	0.45226	6.540222	0.1668206	0.0692	0.0036	0.13447	910	36	917	22	911	50	-0.7	917.0	22.0
(IL14-5)-add-16	6552	20/11 (6)	02:44.0	24	1.518	0.091	0.1598	0.0039	0.11126	6.257822	0.1527253	0.0711	0.0041	0.46777	937	36	956	22	951	67	-0.5	956.0	22.0
(IL14-5)-add-5	6552	20/11 (6)	32:27.0	24	1.608	0.091	0.1608	0.0042	0.56041	6.218905	0.1624341	0.0712	0.0036	-0.0153	973	36	961	23	973	45	1.2	961.0	23.0
(IL14-5)-add-7	6552	20/11 (6)	40:48.0	24	2.498	0.15	0.2164	0.0071	0.84974	4.621072	0.1516156	0.0847	0.0041	-0.1177	1270	43	1270	34	1307	36	2.8	1270.0	34.0
(IL14-5)-add-6	6552	20/11 (6)	39:45.0	25	3.59	0.18	0.2744	0.0066	0.49803	3.644315	0.0876548	0.09536	0.0044	0.36308	1547.1	41	1563	33	1535	19	-1.8	1535.0	19.0
(IL14-5)-add-4	6552	20/11 (6)	31:24.0	24	17.48	0.93	0.582	0.015	0.76369	1.718213	0.0442838	0.2177	0.01	0.2217	2961	51	2956	62	2964	15	0.3	2964.0	15.0
(IL14-5)-add-2	6552	20/11 (6)	29:19.0	23	19.22	1	0.5989	0.015	0.87855	1.669728	0.0418199	0.2327	0.011	0.11558	3052	51	3025	61	3071	12	1.5	3071.0	12.0

Appendix A. Continued.

					Isotopic ratios										Final isopotic ages								
Sample number and analysis[1]	Source file[2]	Date[3]	Time	(s)[4]	$^{207}Pb/^{235}U$	2σ	$^{206}Pb/^{238}U$	2σ	ρ	$^{238}U/^{206}Pb$	2σ	$^{207}Pb/^{206}Pb$	2σ	EC[5]	$^{207}Pb/^{235}U$	2σ	$^{206}Pb/^{238}U$	2σ	$^{207}Pb/^{206}Pb$	2σ	% D[6]	PA[7]	2σ
(IL14-6)-75	6548	19/11 (5)	27:55.0	11	4.902	0.17	0.3131	0.0062	0.04167	3.193868	0.0632449	0.112	0.0038	0.36428	1802	29	1756	31	1831	27	4.1	1831.0	27.0
(IL14-6)-31	6547	19/11 (5)	16:43.0	16	5.128	0.24	0.3283	0.0058	0.52867	3.045995	0.0538129	0.1135	0.0037	0.09131	1840	41	1830	28	1863	25	1.8	1863.0	25.0
(IL14-6)-115	6549	19/11 (5)	12:42.0	25	5.076	0.29	0.3297	0.006	0.80965	3.03306	0.0551967	0.1114	0.0025	0.0149	1832	48	1837	29	1822	16	-0.8	1822.0	16.0
(IL14-6)-92	6549	19/11 (5)	32:01.0	22	5.57	0.36	0.3308	0.011	0.94526	3.022975	0.1005221	0.122	0.0028	-0.2477	1909	55	1842	52	1985	22	7.2	1985.0	22.0
(IL14-6)-87	6549	19/11 (5)	22:36.0	24	5.483	0.32	0.334	0.0069	0.67061	2.994012	0.0618523	0.119	0.0028	0.34066	1897	49	1858	33	1941	21	4.3	1941.0	21.0
(IL14-6)-88	6549	19/11 (5)	23:39.0	23	5.42	0.32	0.3349	0.0069	0.71369	2.985966	0.0615204	0.1174	0.0031	-0.0619	1888	51	1862	33	1916	30	2.8	1916.0	30.0
(IL14-6)-99	6549	19/11 (5)	43:29.0	23	5.529	0.31	0.3363	0.0057	0.71685	2.973536	0.0503989	0.1198	0.0026	-0.2028	1905	49	1869	28	1953	18	4.3	1953.0	18.0
(IL14-6)-107	6549	19/11 (5)	00:11.0	24	5.374	0.29	0.3377	0.0067	0.6068	2.961208	0.0587507	0.1156	0.0024	0.43276	1880	49	1875	32	1888	21	0.7	1888.0	21.0
(IL14-6)-3	6547	19/11 (5)	22:29.0	11	5.307	0.25	0.3402	0.0076	0.53111	2.939447	0.0656667	0.1128	0.0035	0.53402	1870	39	1887	37	1845	20	-2.3	1845.0	20.0
(IL14-6)-23	6547	19/11 (5)	59:59.0	17	5.83	0.28	0.3418	0.0058	0.86455	2.925688	0.049646	0.1244	0.0039	-0.3971	1951	42	1895	28	2025	19	6.4	2025.0	19.0
(IL14-6)-90	6549	19/11 (5)	25:44.0	24	5.72	0.33	0.3419	0.0061	0.71039	2.924832	0.0521833	0.1207	0.0027	0.1014	1934	49	1896	29	1966	17	3.6	1966.0	17.0
(IL14-6)-112	6549	19/11 (5)	09:34.0	25	5.831	0.34	0.3448	0.0076	0.79675	2.900232	0.0639262	0.1222	0.0028	0.47915	1951	50	1909	37	1992	18	4.2	1992.0	18.0
(IL14-6)-86	6549	19/11 (5)	21:33.0	25	5.627	0.32	0.3459	0.0068	0.89931	2.891009	0.0568339	0.11815	0.0025	0.0943	1920	49	1915	32	1928	11	0.7	1928.0	11.0
(IL14-6)-22	6547	19/11 (5)	58:57.0	16	5.756	0.26	0.3463	0.0059	0.65756	2.88767	0.049198	0.1201	0.0036	-0.1434	1940	40	1917	28	1958	17	2.1	1958.0	17.0
(IL14-6)-89	6549	19/11 (5)	24:41.0	24	5.493	0.31	0.3465	0.0064	0.64151	2.886003	0.0533057	0.1154	0.0029	0.19277	1899	49	1918	30	1885	25	-1.8	1885.0	25.0
(IL14-6)-2	6547	19/11 (5)	21:13.0	25	5.894	0.28	0.3477	0.0077	0.77139	2.876043	0.0636915	0.1236	0.0037	0.46367	1960	41	1923	37	2009	17	4.3	2009.0	17.0
(IL14-6)-74	6548	19/11 (5)	26:49.0	17	6.047	0.18	0.3477	0.0069	0.49777	2.876043	0.0570742	0.1249	0.0041	0.19084	1982.5	27	1924	33	2027	20	5.1	2027.0	20.0
(IL14-6)-101	6549	19/11 (5)	49:45.0	24	5.944	0.32	0.3489	0.0059	0.68446	2.866151	0.0484674	0.1249	0.0028	0.09674	1967	45	1929	28	2027	17	4.8	2027.0	17.0
(IL14-6)-5	6547	19/11 (5)	24:21.0	24	5.482	0.25	0.3502	0.0057	0.46018	2.855511	0.0464775	0.1139	0.0036	0.29544	1897	40	1936	27	1861	25	-4.0	1861.0	25.0
(IL14-6)-34	6547	19/11 (5)	19:43.0	24	5.975	0.27	0.3512	0.0065	0.57013	2.84738	0.0526992	0.1237	0.0039	0.4442	1974	43	1940	31	2009	23	3.4	2009.0	23.0
(IL14-6)-29	6547	19/11 (5)	10:19.0	25	5.614	0.25	0.3513	0.0056	0.8138	2.84657	0.0453766	0.11602	0.0034	0.30116	1918	39	1941	27	1896	9.5	-2.4	1895.6	9.5
(IL14-6)-39	6547	19/11 (5)	29:08.0	24	5.926	0.27	0.3517	0.006	0.61374	2.843332	0.0485072	0.12232	0.0036	0.42585	1964.9	40	1943	29	1993	15	2.5	1993.0	15.0
(IL14-6)-35	6547	19/11 (5)	21:01.0	9	5.8	0.31	0.352	0.0079	0.7622	2.840909	0.063759	0.1184	0.0041	-0.0742	1945	45	1944	38	1932	35	-0.6	1932.0	35.0
(IL14-6)-71	6548	19/11 (5)	23:34.0	23	6.004	0.2	0.3521	0.008	0.44421	2.840102	0.0645295	0.1222	0.0042	0.25402	1976	30	1945	38	1987	27	2.1	1987.0	27.0
(IL14-6)-119	6549	19/11 (5)	21:04.0	24	5.813	0.33	0.3522	0.0058	0.09849	2.839296	0.0467573	0.1193	0.0027	0.56802	1948.1	48	1945	27	1945	18	0.0	1945.0	18.0
(IL14-6)-51	6548	19/11 (5)	45:58.0	24	5.866	0.17	0.3551	0.0071	0.47635	2.816108	0.0563063	0.11999	0.0038	0.32867	1956.1	25	1959	36	1956	15	-0.2	1956.0	15.0
(IL14-6)-102	6549	19/11 (5)	50:47.0	24	6.1	0.34	0.3555	0.0072	0.80098	2.81294	0.0569709	0.1247	0.003	-0.4017	1989	49	1961	34	2023	23	3.1	2023.0	23.0
(IL14-6)-42	6548	19/11 (5)	28:12.0	25	5.943	0.18	0.3567	0.0073	0.59995	2.803476	0.0573742	0.1215	0.0039	0.55666	1967.3	26	1966	35	1978	18	0.6	1978.0	18.0
(IL14-6)-52	6548	19/11 (5)	47:01.0	24	6.051	0.18	0.3573	0.0074	0.30231	2.798769	0.057965	0.1227	0.004	0.2696	1983	26	1970	35	1996	18	1.3	1996.0	18.0
(IL14-6)-26	6547	19/11 (5)	07:15.0	21	6.055	0.28	0.3579	0.0069	0.70248	2.794077	0.0538674	0.123	0.0038	0.63996	1983.6	40	1972	33	1999	20	1.4	1999.0	20.0
(IL14-6)-47	6548	19/11 (5)	37:37.0	24	5.927	0.19	0.358	0.0081	0.6947	2.793296	0.0632003	0.12067	0.0038	0.10936	1965	29	1973	39	1966	12	-0.4	1966.0	12.0
(IL14-6)-24	6547	19/11 (5)	01:06.0	12	5.9	0.29	0.359	0.012	0.83486	2.785515	0.0931092	0.12	0.0039	0.38907	1961	43	1977	56	1956	28	-1.1	1956.0	28.0
(IL14-6)-7	6547	19/11 (5)	30:37.0	24	5.666	0.26	0.3592	0.0066	0.79139	2.783964	0.051153	0.1158	0.0035	-0.0414	1930	47	1978	31	1892	18	-4.5	1892.0	18.0
(IL14-6)-80	6548	19/11 (5)	37:08.0	24	6.07	0.18	0.3592	0.0075	0.33063	2.783964	0.0581284	0.1218	0.0039	0.35942	1988.3	27	1978	36	1983	16	0.3	1983.0	16.0
(IL14-6)-38	6547	19/11 (5)	28:05.0	24	6.085	0.29	0.3603	0.007	0.86554	2.775465	0.0539224	0.12345	0.0037	0.00932	1990	43	1983	33	2006	13	1.1	2006.0	13.0
(IL14-6)-56	6548	19/11 (5)	55:22.0	24	6.032	0.19	0.3607	0.0082	0.59466	2.772387	0.0630263	0.121	0.0039	0.28032	1983	23	1986	39	1970	18	-0.8	1970.0	18.0

Appendix A. Continued.

					Isotopic ratios										Final isopotic ages								
Sample number and analysis[1]	Source file[2]	Date[3]	Time	(s)[4]	$^{207}Pb/^{235}U$	2σ	$^{206}Pb/^{238}U$	2σ	ρ	$^{238}U/^{206}Pb$	2σ	$^{207}Pb/^{206}Pb$	2σ	EC[5]	$^{207}Pb/^{235}U$	2σ	$^{206}Pb/^{238}U$	2σ	$^{207}Pb/^{206}Pb$	2σ	% D[6]	PA[7]	2σ
(IL14-6)-41	6548	19/11 (5)	27:10.0	25	6.055	0.18	0.3611	0.0074	0.67765	2.769316	0.0567514	0.1226	0.004	0.16905	1983	26	1987	35	1994	19	0.4	1994.0	19.0
(IL14-6)-59	6548	19/11 (5)	58:45.0	9	6.32	0.35	0.361	0.017	0.99296	2.770083	0.1304471	0.12539	0.004	-0.7023	2019	50	1988	82	2034	14	2.3	2034.0	14.0
(IL14-6)-96	6549	19/11 (5)	40:21.0	24	6.255	0.35	0.3614	0.0073	0.68924	2.767017	0.0558916	0.1259	0.0029	0.2444	2015	53	1988	35	2041	20	2.6	2041.0	20.0
(IL14-6)-30	6547	19/11 (5)	11:22.0	24	5.977	0.28	0.3618	0.0067	0.7469	2.763958	0.0511844	0.12085	0.0036	0.35451	1972	40	1990	32	1968	15	-1.1	1968.0	15.0
(IL14-6)-54	6548	19/11 (5)	49:06.0	25	6.063	0.18	0.3617	0.0075	0.47531	2.764722	0.0573277	0.1214	0.0038	0.35662	1984.9	26	1990	36	1977	13	-0.7	1977.0	13.0
(IL14-6)-63	6548	19/11 (5)	06:51.0	24	6.19	0.22	0.3624	0.01	0.78454	2.759382	0.0761419	0.1236	0.004	0.30405	2002	32	1993	47	2009	16	0.8	2009.0	16.0
(IL14-6)-43	6548	19/11 (5)	29:15.0	24	6.193	0.2	0.3636	0.0088	0.62799	2.750275	0.0665633	0.1232	0.004	0.31156	2003.3	28	1999	42	2007	19	0.4	2007.0	19.0
(IL14-6)-81	6549	19/11 (5)	12:09.0	24	6.247	0.35	0.3636	0.0071	0.71541	2.750275	0.0537045	0.1261	0.0028	0.2793	2011	50	1999	34	2043	19	2.2	2043.0	19.0
(IL14-6)-57	6548	19/11 (5)	56:25.0	24	6.343	0.18	0.364	0.0082	0.76596	2.747253	0.0618887	0.1262	0.004	0.20938	2024	26	2001	39	2045	15	2.2	2045.0	15.0
(IL14-6)-78	6548	19/11 (5)	35:02.0	25	6.313	0.2	0.3639	0.0078	0.42748	2.748008	0.0589021	0.1245	0.0041	0.42785	2020	29	2001	37	2021	21	1.0	2021.0	21.0
(IL14-6)-50	6548	19/11 (5)	40:45.0	24	6.416	0.19	0.3642	0.0071	0.66925	2.745744	0.0535277	0.12821	0.004	0.3564	2034.4	26	2002	34	2076	12	3.6	2076.0	12.0
(IL14-6)-103	6549	19/11 (5)	51:50.0	23	5.83	0.33	0.3651	0.0094	0.47457	2.738976	0.0705187	0.1164	0.0031	-0.2046	1950	51	2006	44	1900	31	-5.6	1900.0	31.0
(IL14-6)-49	6548	19/11 (5)	39:42.0	24	6.103	0.2	0.3658	0.0088	0.56386	2.733734	0.0657651	0.1213	0.0039	0.35723	1990	29	2009	42	1975	18	-1.7	1975.0	18.0
(IL14-6)-108	6549	19/11 (5)	01:14.0	24	6.19	0.34	0.3659	0.0066	0.53879	2.732987	0.0492968	0.123	0.0026	0.19525	2003	50	2010	31	2005	25	-0.2	2005.0	25.0
(IL14-6)-19	6547	19/11 (5)	51:30.0	24	6.313	0.29	0.366	0.0066	0.64031	2.73224	0.0492699	0.1245	0.0038	0.37254	2020	40	2011	31	2021	19	0.5	2021.0	19.0
(IL14-6)-44	6548	19/11 (5)	30:18.0	24	6.375	0.2	0.3671	0.0076	0.59403	2.724053	0.0563956	0.1271	0.0041	0.2337	2028.5	27	2016	36	2058	18	2.0	2058.0	18.0
(IL14-6)-62	6548	19/11 (5)	05:49.0	23	6.455	0.22	0.3672	0.0081	0.49802	2.723312	0.0600731	0.1275	0.0043	0.32426	2039	30	2016	38	2062	24	2.2	2062.0	24.0
(IL14-6)-116	6549	19/11 (5)	17:56.0	24	6.34	0.37	0.368	0.0078	0.658	2.717391	0.0575969	0.1243	0.003	0.31389	2023	50	2019	37	2017	22	-0.1	2017.0	22.0
(IL14-6)-106	6549	19/11 (5)	59:09.0	23	6.42	0.34	0.3682	0.0072	0.51032	2.715915	0.0531086	0.1267	0.0027	0.46525	2034	50	2021	34	2058	25	1.8	2058.0	25.0
(IL14-6)-17	6547	19/11 (5)	49:25.0	25	6.291	0.29	0.3691	0.006	0.70301	2.709293	0.0440416	0.12297	0.0036	0.37591	2016.9	40	2025	28	2000	11	-1.3	2000.0	11.0
(IL14-6)-37	6547	19/11 (5)	27:02.0	25	6.352	0.29	0.3691	0.0068	0.87199	2.709293	0.0499138	0.12447	0.0037	0.09308	2025	40	2025	32	2021	13	-0.2	2021.0	13.0
(IL14-6)-82	6549	19/11 (5)	13:12.0	24	6.516	0.37	0.3691	0.0061	0.73167	2.709293	0.0447756	0.1284	0.0028	-0.0901	2048	50	2025	29	2076	16	2.5	2076.0	16.0
(IL14-6)-45	6548	19/11 (5)	31:20.0	24	6.398	0.2	0.3704	0.0081	0.52626	2.699784	0.0590396	0.12627	0.0039	0.29051	2031.9	25	2031	38	2046	11	0.7	2046.0	11.0
(IL14-6)-6	6547	19/11 (5)	29:35.0	24	6.095	0.29	0.3709	0.0072	0.84898	2.696145	0.0523382	0.1202	0.0036	0.26686	1992	39	2033	34	1958	15	-3.8	1958.0	15.0
(IL14-6)-93	6549	19/11 (5)	33:02.0	24	6.64	0.38	0.371	0.0075	0.47125	2.695418	0.0544896	0.1299	0.0033	0.36683	2064	51	2034	35	2101	27	3.2	2101.0	27.0
(IL14-6)-28	6547	19/11 (5)	09:17.0	23	6.51	0.31	0.3717	0.0076	0.33618	2.690342	0.0550083	0.128	0.0049	0.3659	2047	42	2037	36	2067	44	1.5	2067.0	44.0
(IL14-6)-110	6549	19/11 (5)	03:19.0	24	6.307	0.35	0.3717	0.0074	0.73871	2.690342	0.0535607	0.1233	0.0027	0.36503	2019	50	2037	35	2004	19	-1.6	2004.0	19.0
(IL14-6)-53	6548	19/11 (5)	48:04.0	24	6.553	0.2	0.3723	0.0087	0.51089	2.686006	0.0627673	0.1271	0.0041	0.44171	2053	28	2040	41	2057	19	0.8	2057.0	19.0
(IL14-6)-79	6548	19/11 (5)	36:05.0	24	6.713	0.21	0.3725	0.0083	0.25182	2.684564	0.0598171	0.1299	0.0042	0.27081	2074	29	2041	39	2096	19	2.6	2096.0	19.0
(IL14-6)-21	6547	19/11 (5)	57:47.0	23	6.364	0.29	0.3733	0.0055	0.5852	2.678811	0.0394681	0.12412	0.0037	0.31174	2027.2	40	2044.7	26	2016	12	-1.4	2016.0	12.0
(IL14-6)-64	6548	19/11 (5)	07:54.0	23	6.505	0.21	0.3737	0.0087	0.36792	2.675943	0.0622979	0.127	0.0045	0.37389	2050	28	2046	41	2055	30	0.4	2055.0	30.0
(IL14-6)-105	6549	19/11 (5)	53:55.0	24	6.607	0.34	0.3742	0.0072	0.5327	2.672368	0.0514192	0.1284	0.0031	0.58415	2060	49	2049	34	2075	26	1.3	2075.0	26.0
(IL14-6)-12	6547	19/11 (5)	40:01.0	24	6.503	0.3	0.3747	0.0074	0.78357	2.668802	0.0527065	0.1258	0.0037	0.47362	2046.1	40	2051	34	2040	13	-0.5	2040.0	13.0
(IL14-6)-25	6547	19/11 (5)	02:05.0	16	6.35	0.33	0.3748	0.0098	0.7009	2.66809	0.0697633	0.1224	0.004	0.23899	2024	45	2052	46	1990	29	-3.1	1990.0	29.0
(IL14-6)-67	6548	19/11 (5)	15:13.0	24	6.552	0.19	0.3751	0.0083	0.61192	2.665956	0.0589908	0.1265	0.004	0.42804	2053	26	2053	39	2049	15	-0.2	2049.0	15.0
(IL14-6)-20	6547	19/11 (5)	52:33.0	24	6.72	0.32	0.3759	0.0079	0.68484	2.660282	0.0559091	0.13	0.0041	0.30792	2075	42	2057	37	2097	24	1.9	2097.0	24.0

Appendix A. Continued.

					Isotopic ratios										Final isopotic ages								
Sample number and analysis[1]	Source file[2]	Date[3]	Time	(s)[4]	$^{207}Pb/^{235}U$	2σ	$^{206}Pb/^{238}U$	2σ	ρ	$^{238}U/^{206}Pb$	2σ	$^{207}Pb/^{206}Pb$	2σ	EC[5]	$^{207}Pb/^{235}U$	2σ	$^{206}Pb/^{238}U$	2σ	$^{207}Pb/^{206}Pb$	2σ	% D[6]	PA[7]	2σ
(IL14-6)-48	6548	19/11 (5)	38:40.0	24	6.505	0.2	0.3763	0.0072	0.67811	2.657454	0.0508469	0.1255	0.0039	0.1816	2049	26	2059	34	2036	12	-1.1	2036.0	12.0
(IL14-6)-9	6547	19/11 (5)	32:43.0	24	6.33	0.3	0.3767	0.0081	0.68481	2.654632	0.0570813	0.1231	0.0039	0.28155	2021	42	2060	38	2000	22	-3.0	2000.0	22.0
(IL14-6)-117	6549	19/11 (5)	18:59.0	23	6.53	0.37	0.3766	0.0064	0.41488	2.655337	0.0451252	0.1253	0.003	0.40259	2050	50	2060	30	2033	21	-1.3	2033.0	21.0
(IL14-6)-70	6548	19/11 (5)	18:21.0	24	6.944	0.2	0.3768	0.0081	0.75053	2.653928	0.057051	0.1335	0.0043	0.39125	2104.2	27	2061	38	2144	16	3.9	2144.0	16.0
(IL14-6)-10	6547	19/11 (5)	33:45.0	25	6.35	0.3	0.3771	0.0074	0.80334	2.651816	0.0520378	0.1228	0.0037	0.38755	2028	43	2062	35	1996	18	-3.3	1996.0	18.0
(IL14-6)-33	6547	19/11 (5)	18:41.0	24	6.9	0.34	0.3785	0.0088	0.91508	2.642008	0.0614258	0.1317	0.0039	-0.2659	2098	43	2069	41	2121	14	2.5	2121.0	14.0
(IL14-6)-97	6549	19/11 (5)	41:23.0	24	6.778	0.37	0.379	0.0064	0.47181	2.638522	0.0445555	0.131	0.003	0.34439	2082.7	49	2071	30	2110	20	1.8	2110.0	20.0
(IL14-6)-4	6547	19/11 (5)	23:19.0	24	6.358	0.29	0.3797	0.0069	0.76109	2.633658	0.0478595	0.1218	0.0037	0.42284	2026.3	40	2075	32	1982	16	-4.7	1982.0	16.0
(IL14-6)-11	6547	19/11 (5)	38:59.0	24	6.672	0.3	0.3802	0.0061	0.14011	2.630195	0.0421993	0.1277	0.004	0.63643	2068.7	40	2077	28	2065	22	-0.6	2065.0	22.0
(IL14-6)-100	6549	19/11 (5)	44:31.0	24	6.704	0.37	0.3806	0.007	0.65416	2.62743	0.0483237	0.1278	0.0027	0.28577	2075	47	2079	33	2068	17	-0.5	2068.0	17.0
(IL14-6)-13	6547	19/11 (5)	41:04.0	24	6.498	0.3	0.3809	0.0065	0.29415	2.625361	0.0448014	0.1247	0.004	0.50386	2045	41	2081	31	2023	24	-2.9	2023.0	24.0
(IL14-6)-104	6549	19/11 (5)	52:53.0	23	6.575	0.35	0.3812	0.0075	0.69695	2.623295	0.0516126	0.1245	0.0028	0.32418	2056	49	2082	35	2021	18	-3.0	2021.0	18.0
(IL14-6)-95	6549	19/11 (5)	35:07.0	24	6.838	0.39	0.3815	0.0069	0.72625	2.621232	0.0474089	0.1304	0.0029	0.16214	2090	50	2083	32	2103	17	1.0	2103.0	17.0
(IL14-6)-32	6547	19/11 (5)	17:38.0	24	6.561	0.3	0.3817	0.007	0.59899	2.619859	0.0480456	0.1253	0.0038	0.38044	2056	43	2084	33	2032	18	-2.6	2032.0	18.0
(IL14-6)-58	6548	19/11 (5)	57:27.0	24	6.599	0.21	0.3819	0.0085	0.32999	2.618487	0.05828	0.125	0.0041	0.43446	2059	29	2085	40	2028	21	-2.8	2028.0	21.0
(IL14-6)-120	6549	19/11 (5)	22:06.0	24	6.655	0.38	0.3825	0.0069	0.83203	2.614379	0.0471614	0.125	0.0028	0.19824	2066	50	2088	32	2028	14	-3.0	2028.0	14.0
(IL14-6)-55	6548	19/11 (5)	50:09.0	24	6.84	0.21	0.3834	0.0082	0.35622	2.608242	0.055784	0.1283	0.0042	0.22637	2090.8	28	2092	38	2074	21	-0.9	2074.0	21.0
(IL14-6)-36	6547	19/11 (5)	26:00.0	24	6.532	0.3	0.3838	0.0065	0.89579	2.605524	0.0441269	0.12353	0.0036	-0.1711	2052	39	2094	30	2008	10	-4.3	2008.0	10.0
(IL14-6)-84	6549	19/11 (5)	15:17.0	25	7.277	0.41	0.3839	0.007	0.86733	2.604845	0.0474965	0.13747	0.0029	0.24172	2146	51	2094	32	2195	12	4.6	2195.0	12.0
(IL14-6)-77	6548	19/11 (5)	34:00.0	24	6.89	0.23	0.3842	0.0094	0.74454	2.602811	0.0636815	0.12946	0.0041	0.39669	2097.2	29	2096	44	2090	13	-0.3	2090.0	13.0
(IL14-6)-111	6549	19/11 (5)	08:32.0	24	6.526	0.37	0.3848	0.0066	0.47259	2.598753	0.0445732	0.1231	0.0029	0.41193	2049	50	2099	31	2006	23	-4.6	2006.0	23.0
(IL14-6)-118	6549	19/11 (5)	20:01.0	24	6.61	0.38	0.3918	0.0081	0.68418	2.552323	0.0527662	0.122	0.0029	0.3443	2060	51	2131	37	1985	22	-7.4	1985.0	22.0
(IL14-6)-73	6548	19/11 (5)	25:39.0	24	7.01	0.22	0.397	0.0092	0.7815	2.518892	0.0583723	0.1277	0.0041	0.11329	2111	28	2155	43	2070	17	-4.1	2070.0	17.0
(IL14-6)-85	6549	19/11 (5)	16:20.0	24	7.62	0.46	0.3985	0.0078	0.89702	2.50941	0.0491177	0.1401	0.0032	-0.4421	2186	54	2162	36	2228	21	3.0	2228.0	21.0
(IL14-6)-40	6547	19/11 (5)	30:10.0	24	6.86	0.32	0.3994	0.0088	0.75234	2.503756	0.0551654	0.1251	0.0038	0.24947	2097	45	2166	41	2030	17	-6.7	2030.0	17.0
(IL14-6)-27	6547	19/11 (5)	08:14.0	23	6.88	0.33	0.4001	0.01	0.8293	2.499375	0.0624688	0.1241	0.0039	0.42008	2096	43	2169	47	2015	21	-7.6	2015.0	21.0
(IL14-6)-18	6547	19/11 (5)	50:28.0	24	6.87	0.32	0.4017	0.0077	0.67915	2.48942	0.0477185	0.124	0.0038	0.20621	2095	42	2177	36	2014	20	-8.1	2014.0	20.0
(IL14-6)-61	6548	19/11 (5)	04:49.0	21	7.08	0.28	0.4067	0.014	0.90572	2.458815	0.0846408	0.1276	0.0041	0.09644	2120	32	2199	63	2064	17	-6.5	2064.0	17.0
(IL14-6)-46	6548	19/11 (5)	36:34.0	24	8.458	0.26	0.422	0.0085	0.78464	2.369668	0.0477303	0.14593	0.0046	0.23288	2281.1	27	2269	39	2299	11	1.3	2299.0	11.0
(IL14-6)-1	6547	19/11 (5)	20:10.0	24	9.967	0.45	0.4611	0.0083	0.25619	2.168727	0.039038	0.1583	0.005	0.58833	2431.5	42	2444	36	2437	21	-0.3	2437.0	21.0
(IL14-6)-72	6548	19/11 (5)	24:36.0	24	10.48	0.32	0.4645	0.0098	0.60956	2.152853	0.0454208	0.1623	0.0052	0.37686	2478	29	2459	43	2479	17	0.8	2479.0	17.0
(IL14-6)-76	6548	19/11 (5)	32:57.0	24	10.47	0.32	0.4663	0.01	0.49421	2.144542	0.0459906	0.1618	0.0052	0.31486	2477.1	29	2467	44	2474	14	0.3	2474.0	14.0
(IL14-6)-94	6549	19/11 (5)	34:05.0	24	10.55	0.59	0.4683	0.0072	0.59872	2.135383	0.032831	0.1629	0.0035	-0.0823	2484	52	2476	32	2490	19	0.6	2490.0	19.0
(IL14-6)-98	6549	19/11 (5)	42:26.0	24	10.82	0.61	0.4688	0.0092	0.87852	2.133106	0.0418613	0.1675	0.0034	0.03749	2507	47	2478	40	2533	12	2.2	2533.0	12.0
(IL14-6)-8	6547	19/11 (5)	31:40.0	24	11.12	0.51	0.4749	0.009	0.8638	2.105706	0.039906	0.1713	0.0051	0.4826	2533	43	2505	39	2570	12	2.5	2570.0	12.0
(IL14-6)-83	6549	19/11 (5)	14:15.0	24	11.51	0.66	0.4762	0.0096	0.89887	2.099958	0.0423343	0.176	0.0036	0.03668	2565	54	2510	42	2615	11	4.0	2615.0	11.0

Appendix A. Continued.

					Isotopic ratios										Final isopotic ages								
Sample number and analysis[1]	Source file[2]	Date[3]	Time	(s)[4]	$^{207}Pb/^{235}U$	2σ	$^{206}Pb/^{238}U$	2σ	ρ	$^{238}U/^{206}Pb$	2σ	$^{207}Pb/^{206}Pb$	2σ	EC[5]	$^{207}Pb/^{235}U$	2σ	$^{206}Pb/^{238}U$	2σ	$^{207}Pb/^{206}Pb$	2σ	% D[6]	PA[7]	2σ
(IL14-6)-14	6547	19/11 (5)	42:07.0	23	10.73	0.5	0.4821	0.0091	0.32439	2.074258	0.0391532	0.1599	0.0051	0.4556	2500	43	2536	39	2453	24	-3.4	2453.0	24.0
(IL14-6)-114	6549	19/11 (5)	11:40.0	24	11.288	0.64	0.4825	0.0082	0.77626	2.072539	0.0352224	0.1692	0.0037	0.40751	2547.1	52	2538	36	2550	14	0.5	2550.0	14.0
(IL14-6)-66	6548	19/11 (5)	14:10.0	24	12.33	0.36	0.4873	0.01	0.53208	2.052124	0.0421121	0.1808	0.0058	0.4752	2629.5	28	2559	44	2660	16	3.8	2660.0	16.0
(IL14-6)-16	6547	19/11 (5)	48:23.0	24	10.78	0.51	0.4878	0.0088	0.95197	2.050021	0.0369827	0.16119	0.0047	-0.3361	2504	44	2561	38	2468	9.4	-3.8	2468.0	9.4
(IL14-6)-109	6549	19/11 (5)	02:16.0	24	11.19	0.62	0.4883	0.0091	0.76045	2.047921	0.0381652	0.1647	0.0038	-0.2014	2539	55	2563	39	2503	24	-2.4	2503.0	24.0
(IL14-6)-15	6547	19/11 (5)	43:09.0	25	12.31	0.61	0.4963	0.012	0.96978	2.01491	0.0487184	0.1802	0.0053	-0.3519	2627	46	2597	50	2654	9.5	2.2	2654.3	9.5
(IL14-6)-68	6548	19/11 (5)	16:15.0	24	11.85	0.37	0.4982	0.011	0.53801	2.007226	0.0443185	0.1711	0.0055	0.2738	2592	27	2606	48	2568	14	-1.5	2568.0	14.0
(IL14-6)-60	6548	19/11 (5)	59:33.0	24	12.75	0.37	0.5024	0.01	0.60339	1.990446	0.0396188	0.1832	0.006	0.51253	2661.4	27	2624	44	2686	20	2.3	2686.0	20.0
(IL14-6)-91	6549	19/11 (5)	30:57.0	24	13.2	0.73	0.5146	0.0083	0.54738	1.943257	0.0313429	0.1865	0.0039	0.37175	2694.2	53	2680	32	2711	12	1.1	2711.0	12.0
(IL14-6)-113	6549	19/11 (5)	10:37.0	24	13.39	0.79	0.522	0.011	0.84474	1.915709	0.0403693	0.1863	0.0042	-0.0009	2707	55	2707	46	2710	16	0.1	2710.0	16.0
(IL14-6)-65	6548	19/11 (5)	08:57.0	23	13.59	0.43	0.5226	0.012	0.43874	1.913509	0.0439382	0.1887	0.0063	0.47574	2721	30	2710	52	2735	23	0.9	2735.0	23.0
(IL14-6)-69	6548	19/11 (5)	17:18.0	23	14.3	0.47	0.5429	0.014	0.50488	1.84196	0.0474994	0.19	0.0065	0.54232	2769	34	2795	58	2741	25	-2.0	2741.0	25.0
(IL14-4)-115	6546	18/11 (4)	0.6684	24	0.67	0.014	0.0808	0.0017	0.67959	12.37624	0.2603911	0.06006	0.0013	0.04265	520.5	8.2	500.8	10	604	33	17.1	500.8	10.0
(IL14-4)-51	6545	18/11 (4)	0.5847	24	0.663	0.03	0.0826	0.0012	0.07129	12.11387	0.176095	0.0583	0.0024	0.30981	516	18	511.3	7	536	64	4.6	511.3	7.0
(IL14-4)-87	6546	18/11 (4)	0.6481	24	0.68	0.013	0.0839	0.0017	0.59854	11.91895	0.2415044	0.0588	0.0014	0.21925	526.5	7.7	519.1	10	558	38	7.0	519.1	10.0
(IL14-4)-8	6544	18/11 (4)	0.5018	24	0.652	0.13	0.0841	0.0023	0.43842	11.89061	0.325189	0.0585	0.0027	-0.3042	509	16	520.3	14	541	58	3.8	520.3	14.0
(IL14-4)-61	6545	18/11 (4)	0.5977	24	0.863	0.042	0.0912	0.0022	0.22618	10.96491	0.2645045	0.0678	0.0034	0.31426	631	23	562	13	851	81	34.0	562.0	13.0
(IL14-4)-79	6545	18/11 (4)	0.6195	24	0.752	0.037	0.0931	0.0017	0.4683	10.74114	0.1961325	0.0584	0.0025	0.1291	569	22	573.9	9.8	538	67	-6.7	573.9	9.8
(IL14-4)-118	6546	18/11 (4)	0.6706	24	0.77	0.015	0.0939	0.0019	0.73843	10.64963	0.2154877	0.05951	0.0012	0.13993	579.3	8.6	578.5	11	584	31	0.9	578.5	11.0
(IL14-4)-89	6546	18/11 (4)	0.6495	24	0.772	0.02	0.094	0.002	0.38617	10.6383	0.2263468	0.0597	0.002	0.328	581	11	579.4	12	586	62	1.1	579.4	12.0
(IL14-4)-66	6545	18/11 (4)	0.6043	24	0.804	0.033	0.0964	0.0019	0.52531	10.37344	0.2044558	0.0595	0.0021	0.27371	598.6	19	594	11	580	45	-2.4	594.0	11.0
(IL14-4)-77	6545	18/11 (4)	0.6181	24	0.799	0.033	0.0966	0.0022	0.34835	10.35197	0.2357591	0.0599	0.0023	0.55899	598.4	17	595	13	607	53	2.0	595.0	13.0
(IL14-4)-35	6544	18/11 (4)	0.5359	24	0.837	0.16	0.0996	0.0027	0.377	10.04016	0.272173	0.0613	0.0026	0.22492	617	11	612.2	16	645	51	5.1	612.2	16.0
(IL14-4)-110	6546	18/11 (4)	0.6648	24	0.932	0.023	0.0998	0.0019	0.38288	10.02004	0.1907623	0.0679	0.0023	0.1684	668	12	613.1	11	875	56	29.9	613.1	11.0
(IL14-4)-37	6544	18/11 (4)	0.5403	23	0.832	0.16	0.1009	0.0028	0.46144	9.910803	0.2750272	0.0602	0.0025	0.30592	617	12	619	16	608	47	-1.8	619.0	16.0
(IL14-4)-76	6545	18/11 (4)	0.6173	25	0.87	0.034	0.1013	0.0015	0.58411	9.871668	0.1461748	0.06186	0.0019	0.31834	637	20	622.1	9	668	26	6.9	622.1	9.0
(IL14-4)-71	6545	18/11 (4)	0.6108	24	0.845	0.039	0.1015	0.0016	0.41568	9.852217	0.1553059	0.0598	0.0025	-0.0213	621	22	623	9.6	589	64	-5.8	623.0	9.6
(IL14-4)-22	6544	18/11 (4)	0.5207	24	0.852	0.16	0.1017	0.0026	0.32996	9.832842	0.2513804	0.0599	0.0028	0.12589	625	14	624.1	15	609	54	-2.5	624.1	15.0
(IL14-4)-16	6544	18/11 (4)	0.5134	24	0.892	0.17	0.1021	0.003	0.001	9.794319	0.2877861	0.0618	0.0035	0.56767	646	18	626	17	650	95	3.7	626.0	17.0
(IL14-4)-108	6546	18/11 (4)	0.6633	24	0.86	0.022	0.102	0.0017	0.65304	9.803922	0.1633987	0.0608	0.0015	-0.2282	630	12	626	10	630	42	0.6	626.0	10.0
(IL14-4)-112	6546	18/11 (4)	0.6662	24	0.843	0.022	0.1021	0.0019	0.16409	9.794319	0.1822645	0.0605	0.0021	0.43878	620	12	626.6	11	612	67	-2.4	626.6	11.0
(IL14-4)-85	6546	18/11 (4)	0.6466	24	0.828	0.031	0.1022	0.002	0.06253	9.784736	0.1914821	0.0589	0.0025	0.32572	612	17	627.1	11	550	89	-14.0	627.1	11.0
(IL14-4)-27	6544	18/11 (4)	0.5272	24	0.757	0.16	0.1023	0.0028	0.48306	9.775171	0.2675511	0.0581	0.0025	0.20842	572	10	627.8	16	555	41	-13.1	627.8	16.0
(IL14-4)-48	6545	18/11 (4)	0.5796	24	0.881	0.04	0.103	0.0017	0.70644	9.708738	0.1602413	0.0617	0.0022	-0.2067	641	22	632.1	10	661	45	4.4	632.1	10.0
(IL14-4)-91	6546	18/11 (4)	0.651	24	0.935	0.025	0.1033	0.0022	0.55945	9.680542	0.2061684	0.0648	0.0018	-0.1157	670	13	634	13	778	53	18.5	634.0	13.0

Appendix A. Continued.

					Isotopic ratios										Final isopotic ages								
Sample number and analysis[1]	Source file[2]	Date[3]	Time	(s)[4]	$^{207}Pb/^{235}U$	2σ	$^{206}Pb/^{238}U$	2σ	ρ	$^{238}U/^{206}Pb$	2σ	$^{207}Pb/^{206}Pb$	2σ	EC[5]	$^{207}Pb/^{235}U$	2σ	$^{206}Pb/^{238}U$	2σ	$^{207}Pb/^{206}Pb$	2σ	% D[6]	PA[7]	2σ
(IL14-4)-113	6546	18/11 (4)	0.6669	24	0.875	0.018	0.1038	0.0019	0.48453	9.633911	0.1763433	0.0605	0.0015	0.26479	638.1	9.6	636.8	11	620	42	-2.7	636.8	11.0
(IL14-4)-68	6545	18/11 (4)	0.6057	24	0.894	0.055	0.1042	0.0022	0.56468	9.596929	0.2026223	0.063	0.0035	-0.1144	647	30	639	13	690	100	7.4	639.0	13.0
(IL14-4)-44	6545	18/11 (4)	0.5738	24	0.889	0.036	0.1044	0.0016	0.71716	9.578544	0.1467976	0.06086	0.0019	0.08251	645.7	19	640.2	9.1	633	28	-1.1	640.2	9.1
(IL14-4)-80	6545	18/11 (4)	0.6202	24	0.881	0.036	0.1054	0.0018	0.42103	9.487666	0.1620285	0.0607	0.0021	0.50107	641.4	19	645.8	10	625	42	-3.3	645.8	10.0
(IL14-4)-45	6545	18/11 (4)	0.5745	24	0.892	0.038	0.1055	0.0018	0.41849	9.478673	0.1617214	0.0607	0.0022	0.29761	647	21	646.4	11	623	47	-3.8	646.4	11.0
(IL14-4)-2	6544	18/11 (4)	0.4946	24	0.989	0.17	0.1062	0.0029	0.46014	9.416196	0.2571278	0.0638	0.0024	0.20224	698	13	651	17	731	40	10.9	651.0	17.0
(IL14-4)-93	6546	18/11 (4)	0.6524	24	0.903	0.02	0.1069	0.0021	0.706	9.354537	0.1837655	0.062	0.0015	0.25367	653	11	654.4	12	670	40	2.3	654.4	12.0
(IL14-4)-4	6544	18/11 (4)	0.496	24	0.951	0.17	0.1078	0.0029	0.001	9.276438	0.2495517	0.062	0.0026	0.59548	678.6	8.6	660.2	17	679	57	2.8	660.2	17.0
(IL14-4)-5	6544	18/11 (4)	0.4967	24	1.528	0.28	0.1083	0.0035	0.48603	9.23361	0.2984085	0.0992	0.0048	0.0988	940	25	663	20	1601	66	58.6	663.0	20.0
(IL14-4)-53	6545	18/11 (4)	0.5861	24	0.94	0.04	0.1084	0.0016	0.5832	9.225092	0.1361637	0.0632	0.0021	0.12376	673	21	663.5	9.2	712	35	6.8	663.5	9.2
(IL14-4)-23	6544	18/11 (4)	0.5214	24	0.927	0.18	0.1087	0.0027	0.14137	9.199632	0.2285097	0.0604	0.0027	0.56485	665.6	9.5	665.3	16	612	53	-8.7	665.3	16.0
(IL14-4)-15	6544	18/11 (4)	0.5098	24	0.977	0.18	0.1094	0.0028	0.39314	9.140768	0.2339502	0.0632	0.0025	0.38329	692	10	669.5	17	712	38	6.0	669.5	17.0
(IL14-4)-116	6546	18/11 (4)	0.6691	24	1.158	0.049	0.1097	0.0025	0.001	9.11577	0.2077432	0.0769	0.0045	0.69739	780	23	671	15	1100	110	39.0	671.0	15.0
(IL14-4)-52	6545	18/11 (4)	0.5854	25	0.941	0.039	0.1098	0.002	0.64757	9.107468	0.165892	0.062	0.002	0.2363	673.1	20	672	12	680	32	1.2	672.0	12.0
(IL14-4)-117	6546	18/11 (4)	0.6698	24	1.124	0.066	0.1101	0.0025	0.50605	9.082652	0.2062364	0.0726	0.0035	-0.1988	762	31	673	15	989	92	32.0	673.0	15.0
(IL14-4)-62	6545	18/11 (4)	0.5985	24	0.952	0.036	0.1107	0.0018	0.35628	9.033424	0.1468849	0.0614	0.0021	0.55958	679.1	19	677	10	650	38	-4.2	677.0	10.0
(IL14-4)-36	6544	18/11 (4)	0.5395	24	0.984	0.19	0.1113	0.0028	0.26756	8.984726	0.2260308	0.0641	0.0027	0.36493	695	14	680.4	16	743	47	8.4	680.4	16.0
(IL14-4)-74	6545	18/11 (4)	0.613	24	0.96	0.04	0.1115	0.0022	0.55466	8.96861	0.1769591	0.0615	0.0021	0.41192	683	21	681	13	653	37	-4.3	681.0	13.0
(IL14-4)-28	6544	18/11 (4)	0.5279	23	0.877	0.18	0.1118	0.0033	0.27754	8.944544	0.2640161	0.0607	0.0027	0.4985	642	10	683	19	623	58	-9.6	683.0	19.0
(IL14-4)-109	6546	18/11 (4)	0.664	24	0.97	0.016	0.1124	0.0019	0.25849	8.896797	0.1503907	0.0627	0.0015	0.34409	688.5	8.3	686.8	11	695	37	1.2	686.8	11.0
(IL14-4)-47	6545	18/11 (4)	0.5789	24	0.971	0.041	0.1128	0.002	0.75308	8.865248	0.1571853	0.06196	0.002	-0.1858	689	21	688.8	11	671	30	-2.7	688.8	11.0
(IL14-4)-92	6546	18/11 (4)	0.6517	24	0.981	0.02	0.1136	0.0022	0.34064	8.802817	0.1704771	0.0623	0.0017	0.31704	694	10	693.3	13	682	49	-1.7	693.3	13.0
(IL14-4)-49	6545	18/11 (4)	0.5803	24	0.987	0.043	0.1154	0.002	0.69231	8.665511	0.1501822	0.0619	0.0022	-0.1603	697	22	704.1	12	668	45	-5.4	704.1	12.0
(IL14-4)-7	6544	18/11 (4)	0.5011	24	0.944	0.19	0.1158	0.0058	0.8653	8.635579	0.4325247	0.0618	0.0025	-0.048	673	25	706	34	664	47	-6.3	706.0	34.0
(IL14-4)-3	6544	18/11 (4)	0.4953	24	1.105	0.19	0.1181	0.0032	0.51684	8.467401	0.22943	0.0639	0.0024	0.32582	755.3	9.5	719	19	737	34	2.4	719.0	19.0
(IL14-4)-17	6544	18/11 (4)	0.5142	24	1.51	0.28	0.1525	0.0037	0.59511	6.557377	0.159097	0.0699	0.0027	0.05467	934	13	915	21	923	34	0.9	915.0	21.0
(IL14-4)-73	6545	18/11 (4)	0.6123	25	2.03	0.088	0.1582	0.0039	0.85335	6.321113	0.1558302	0.0935	0.0029	0.1552	1125	30	947	22	1496	23	36.7	947.0	22.0
(IL14-4)-1	6544	18/11 (4)	0.4939	24	2.11	0.36	0.1704	0.0069	0.94741	5.868545	0.2376347	0.0837	0.0031	-0.4083	1157	24	1014	38	1285	31	21.1	1014.0	38.0
(IL14-4)-55	6545	18/11 (4)	0.5876	24	1.802	0.073	0.1755	0.0033	0.53693	5.698006	0.107142	0.0748	0.0025	0.46156	1046	26	1042	18	1069	31	2.5	1042.0	18.0
(IL14-4)-83	6546	18/11 (4)	0.6452	24	1.898	0.043	0.1824	0.0044	0.78827	5.482456	0.1322522	0.0756	0.0016	0.27288	1080	15	1080	24	1084	28	0.4	1080.0	24.0
(IL14-4)-106	6546	18/11 (4)	0.6619	25	2.139	0.043	0.1956	0.0043	0.90348	5.112474	0.1123908	0.07966	0.0014	-0.0225	1161	14	1151	23	1188	17	3.1	1151.0	23.0
(IL14-4)-72	6545	18/11 (4)	0.6115	25	2.159	0.083	0.1966	0.0033	0.69543	5.08647	0.0853782	0.07903	0.0024	0.54824	1168	27	1157	18	1172	21	1.3	1157.0	18.0
(IL14-4)-41	6545	18/11 (4)	0.5716	24	2.209	0.093	0.1997	0.0032	0.66721	5.007511	0.0802405	0.0796	0.0026	-0.0614	1187	31	1174	17	1187	29	1.1	1174.0	17.0
(IL14-4)-96	6546	18/11 (4)	0.6546	24	2.291	0.054	0.2011	0.004	0.72828	4.97265	0.098909	0.082	0.0018	-0.053	1209	17	1181	21	1245	29	5.1	1181.0	21.0
(IL14-4)-14	6544	18/11 (4)	0.5091	24	2.307	0.42	0.2029	0.0055	0.83762	4.928536	0.1335976	0.0801	0.003	-0.1498	1214	12	1191	30	1198	25	0.6	1191.0	30.0
(IL14-4)-82	6546	18/11 (4)	0.6445	24	2.233	0.055	0.2041	0.0038	0.59187	4.899559	0.0912216	0.0805	0.0019	0.18277	1191	17	1197	20	1207	36	0.8	1197.0	20.0

Appendix A. Continued.

					Isotopic ratios										Final isopotic ages								
Sample number and analysis[1]	Source file[2]	Date[3]	Time	(s)[4]	$^{207}Pb/^{235}U$	2σ	$^{206}Pb/^{238}U$	2σ	ρ	$^{238}U/^{206}Pb$	2σ	$^{207}Pb/^{206}Pb$	2σ	EC[5]	$^{207}Pb/^{235}U$	2σ	$^{206}Pb/^{238}U$	2σ	$^{207}Pb/^{206}Pb$	2σ	% D[6]	PA[7]	2σ
(IL14-4)-94	6546	18/11 (4)	0.6532	24	2.315	0.041	0.2046	0.0039	0.71712	4.887586	0.0931651	0.0822	0.0017	0.1007	1219	13	1200	21	1249	28	3.9	1200.0	21.0
(IL14-4)-58	6545	18/11 (4)	0.5927	24	2.336	0.096	0.2059	0.0044	0.79128	4.856727	0.1037863	0.0806	0.0028	0.16007	1223	29	1207	23	1210	36	0.2	1207.0	23.0
(IL14-4)-60	6545	18/11 (4)	0.5941	24	2.361	0.097	0.2064	0.0032	0.59719	4.844961	0.0751157	0.0826	0.0026	0.01021	1230	29	1210	17	1260	25	4.0	1210.0	17.0
(IL14-4)-59	6545	18/11 (4)	0.5934	24	2.361	0.094	0.2103	0.0034	0.84704	4.755112	0.0768777	0.0811	0.0025	0.06471	1231	29	1230	18	1223	17	-0.6	1230.0	18.0
(IL14-4)-6	6544	18/11 (4)	0.5004	24	2.268	0.44	0.2118	0.0052	0.69907	4.721435	0.1159181	0.08029	0.003	-0.0338	1205	12	1238	28	1203	23	-2.9	1238.0	28.0
(IL14-4)-81	6546	18/11 (4)	0.6437	24	2.791	0.046	0.2342	0.0043	0.35625	4.269855	0.0783961	0.0868	0.002	0.55294	1353	12	1356	22	1355	34	-0.1	1355.0	34.0
(IL14-4)-33	6544	18/11 (4)	0.5345	23	3.007	0.54	0.234	0.0059	0.16181	4.273504	0.1077507	0.0901	0.0038	0.43759	1409	18	1355	31	1423	44	4.8	1423.0	44.0
(IL14-4)-40	6544	18/11 (4)	0.5425	23	3.302	0.62	0.2562	0.0066	0.40905	3.903201	0.1005508	0.0921	0.0037	0.49781	1481.3	7.7	1470	34	1467	33	-0.2	1467.0	33.0
(IL14-4)-10	6544	18/11 (4)	0.5033	24	3.155	0.61	0.2501	0.0061	0.001	3.998401	0.097522	0.0932	0.004	0.54485	1445	17	1439	31	1488	45	3.3	1488.0	45.0
(IL14-4)-38	6544	18/11 (4)	0.541	24	3.353	0.63	0.2603	0.0069	0.33309	3.841721	0.1018359	0.0931	0.0037	0.63205	1493.3	8.2	1491	36	1489	30	-0.1	1489.0	30.0
(IL14-4)-101	6546	18/11 (4)	0.6582	24	3.463	0.052	0.2664	0.005	0.61152	3.753754	0.0704533	0.094	0.0018	0.29256	1519	12	1522	26	1507	21	-1.0	1507.0	21.0
(IL14-4)-9	6544	18/11 (4)	0.5026	23	3.396	0.66	0.2709	0.0064	0.44306	3.691399	0.0872091	0.0943	0.0036	0.52697	1503.2	9.8	1545	33	1513	27	-2.1	1513.0	27.0
(IL14-4)-107	6546	18/11 (4)	0.6626	24	3.588	0.047	0.2746	0.0048	0.53785	3.641661	0.0636561	0.0952	0.0021	0.14412	1547	10	1564	24	1530	30	-2.2	1530.0	30.0
(IL14-4)-99	6546	18/11 (4)	0.6568	24	3.343	0.061	0.2546	0.0043	0.59029	3.92773	0.0663364	0.0953	0.0024	0.03294	1491	14	1462	22	1532	38	4.6	1532.0	38.0
(IL14-4)-11	6544	18/11 (4)	0.5069	24	3.729	0.69	0.2744	0.0073	0.89875	3.644315	0.0969515	0.096	0.0036	-0.2841	1582	17	1563	37	1546	21	-1.1	1546.0	21.0
(IL14-4)-78	6545	18/11 (4)	0.6188	23	3.695	0.15	0.2724	0.0054	0.50744	3.671072	0.0727746	0.0976	0.0034	0.60143	1573	29	1559	30	1578	34	1.2	1578.0	34.0
(IL14-4)-88	6546	18/11 (4)	0.6488	24	3.968	0.064	0.2864	0.0052	0.40942	3.49162	0.0633953	0.1003	0.0023	0.41947	1627	13	1623	26	1628	32	0.3	1628.0	32.0
(IL14-4)-114	6546	18/11 (4)	0.6677	24	3.546	0.052	0.2557	0.0044	0.68406	3.910833	0.0672963	0.101	0.0019	0.22939	1537	12	1467	23	1643	21	10.7	1643.0	21.0
(IL14-4)-29	6544	18/11 (4)	0.5287	23	3.515	0.71	0.2638	0.0071	0.56131	3.790751	0.1020255	0.1013	0.0042	0.03886	1529	22	1509	36	1646	40	8.3	1646.0	40.0
(IL14-4)-31	6544	18/11 (4)	0.533	24	4.409	0.76	0.2892	0.0075	0.75602	3.457815	0.0896736	0.10159	0.0037	0.05656	1713	14	1637	37	1653	17	1.0	1653.0	17.0
(IL14-4)-67	6545	18/11 (4)	0.605	24	4.114	0.15	0.2896	0.0043	0.69208	3.453039	0.051271	0.1019	0.0031	0.5134	1657	30	1639	21	1658	19	1.1	1658.0	19.0
(IL14-4)-119	6546	18/11 (4)	0.6713	24	4.273	0.083	0.3005	0.006	0.837	3.327787	0.066445	0.10404	0.0019	-0.0152	1691	17	1694	30	1697	17	0.2	1697.0	17.0
(IL14-4)-50	6545	18/11 (4)	0.5811	24	4.502	0.18	0.3081	0.0061	0.83418	3.245699	0.0642609	0.1053	0.0034	0.22008	1731	33	1731	30	1718	24	-0.8	1718.0	24.0
(IL14-4)-39	6544	18/11 (4)	0.5417	24	4.677	0.88	0.3147	0.0093	0.47096	3.177629	0.0939052	0.1069	0.0046	0.53251	1762	16	1764	46	1744	43	-1.1	1744.0	43.0
(IL14-4)-95	6546	18/11 (4)	0.6539	24	4.77	0.078	0.3168	0.007	0.8381	3.156566	0.0697474	0.1084	0.002	0.1748	1779	14	1774	34	1772	18	-0.1	1772.0	18.0
(IL14-4)-90	6546	18/11 (4)	0.6503	24	4.539	0.062	0.3044	0.0054	0.86404	3.285151	0.058278	0.10857	0.0018	0.26927	1738	11	1713	27	1775	13	3.5	1775.0	13.0
(IL14-4)-24	6544	18/11 (4)	0.5221	23	4.62	0.91	0.2947	0.0087	0.62004	3.393281	0.1001749	0.1103	0.0071	-0.3953	1746	49	1665	43	1789	96	6.9	1789.0	96.0
(IL14-4)-102	6546	18/11 (4)	0.659	24	4.786	0.086	0.3176	0.0059	0.48283	3.148615	0.0584913	0.1099	0.0026	0.24963	1782	15	1778	29	1795	33	0.9	1795.0	33.0
(IL14-4)-84	6546	18/11 (4)	0.6459	24	4.989	0.068	0.3266	0.0059	0.84255	3.061849	0.055312	0.11107	0.0019	0.35469	1817	12	1822	29	1817	15	-0.3	1817.0	15.0
(IL14-4)-69	6545	18/11 (4)	0.6065	24	5.214	0.2	0.3323	0.0053	0.77455	3.009329	0.0479971	0.11276	0.0034	0.2251	1854	33	1854	24	1844	16	-0.5	1844.0	16.0
(IL14-4)-103	6546	18/11 (4)	0.6597	24	4.638	0.045	0.2987	0.0047	0.66106	3.347841	0.0526778	0.11304	0.0019	0.28599	1756	8.1	1685	23	1852	13	9.0	1852.0	13.0
(IL14-4)-43	6545	18/11 (4)	0.5731	24	5.418	0.21	0.3418	0.0052	0.84668	2.925688	0.0445102	0.11348	0.0034	0.24446	1887	33	1895	25	1855	15	-2.2	1855.0	15.0
(IL14-4)-120	6546	18/11 (4)	0.672	24	5.277	0.077	0.3349	0.0058	0.8114	2.985966	0.0517128	0.11417	0.002	0.42241	1865	12	1862	28	1866	15	0.2	1866.0	15.0
(IL14-4)-100	6546	18/11 (4)	0.6575	23	5.35	0.11	0.3372	0.0069	0.71639	2.965599	0.060684	0.1149	0.0029	0.02689	1876	18	1873	33	1875	36	0.1	1875.0	36.0
(IL14-4)-86	6546	18/11 (4)	0.6474	24	5.372	0.097	0.3413	0.0064	0.71738	2.929974	0.0549424	0.1148	0.0022	0.28992	1880	15	1893	31	1876	22	-0.9	1876.0	22.0
(IL14-4)-70	6545	18/11 (4)	0.6072	24	5.24	0.22	0.3249	0.0065	0.93412	3.07787	0.0615764	0.1151	0.0035	-0.112	1858	36	1813	32	1881	17	3.6	1881.0	17.0

Appendix A. Continued.

					Isotopic ratios										Final isopotic ages								
Sample number and analysis[1]	Source file[2]	Date[3]	Time	(s)[4]	$^{207}Pb/^{235}U$	2σ	$^{206}Pb/^{238}U$	2σ	ρ	$^{238}U/^{206}Pb$	2σ	$^{207}Pb/^{206}Pb$	2σ	EC[5]	$^{207}Pb/^{235}U$	2σ	$^{206}Pb/^{238}U$	2σ	$^{207}Pb/^{206}Pb$	2σ	% D[6]	PA[7]	2σ
(IL14-4)-98	6546	18/11 (4)	0.6561	24	5.426	0.064	0.343	0.0057	0.76592	2.915452	0.0484492	0.11511	0.002	0.01511	1889	10	1901	27	1881	15	-1.1	1881.0	15.0
(IL14-4)-42	6545	18/11 (4)	0.5724	23	5.35	0.22	0.3377	0.0064	0.75311	2.961208	0.05612	0.1152	0.0037	0.07528	1880	40	1875	31	1882	27	0.4	1882.0	27.0
(IL14-4)-21	6544	18/11 (4)	0.52	24	5.844	1.1	0.357	0.0085	0.81766	2.80112	0.0666933	0.1174	0.0044	0.16967	1952.7	9.9	1968	41	1917	16	-2.7	1917.0	16.0
(IL14-4)-111	6546	18/11 (4)	0.6655	24	5.475	0.099	0.3331	0.0064	0.63746	3.002101	0.0576807	0.119	0.0026	0.14501	1896	15	1853	31	1940	27	4.5	1940.0	27.0
(IL14-4)-18	6544	18/11 (4)	0.5149	23	5.89	1.1	0.3445	0.0081	0.52828	2.902758	0.0682506	0.1192	0.0047	0.18346	1963	16	1908	39	1942	31	1.8	1942.0	31.0
(IL14-4)-105	6546	18/11 (4)	0.6611	24	5.651	0.081	0.3409	0.0068	0.70044	2.933412	0.0585133	0.1199	0.0024	0.4267	1924	12	1891	33	1959	21	3.5	1959.0	21.0
(IL14-4)-19	6544	18/11 (4)	0.5156	24	6.288	1.1	0.3645	0.01	0.82681	2.743484	0.0752671	0.1202	0.0044	0.46399	2016	14	2003	47	1959	18	-2.2	1959.0	18.0
(IL14-4)-12	6544	18/11 (4)	0.5076	24	6.27	1.2	0.3681	0.0094	0.77299	2.716653	0.0693739	0.1205	0.0044	0.38239	2014	14	2020	44	1963	18	-2.9	1963.0	18.0
(IL14-4)-104	6546	18/11 (4)	0.6604	24	5.591	0.072	0.3352	0.006	0.80495	2.983294	0.0534002	0.1206	0.0022	0.36279	1914	11	1863	29	1969	19	5.4	1969.0	19.0
(IL14-4)-63	6545	18/11 (4)	0.5992	24	6.05	0.26	0.3556	0.0062	0.50817	2.812148	0.0490307	0.1211	0.0042	0.18161	1982	37	1961	30	1970	34	0.5	1970.0	34.0
(IL14-4)-54	6545	18/11 (4)	0.5869	24	6.2	0.26	0.3684	0.0054	0.57649	2.714441	0.0397882	0.1226	0.0041	0.21814	2003	36	2022	25	1993	29	-1.5	1993.0	29.0
(IL14-4)-13	6544	18/11 (4)	0.5083	24	6.15	1.1	0.3532	0.0095	0.7583	2.831257	0.0761522	0.1224	0.0045	0.1878	1996	16	1949	45	1995	17	2.3	1995.0	17.0
(IL14-4)-34	6544	18/11 (4)	0.5352	24	6.053	1.1	0.3478	0.0087	0.67612	2.875216	0.0719217	0.1233	0.0048	0.20686	1983	13	1924	42	2003	29	3.9	2003.0	29.0
(IL14-4)-20	6544	18/11 (4)	0.5163	24	6.642	1.2	0.371	0.0099	0.71576	2.695418	0.0719262	0.1244	0.0047	0.35829	2064	12	2034	47	2019	22	-0.7	2019.0	22.0
(IL14-4)-97	6546	18/11 (4)	0.6553	24	6.44	0.12	0.3782	0.0091	0.82603	2.644104	0.0636207	0.1246	0.0024	0.13856	2041	18	2067	43	2023	20	-2.2	2023.0	20.0
(IL14-4)-64	6545	18/11 (4)	0.5999	24	6.422	0.24	0.3667	0.005	0.83911	2.727025	0.0371833	0.12536	0.0037	0.34134	2035	33	2013	24	2034	11	1.0	2034.0	11.0
(IL14-4)-30	6544	18/11 (4)	0.5294	23	5.962	1.2	0.3586	0.0083	0.64514	2.788622	0.0645442	0.1257	0.0047	0.24045	1970	12	1976	39	2038	20	3.0	2038.0	20.0
(IL14-4)-56	6545	18/11 (4)	0.5912	24	6.58	0.27	0.3762	0.0059	0.85089	2.658161	0.0416883	0.1281	0.0039	0.12855	2056	36	2058	28	2071	16	0.6	2071.0	16.0
(IL14-4)-65	6545	18/11 (4)	0.6006	23	11.33	0.44	0.4764	0.008	0.7841	2.099076	0.035249	0.1707	0.0053	0.29871	2551	37	2511	35	2564	19	2.1	2564.0	19.0
(IL14-4)-46	6545	18/11 (4)	0.5782	23	12.19	0.48	0.4996	0.0073	0.79863	2.001601	0.0292468	0.1753	0.0053	0.1423	2622	35	2612	31	2608	16	-0.2	2608.0	16.0
(IL14-4)-25	6544	18/11 (4)	0.5228	24	12.87	2.4	0.5118	0.013	0.77337	1.953888	0.0496298	0.1785	0.0068	0.51696	2670	10	2664	55	2638	16	-1.0	2638.0	16.0
(IL14-4)-32	6544	18/11 (4)	0.5337	24	13.1	2.3	0.4841	0.012	0.7724	2.065689	0.0512049	0.1828	0.0066	0.27428	2686.9	9.7	2545	51	2678	14	5.0	2678.0	14.0
(IL14-4)-75	6545	18/11 (4)	0.6137	24	13.44	0.52	0.5242	0.0096	0.59659	1.907669	0.0349363	0.1849	0.0062	0.45059	2714	40	2717	40	2696	28	-0.8	2696.0	28.0
(IL14-4)-26	6544	18/11 (4)	0.5265	24	12.59	2.6	0.5236	0.014	0.87447	1.909855	0.0510656	0.187	0.0069	-0.0663	2649	17	2714	59	2716	15	0.1	2716.0	15.0
(IL14-4)-57	6545	18/11 (4)	0.5919	24	13.37	0.52	0.5169	0.0074	0.73663	1.93461	0.0276961	0.1878	0.0057	0.3961	2706	36	2686	32	2722	14	1.3	2722.0	14.0

Notes: [1] Sample number in parenthses; [2] Source file number followed by "TRA_Analysis.csv"; [3] day/mouth and completed in 2015; [4] duration of analyis in seconds; [5] ErrorCorrelation $^{238}U/^{206}Pb$ vs $^{207}Pb/^{206}Pb$; [6] % Discordant; [7] Preferred Age used in interpretations.